Problems of the Standard Model and their relations to Planck/String scale physics

Kiyoharu Kawana*

Department of Physics, Kyoto University, Kyoto 606-8502, Japan

January 20, 2017

*E-mail: kiyokawa@gauge.scphys.kyoto-u.ac.jp

Abstract

Since the discovery of the Higgs boson [1, 2], we are now living in an exciting era: We already know all the Standard Model (SM) particles and their couplings ! In particular, the observed quartic coupling $\lambda \sim 0.12$ indicates that the SM can be perturbatively valid up the the Planck scale, and also that the Higgs potential can have another degenerate vacuum around the Planck scale. This non-trivial behavior of the Higgs vacua called the *SM criticality*, and it opened new phenomenological possibilities such as the Higgs inflation. However, we all know that this is not the end of the story: There are various phenomenological and theoretical problems in the SM. For examples, as for the phenomenological problems, the various cosmological observations strongly suggest the existence of Dark Matter (DM) and the asymmetry of baryon number. Because they are difficult to answer within the SM, people usually expect that they must be evidences of new particles. Besides, we also have various theoretical problems such as the quadratic divergence of the Higgs mass, and they are often called the *naturalness problem*. These problems are more fundamental than the phenomenological ones in the sense that they always appear in any quantum field theory (QFT). In other words, the naturalness problem suggests us the necessity of new physics beyond QFT. The purpose of this thesis is to investigate these problems from the point of view of physics at the Planck/String scale.

The first part of this thesis is devoted to possible solutions of DM and the baryon asymmetry. First, we consider the so-called minimal dark matter models, and study its theoretical consistencies: We check perturbativity of these models up to the Planck scale based on the one or two loop renormalization group equations (RGEs). As a result, we find that only such candidates that have small (triplet or quintet) $SU(2)_L$ representations are valid up to the Planck scale. Then, we study the Higgs potential for these safe candidates, and find that only the triplet Majorana fermion or real scalar can realize the degenerate vacua between the weak scale and the Planck scale. Second, we propose a novel leptogenesis scenario at the reheating era: We assume an heavy inflaton which decays to the SM particles. Then, by considering the scatterings of the SM leptons through the higher dimensional operators, we show that the enough lepton asymmetry can be obtained at the reheating era. Because our mechanism does not assume a specific model, this can be applicable to various extensions of the SM such as the seesaw models.

The second part of this thesis is devoted to the naturalness problem and gravity. First, we formulate the Minkowski version of the Coleman's theory, and show that a few naturalness problems, the strong CP problem, the SM criticality and the cosmological constant problem, can be simultaneously solved by it. Finally, we discuss a possible origin of gravity from the matrix model. We interpret the large N matrix model as the noncommutative $U(1)$ gauge theory, and discuss whether we can regard the $U(1)$ gauge field $A_\mu(x)$ as usual graviton. By using the one-loop effective action of $A_\mu(x)$, we show that the amplitude of the ordinary graviton exchange can be reproduced

by the exchange of $A_\mu(x)$.

Contents

1 Introduction and Motivation **4**

2 Dark Matter **11**
2.1 Minimal Dark Matter . . . 11
2.2 Perturbativity . . . 12
2.3 The Standard Model Criticality . . . 21
2.3.1 The criticality in the Standard Model . . . 21
2.3.2 The criticality in Minimal Dark Matter Models . . . 22

3 Leptogenesis **30**
3.1 Theoretical foundations and ordinary thermal leptogenesis . . . 30
3.2 Leptogenesis at the reheating era . . . 33

4 Theoretical Approaches to the Naturalness Problem **43**
4.1 Froggatt-Nielsen mechanism . . . 44
4.2 Multi-local theory and the naturalness problem . . . 48
4.2.1 Coleman's first idea . . . 48
4.2.2 Minkowski version . . . 53
4.3 Strong CP problem . . . 54
4.4 The SM criticality . . . 54
4.5 Cosmological constant problem . . . 56

5 Origin of Gravity **60**
5.1 Noncommutative field theory from the matrix model . . . 61
5.2 Emergent gravity from NC $U(1)$ gauge theory . . . 63

6 Summary **71**

A Renormalization Group equations **73**

B Sphaleron process and relation between number densities **76**

C Multi-local theory from the matrix model **80**

D Effect of the expansion of the universe **87**

E Wheeler-Dewitt generalization **87**

F Principal value and Wheeler-Dewitt state **89**

1 Introduction and Motivation

In the history of particle physics, the Standard Model (SM) is the most successful theory that can explain the various experiments and observations. It is a gauge theory whose gauge group is $SU(3)_C \times SU(2)_L \times U(1)_Y$, and it consists of quark (Q_i, q_{Ri}), lepton (L_i, l_{Ri}), gauge boson $(G^a_\mu, A_\mu, W^\pm_\mu, Z_\mu)$ and Higgs boson H, where $i = 1, 2, 3$ represents the generation. Surprisingly, their quantum charges are correctly chosen so that the theory becomes gauge invariant. By the discovery of the Higgs boson, we already know the precise values of the SM couplings and can discuss its various aspects including its relation to the Planck scale physics. In particular, recent analyses based on renormalization group equations (RGEs) [3, 4, 5, 6, 7, 8, 9] indicate that the SM can be interpolated to the Planck scale without any contradiction or divergence. This fact is not so trivial in the framework of quantum field theory (QFT) and suggests an interesting possibility: There might be no new physics between the weak scale and the Planck scale. This scenario is often called *desert scenario*, and the half part of this thesis is devoted to this possibility. (See Sections 4 and 5.)

Although the SM itself can be valid up to the Planck scale, it has many phenomenological and theoretical problems. Here, let us summarize the ones that are related with my works. The purpose of this thesis is to investigate those problems from the point of view of the Planck/String scale physics.

Problems of the Standard Model

- *Dark Matter (DM)*
- *Baryon (Lepton) Asymmetry*
- *Vacuum structure of the SM*
- *Naturalness (Fine-tuning) problem*
- *Origin of Gravity*

The existence of Dark Matter (DM) is supported by various cosmological observations [10, 11, 12, 13, 14, 15]. These observations indicate the following properties of DM:

- It is a non-relativistic particle [10, 12, 13]. People usually call it *cold Dark Matter*.

- Its life time must be larger than the age of the universe.
- It is neutral under $SU(3)_C \times U(1)_{\rm em}$ [11, 14, 15].
- Its energy density $\rho_{\rm DM}$ is given by [10]

$$\Omega_{\rm DM} = \frac{\rho_{\rm DM}}{\rho_{\rm cri}} = 0.308 \pm 0.012, \tag{1}$$

  where $\rho_{\rm cri} := 3M_{pl}H^2$ is the critical energy density.

Unfortunately, there is no possible candidate in the SM that can satisfy the above properties. Therefore, we must attribute its origin to new physics. Among various possibilities (see [] for example), *weakly interacting massive particle* (WIMP) attracts much attention because of its simplicity and its collider experimental interest: This scenario explains the DM abundance as a relic abundance of a new particle whose annihilation cross section is determined as

$$\langle \sigma v \rangle \sim \frac{\alpha_{\rm DM}^2}{M_{\rm DM}^2} \sim \mathcal{O}(10^{-8}){\rm GeV}^{-2} \tag{2}$$

in order to explain Eq.(1). Here, $M_{\rm DM}^2$ is the DM mass, and $\alpha_{\rm DM}^2$ is the structure constant of the annihilation process. Remarkably, Eq.(2) holds when $M_{\rm DM} \sim 100{\rm GeV}$ and $\alpha_{\rm DM} \sim 10^{-2}$! Because they are close to the electroweak scale and the weak coupling in the SM, the above coincidence is called *WIMP Miracle*. This miracle motivates us to consider a new weakly interacting fermion χ or scalar X, which is a $n_{\chi(X)}$ representation of $SU(2)_L$ with the hypercharge $Y_{\chi(X)}$. Its neutral component can naturally become a DM candidate, and those models are called *Minimal Dark Matter Models* [16, 17, 18, 19]. Because its cosmological and experimental implications are already well studied [16, 17, 18, 19], we in particular focus on its theoretical consistency as a low energy effective theory below the Planck scale: We study *perturbativity* and the criticality of minimal dark matter models in Section 2. Here, we briefly explain them: (See Section 2 for the detail analyses.)

Perturbativity is a good theoretical criterion in order to check whether a theory can be valid up to the Planck scale. Couplings of a field theory generally suffer loop corrections, and they change as a function of the renormalization scale μ by the renormalization group equations. If a few of them monotonically increase, they finally diverge or hit the Landau pole (LP) in some scale $\Lambda_{\rm LP}$, and we can no longer use perturbation around that scale. Therefore, if one want to study some phenomenological model, and regard it as a low energy effective theory below the Planck scale, one must always take care of the existence of the LP. In this sense, we can use perturbativity as a theoretical consistency check of various models. In particular, it is notable that there is no LP in the SM. The runnings of the SM couplings based on two-loop RGEs are shown in Fig.1. Here, we drop the Yukawa couplings except for the top Yukawa because they are not relevant. From this figure, one can actually see that the SM is perturbative up to the Planck scale though the

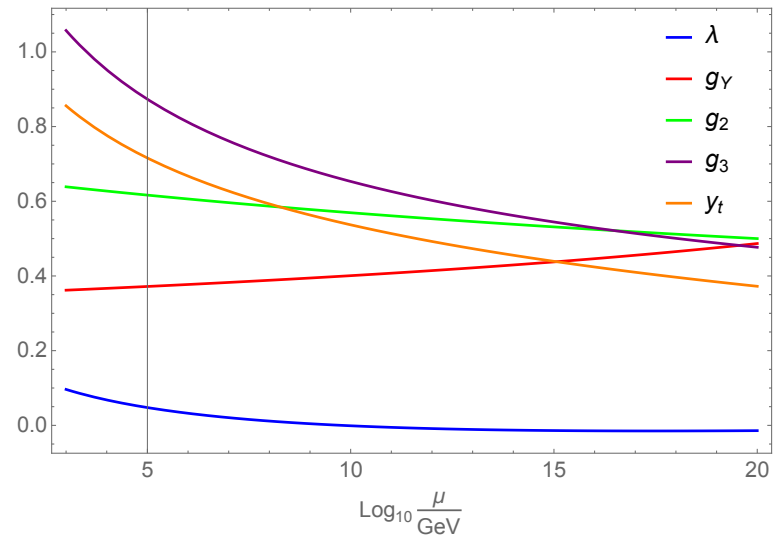

Figure 1: The runnings of the SM couplings based on the two-loop RGEs.

$U(1)_Y$ gauge coupling g_Y monotonically increases. This result is not so trivial because, as we will see in Section 2, we often encounter the LP in its various extensions. Therefore, this fact is often regarded as one of the evidences of the desert scenario. However, even in this situation, people usually think that there must be new physics above the weak scale because of the phenomenological problems mentioned before. In the first part of Section 2, we systematically examine perturbativity of minimal dark matter models. As a result, we find that perturbativity gives a strong constraint on the representations and the charges of the DM. Our results are rather general, and can be applicable to other various models.

In addition to perturbativity, the SM has an interesting vacuum structure: The observed Higgs mass indicates that the Higgs potential can have another minimum around the Planck scale, and it can degenerate with the electroweak vacuum $v_h = 246\mathrm{GeV}$ depending on the other SM couplings. See Fig.2 for example. This shows the one-loop effective Higgs potential where the blue contour corresponds to the critical case where the top mass M_t is fine tuned. Although the existence of another vacuum generally depends on the SM couplings, this critical behavior of the SM vacua is quite non-trivial and recently attracts much attention [20, 21, 22, 23, 24, 25, 26, 27, 28, 29, 30, 31]. Among them, the best known application of the criticality is the Higgs inflation [32, 33, 34, 35, 36, 37, 38, 39, 40]: Before the discovery of the Higgs, it was believed that it was difficult to realize the Higgs inflation *naturally* because the Higgs potential could not be so flat around the Planck scale. Thus, in order to make the Higgs potential flat, an interaction between gravity $\xi\phi^2 R$ was introduced, and ξ was chosen to be very large $\sim 10^5$. However, as one can see from Fig.2, the observed value of the Higgs mass indicates that the Higgs potential can be very flat even without

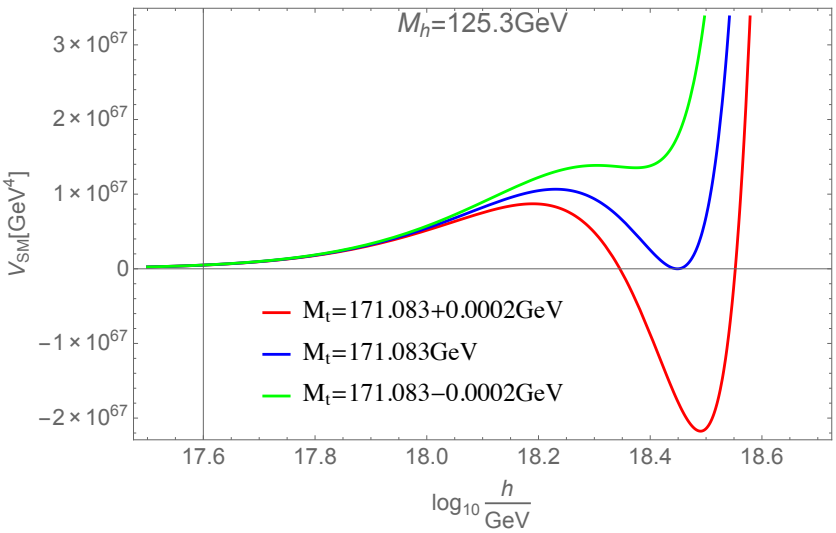

Figure 2: The one-loop effective Higgs potential. The blue one corresponds to the critical value of the top mass M_t such that the two vacua degenerate.

introducing unnaturally large coupling. By using this result, it is now possible to realize the Higgs inflation even if $\xi \sim \mathcal{O}(10)$ [37]. Of course, this peculiar behavior of the Higgs potential can be spoiled by the effects of new particles. Therefore, it is meaningful to study whether we can maintain the criticality even in some extensions of the SM. In subsection 2.2, we actually study the Higgs potential in minimal dark matter models. Then, we find that only the $SU(2)_L$ triplet extensions can realize the degeneracy of two vacua as maintaining perturbativity. In this sense, perturbativity and the SM criticality give strong constrains to possible extensions of the SM. At this point, however, readers might have a following question: " Ok, I understand that the criticality is interesting. But, is there any theoretical reason to believe it ? ". In section 4, we discuss a few theoretical explanations of the SM criticality in addition to the naturalness problem.

The baryon asymmetry of the universe is also one of the important problems of the SM. It is usually measured by the baryon to photon ratio [10]:

$$\eta_B := \frac{n_B}{s} = (8.67 \pm 0.05) \times 10^{-10} \tag{3}$$

where n_B is the number density of baryons, and s is the entropy density of photons. This fact is usually considered as an evidence of new physics because it is difficult to obtain the above asymmetry in the SM. Actually, various models and mechanisms have been proposed so far [41, 42, 43, 44, 45, 46, 47, 48] in connection with physics beyond the SM. Among them, the thermal leptogenesis [43, 48] by the decays of heavy right handed neutrinos attracts much attention

because it is a minimum extension of the SM, and the heavy neutrinos can also realize the small neutrino masses by the seesaw mechanism. In this scenario, the lepton asymmetry is produced by the decays of thermalized right handed neutrinos, and this asymmetry is converted baryons by Sphaleron process [49, 50, 51]. Therefore, in order to obtain thermalized heavy neutrinos, the reheating temperature of the universe must be larger than these neutrinos $\sim \mathcal{O}(10^{15}\text{GeV})$. However, realizing such a high temperature is not so easy in typical inflationary scenario [1]. In Section 3, taking this situation into account, we propose a novel leptogenesis scenario which can realize the observed asymmetry even when the reheating temperature T_R is lower than $\mathcal{O}(10^{15}\text{GeV})$: We consider the reheating era where the SM particles are produced by an heavy inflaton. These particles are inevitably out of equilibrium, and scatter each other. Then, by considering the effects of the higher dimensional operators in the SM, we show that the enough lepton asymmetry can be actually produced during the reheating era. See section 3 for the details. Because heavy right hand neutrino can be a natural origin of such higher dimensional operators, our scenario can be a promising alternative of the ordinary thermal leptogenesis scenario. Furthermore, our mechanism can be applicable to various extensions [52] of the SM because we do not assume a specific model in our argument.

In addition to the above phenomenological problems, the SM also has various fine-tuning problems: In flat spacetime, the most well known one is the quadratic divergence of the Higgs mass:

$$m_B^2 + \Lambda^2 \sim \mathcal{O}(100^2)\text{GeV}^2, \tag{5}$$

where m_B is the bare Higgs mass, and Λ is a cutoff scale. Thus, we must drastically fine tune the bare mass to obtain the observed mass. Note that this problem is not unique for the SM, and always exists as long as we consider scalar fields in QFT. Moreover, in quantum chromodynamics (QCD), the Strong CP problem [53, 127, 128] exits, and the small Yukawa couplings are also one of the mysteries of the SM. In curved spacetime, however, situation becomes more and more worse: The cosmological constant problem (CCP) [54, 55] is the worst fine-tuning problem in the universe [10]:

$$\Lambda_B + (\Lambda^4/M_{pl}^2) = \mathcal{O}(H_0^2) \sim \mathcal{O}(10^{-42\times 2})\text{GeV}, \tag{6}$$

where Λ_B is the bare cosmological constant (CC), and H_0 is the Hubble constant of the present universe. In Section 4, we discuss a few possible solutions of these problems in addition to the

[1] For example, if the reheating occurs by the decay of heavy inflatons, and its decay rate Γ_{inf} satisfies $\Gamma_{\text{inf}} \ll H$ at the end of the inflation, the reheating temperature T_R is roughly given by

$$T_R \sim \sqrt{M_{pl}\Gamma_{\text{inf}}} \ll \sqrt{HM_{pl}} \sim \mathcal{O}(10^{14})\text{GeV}, \tag{4}$$

where we have assumed $H \sim 10^{13}\text{GeV}$.

SM criticality. We first consider the so-called Froggatt-Nielsen mechanism (FNM) [56, 57, 58, 59]. Froggatt and Nielsen originally proposed this mechanism in order to explain the SM criticality. In particular, because the predicted Higgs mass $\sim$ 130GeV was very close to the observed value 125GeV, this mechanism has came to attract much attention recently [20, 21, 22, 23, 24, 25, 26, 27, 28, 29, 30, 31]. The fundamental assumption of the FNM is to start from a micro-canonical partition function like statistical mechanics. Then, as the temperature is naturally determined in statistical mechanics, the couplings in QFT become dynamical, and they can be fixed dynamically. See subsection 4.1 for the details. However, while its phenomenological applications are well studied, its physical origin has not been discussed so far. In the following, we will see that it can be actually obtained from the Planck scale physics by reinterpreting this mechanism as the Coleman's theory mentioned below.

As a second possibility, we discuss recent progresses [60, 61, 62, 63, 64, 31, 65] of the Coleman's approach in subsection 4.2. This approach was originally based on Euclidean gravity, and it was argued that couplings of ordinary field theory become dynamical quantities by the effects of the classical solutions of Euclidean gravity (wormholes). In the original paper [66], Coleman actually applied this theory to the CCP, and showed that the partition function of Euclidean gravity has a strong peak at $\Lambda = 0$. However, because the path integral of Euclidean gravity is not well-defined, the validity of this argument is unclear as long as we use Euclidean gravity. Therefore, its Minkowski analysis is essential needed in order to give meaningful predictions.

In subsection 4.2, we actually formulate the Minkowski version of the Coleman's theory. As a result, we find that a few naturalness problems, the Strong CP problem and the CCP, can be simultaneously solved including the SM criticality. In Appendix C, its possible origin from the matrix model is also discussed.

The final section of this thesis is devoted to the matrix model and its possible relation to gravity: The IIB matrix model [69, 70, 71, 72] is known as a promising candidate for the non-perturbative formulation of type-IIB superstring theory. Because string theory contains gravity as its fluctuation, it is also expected that the matrix model includes gravity. However, there are many possibilities and interpretations of the appearances of spacetime and gravity [61, 65, 73, 74, 75, 76, 77, 78, 79, 80, 81, 82, 83, 84], and we do not yet obtain a correct picture. In particular, it is well known that there is a close relation between the matrix model and noncommutative (NC) field theory [85, 86, 87]: The fluctuation of matrices around some noncommutative classical solution is equivalent to a $U(1)$ gauge field of a NC $U(1)$ gauge theory, where the product of fields is defined by the star product. Because of the noncommutativity, this gauge field is uniformly coupled with all the matters including real scalar and Majorana fermion. This peculiar behavior of the $U(1)$ gauge field reminds us the property of gravity, and many studies have been done so far [88, 89, 90, 91, 92, 93, 94, 95, 97, 98] with the aim of understanding the

relation between the NC theory and gravity. This possibility is usually called *emergent gravity*.

The purpose of section 5 is to investigate this possibility. At a first glance, it seemingly does not work because of the mismatch of the off-shell degrees of freedom: The $U(1)$ gauge field has only four, while a graviton does ten. Furthermore, we have not yet obtained the explicit diffeomorphism invariance in this NC picture [2]. Therefore, it is quite necessary to check whether the emergent gravity scenario can actually explain the results of the ordinary gravity. As a fist step, we calculate a two-body scattering amplitude of scalar particles exchanging the NC $U(1)$ gauge field, and compare it with that of the usual graviton exchange. As a result, we will see that the NC $U(1)$ gauge theory correctly reproduces the usual graviton exchange if the noncommutativity is appropriately averaged and the test particles are massless. (See subsection 5.2 for the details.) Of course, this is just one example, and we need more detail studies in order to confirm the emergent scenario. We leave them as our future works.

This thesis is organized as follows. In Section 2, we study the theoretical consistencies of the minimal dark matter models. In particular, we examine perturbativity of these models in subsection 2.1. Then, in subsection 2.2, we consider the Higgs potential for those models that are perturbative up to the Planck scale. In Section 3, we focus on the baryon asymmetry of the universe. We first summarize theoretical foundations of leptogenesis and the thermal leptogenesis scenario in subsection 3.1. After that, we propose a new leptogenesis scenario at the reheating era in subsection 3.2. In Section 4, we consider possible solutions of the naturalness problem. In subsection 4.1, we first consider the FNM, and discuss how fine-tunings occur in this mechanism. In subsection 4.2, we formulate the Minkowski version of the Coleman theory. Then we apply it to a few fine-tuning problems in subsections 4.3 - 4.5. In Section 5, we study the matrix model and its relation to gravity. Before discussing gravity, we first review the matrix model and its NC interpretation in subsection 5.1. Then, we study the relation between the NC $U(1)$ theory and gravity in subsection 5.2. In particular, we calculate the scattering amplitude of scalar test particles exchanging the NC $U(1)$ gauge field, and compare it with that of the usual graviton exchange. In Section 6, we summarize this thesis.

[2] On the other hand, the diffeomorphism can be explicitly seen in other interpretations of the matrix model such as the covariant derivative interpretation [80, 81].

2 Dark Matter

In this section, we consider perturbativity and the Higgs potential in minimal dark matter models. In subsection 2.1, we briefly explain the models. In subsection 2.2, we first give a general argument of perturbativity, and apply it to minimal dark matter models. In subsection 2.3, we study whether the Higgs potential can have another degenerate vacuum at the Planck scale. Then, we also examine the bare Higgs mass.

2.1 Minimal Dark Matter

We consider a new fermion χ or scalar X, which is a $n_{\chi(X)}$ representation of $SU(2)_L$ with a hypercharge $Y_{\chi(X)}$. The Lagrangian of this model is given by

$$\mathcal{L} = \mathcal{L}_{\rm SM} + \eta \begin{cases} \chi \left(i\not{D} - M_{\rm DM} \right) \chi + \mathcal{L}_{\rm Yukawa} \text{ for fermionic DM,} \\ (D_\mu X)^\dagger (D^\mu X) - M_{\rm DM}^2 (X^\dagger X) - V(X) \text{ for scalar DM,} \end{cases} \tag{7}$$

where

$$\eta = \begin{cases} 1 \text{ for Dirac fermion and complex scalar,} \\ 1/2 \text{ for Majorana fermion and real scalar,} \end{cases} \tag{8}$$

$\not{D} = D\mu\gamma^\mu$, D_μ is the covariant derivative of $SU(2)_L \times U(1)_Y$, $\mathcal{L}_{\rm Yukawa}$ represents an additional Yukawa term, and $V(X)$ is the potential of χ. Note that the hipercharge of the DM $Y_{\chi(X)}$ is zero for the Majorana fermion and the real scalar. Furthermore, we must choose $Y_{\chi(X)}$ correctly so that

$$Q_{\rm DM} = T_3 + Y_{\chi(X)} = 0 \tag{9}$$

is satisfied for a component of χ or X. In table 1, we present all the possibilities for $n_{\chi(X)} \leq 7$: In the 4th column, the possible decay channels are shown. Candidates that have an open decay channel can be excluded as long as we do not assume additional symmetries such as $\mathbf{Z}_2$ symmetry. In the following, we assume such an ad hoc symmetry. In the 5th column, we show whether these candidates are excluded by direct detection searches [101, 102]. Here, candidates with $Y \neq 0$ are all excluded because they have a tree-level spin-independent cross section [103]

$$\sigma({\rm DM} + \mathcal{N} \to {\rm DM} + \mathcal{N}) = \frac{G_F^2 M_{\mathcal{N}}^2}{2\pi} Y^2 \left(N - (1 - 4s_W^2) Z \right)^2 , \tag{10}$$

through the Z boson exchange. Here, $c = 1$ for fermionic DM, and $c = 4$ for scalar DM, $\mathcal{N}$ represents the target nucleus, and Z (N) is the number of its protons (neutrons). Thus, only the real representations

$$(n_{\chi(X)}, Y_{\chi(X)}) = (\mathbf{2n+1}, 0), \ n = 1, 2, \cdots , \tag{11}$$

are allowed. In the next subsections, we further constrain these candidates by perturbativity and the criticality.

Representation and charge			Coupling with the	Direct detection	Perturbativity
$SU(2)_L$	$U(1)_Y$	Spin	SM particles	bound	up to the Planck scale
2	1/2	S	$E\bar{L}$	$\times$	$\bigcirc$
2	1/2	F	EH	$\times$	$\bigcirc$
3	0	S	HH^*	$\bigcirc$	$\bigcirc$
3	0	F	LH	$\bigcirc$	$\bigcirc$
3	1	S	H^*H^*, LL	$\times$	$\bigcirc$
3	1	F	LH^*	$\times$	$\bigcirc$
4	1/2	S	HH^*H^*	$\times$	$\times$
4	1/2	F	LHH^*	$\times$	$\bigcirc$
4	3/2	S	$H^*H^*H^*$	$\times$	$\times$
4	3/2	F	LHH	$\times$	$\bigcirc$
5	0	S	HHH^*H^*	$\bigcirc$	$\times$
5	0	F	$-$	$\bigcirc$	$\bigcirc$
5	1	S	$HH^*H^*H^*$	$\times$	$\times$
5	1	F	$-$	$\times$	$\times$
5	2	S	$H^*H^*H^*H^*$	$\times$	$\times$
5	2	F	$-$	$\times$	$\times$
6	1/2, 3/2, 5/2	S	$HHH^*H^*H^*, \cdots$	$\times$	$\times$
6	1/2, 3/2, 5/2	F	$-$	$\times$	$\times$
7	0	S	$XXHH^*, \cdots$	$\bigcirc$	$\times$
7	0	F	$-$	$\bigcirc$	$\times$

Table 1: The possible candidates of the minimal dark matter models. Here, we also show additional couplings with the SM particles and the constraints from direct detection searches [101, 102] and the LP. Note that the models with $Y_{\chi(X)} \neq 0$ are excluded by direct detection serches. All the candidates that have the couplings between the SM particles are not allowed as long as we do not assume additional symmetries such as $\mathbf{Z}_2$ symmetry.

2.2 Perturbativity

In this section, we examine perturbativity up to the Planck scale. In order to understand the LP, let us first consider ϕ^4 theory as a simple example:

$$S = \int d^4x \left(\frac{1}{2}\partial_\mu \phi \partial^\mu \phi - \frac{m^2}{2}\phi^2 - \frac{\lambda}{4!}\phi^4 \right). \tag{12}$$

The one-loop RGE of the scalar quartic coupling λ is given by

$$\frac{d\lambda}{d\log\mu} = \frac{6\lambda^2}{16\pi^2} := c\lambda^2, \tag{13}$$

where μ is the renormalization scale. This can be analytically solved as

$$\lambda(\mu) = \frac{\lambda(\mu_0)}{1-\lambda(\mu_0)c\log\left(\frac{\mu}{\mu_0}\right)}, \tag{14}$$

where μ_0 is an initial scale. Because $c > 0$, $\lambda(\mu)$ diverges at

$$\Lambda_{\rm LP} = \mu_0 \exp\left(\frac{1}{c\lambda(\mu_0)}\right), \tag{15}$$

and this is the LP. In the following argument, we take the weak scale $v_h = 246$GeV as μ_0. Note that $\Lambda_{\rm LP}$ is mainly determined by the coefficient of the RGE and the initial value. This property generally holds even if we consider more general models.

Before considering extensions of the SM, let us briefly summarize the RGEs of the SM here. The two-loop RGEs of the relevant SM couplings are given by as follows:

$$\frac{dg_Y}{dt} = \frac{1}{(4\pi)^2}\frac{41}{6}g_Y^3 + \frac{g_Y^3}{(4\pi)^4}\left(\frac{199}{18}g_Y^2 + \frac{9}{2}g_2^2 + \frac{44}{3}g_3^2 - \frac{17}{6}y_t^2 - \frac{3}{2}y_\nu^2\right), \tag{16}$$

$$\frac{dg_2}{dt} = -\frac{1}{(4\pi)^2}\frac{19}{6}g_2^3 + \frac{g_2^3}{(4\pi)^4}\left(\frac{3}{2}g_Y^2 + \frac{35}{6}g_2^2 + 12g_3^2 - \frac{3}{2}\left(y_t^2 + y_\nu^2\right)\right), \tag{17}$$

$$\frac{dg_3}{dt} = -\frac{7}{(4\pi)^2}g_3^3 + \frac{g_3^3}{(4\pi)^4}\left(\frac{11}{6}g_Y^2 + \frac{9}{2}g_2^2 - 26g_3^2 - 2y_t^2\right), \tag{18}$$

$$\begin{aligned}\frac{dy_t}{dt} &= \frac{y_t}{(4\pi)^2}\left(\frac{9}{2}y_t^2 + 3y_\nu^2 - \frac{17}{12}g_Y^2 - \frac{9}{4}g_2^2 - 8g_3^2\right)\\ &+ \frac{y_t}{(4\pi)^4}\Bigg\{-12y_t^4 - \frac{27}{4}y_\nu^4 - \frac{27}{4}y_t^2y_\nu^2 - \frac{9}{8}Y_R^2y_\nu^2 + 6\lambda^2 + \frac{1}{4}\kappa^2 - 12\lambda y_t^2 + g_Y^2\left(\frac{131}{16}y_t^2 + \frac{15}{8}y_\nu^2\right)\\ &\quad + g_2^2\left(\frac{225}{16}y_t^2 + \frac{45}{8}y_\nu^2\right) + 36g_3^2y_t^2 + \frac{1187}{216}g_Y^4 - \frac{23}{4}g_2^4 - 108g_3^4 - \frac{3}{4}g_Y^2g_2^2 + 9g_2^2g_3^2 + \frac{19}{9}g_3^2g_Y^2\Bigg\},\end{aligned} \tag{19}$$

$$\begin{aligned}\frac{dy_\nu}{dt} &= \frac{y_\nu}{(4\pi)^2}\left(\frac{9}{2}y_\nu^2 + 3y_t^2 - \frac{3}{4}g_Y^2 - \frac{9}{4}g_2^2\right)\\ &+ \frac{y_\nu}{(4\pi)^4}\Bigg\{-12y_\nu^4 - \frac{27}{4}y_t^4 - \frac{27}{4}y_t^2y_\nu^2 + 6\lambda^2 + \frac{1}{4}\kappa^2 - 12\lambda y_\nu^2\\ &\quad + g_Y^2\left(\frac{123}{16}y_\nu^2 + \frac{85}{24}y_t^2\right) + g_2^2\left(\frac{225}{16}y_\nu^2 + \frac{45}{8}y_t^2\right) + 20g_3^2y_t^2 + \frac{35}{24}g_Y^4 - \frac{23}{4}g_2^4 - \frac{9}{4}g_Y^2g_2^2\Bigg\},\end{aligned} \tag{20}$$

$$
\begin{aligned}
\frac{d\lambda}{dt} &= \frac{1}{(4\pi)^2}\left(\lambda\left(24\lambda - 9g_2^2 - 3g_Y^2 + 12y_\nu^2 + 12y_t^2\right) + \frac{3}{4}g_2^2 g_Y^2 + \frac{9g_2^4}{8} + \frac{3g_Y^4}{8} + \frac{\kappa^2}{2} - 6y_\nu^4 - 6y_t^4\right) \\
&+ \frac{1}{(4\pi)^4}\Bigg\{-2\kappa^3 - 5\kappa^2\lambda - 312\lambda^3 + 36\lambda^2\left(g_Y^2 + 3g_2^2\right) + \lambda\left(\frac{629}{24}g_Y^4 + \frac{39}{4}g_2^2 g_Y^2 - \frac{73}{8}g_2^4\right) \\
&\quad + \frac{305}{16}g_2^6 - \frac{289}{48}g_Y^2 g_2^4 - \frac{559}{48}g_Y^4 g_2^2 - \frac{379}{48}g_Y^6 - 32g_3^2 y_t^4 - \frac{8}{3}g_Y^2 y_t^4 - \frac{9}{4}g_2^4\left(y_t^2 + y_\nu^2\right) \\
&\quad + \lambda y_t^2\left(\frac{85}{6}g_Y^2 + \frac{45}{2}g_2^2 + 80g_3^2\right) + \lambda y_\nu^2\left(\frac{15}{2}g_Y^2 + \frac{45}{2}g_2^2\right) + g_Y^2 y_t^2\left(-\frac{19}{4}g_Y^2 + \frac{21}{2}g_2^2\right) \\
&\quad - g_Y^2 y_\nu^2\left(\frac{3}{4}g_Y^2 + \frac{3}{2}g_2^2\right) - 144\lambda^2\left(y_t^2 + y_\nu^2\right) - 3\lambda\left(y_t^4 + y_\nu^4\right) + 30\left(y_t^6 + y_\nu^6\right)\Bigg\}, \qquad (21)
\end{aligned}
$$

Here, g_Y, g_2 and g_3 are the gauge couplings, y_t is the top Yukawa, and we have also included the Yukawa couplings of the right handed neutrinos:

$$
\mathcal{L} \ni \sum_{i,j} y_{\nu ij}\bar{L}_i\tilde{H}\nu_{jR} + \text{h.c}, \qquad (22)
$$

where we have assumed that $y_{\nu ij}$'s are diagonalized and satisfy $y_{\nu 11} = y_{\nu 22} = y_{\nu 33}$ for simplicity. Note that the SM has the LP determined by g_Y. At one-loop level, it is given by

$$
\Lambda_{LP}^{(SM)} = v_h \times \exp\left(\frac{48\pi^2}{41}\frac{1}{g_Y(v_h)^2}\right) \sim 10^{41}\text{GeV}. \qquad (23)
$$

Therefore, the SM itself can be perturbative up to the Planck scale. The runnings of the SM couplings are already shown in Fig.1 where we have put $y_\nu = 0$ for simplicity.

□ **Fermionic extensions**

Now, let us consider the fermionic extensions of the SM. Here, we concentrate on a new fermion which has the SM weak charges only, and do not consider new fermions which have some hidden gauge symmetries because such new degrees of freedom typically decrease Λ_{LP}. The analyses of the LP in these fermionic extensions are already done in details [104], but our study is more complete because we also include the top Yukawa in their RGEs. The two-loop RGEs of the gauge couplings are given by

$$
\frac{dg_Y}{dt} = \frac{g_Y^3}{(4\pi)^2}\left(\frac{41}{6} + \eta\, n_\chi \frac{4}{3}Y_\chi^2\right) + \frac{g_Y^3}{(4\pi)^4}\left\{\left(\frac{199}{18} + 4\eta\, n_\chi Y_\chi^4\right)g_Y^2 + \left(\frac{9}{2} + 4\eta Y_\chi^2 C_n\right)g_2^2 + \frac{44}{3}g_3^2 - \frac{17}{6}y_t^2\right\}, \qquad (24)
$$

$$\frac{dg_2}{dt} = \frac{g_2^3}{(4\pi)^2}\left(-\frac{19}{6}+\eta\frac{4}{3}S_n\right) + \frac{g_2^3}{(4\pi)^4}\left\{\left(\frac{3}{2}+\eta 4Y_\chi^2 S_n\right)g_Y^2 + \left(\frac{35}{6}+\eta\frac{40}{3}S_n+\eta 4C_n S_n\right)g_2^2 + 12g_3^2 - \frac{3}{2}y_t^2\right\}, \tag{25}$$

$$\frac{dg_3}{dt} = -\frac{7}{(4\pi)^2}g_3^3 + \frac{g_3^3}{(4\pi)^4}\left(\frac{11}{6}g_Y^2+\frac{9}{2}g_2^2-26g_3^2-2y_t^2\right), \tag{26}$$

where C_n and S_n are the Casimir and Dynkin index, and $\eta = 1, \frac{1}{2}$ for Dirac and Weyl fermion. Note that they are agreement with [104] by putting $y_t = 0$.

By using these RGEs, we can now evaluate the runnings and the LP of the minimal dark matter fermions. In Fig.3, we show the runnings of g_2 for each of the fermionic candidates. Here, we use the RGEs of the SM for $\mu < M_{\rm DM}$, and use Eq.(25) for $\mu > M_{\rm DM}$. In this figure, $M_{\rm DM}$ is chosen to be 1TeV. One can see that the triplet fermion never hit the LP, while the fermions with $n_\chi \geq 5$ can hit the LP. For the $n_\chi = 5$ case, however, it is actually valid up to the Planck scale because its mass is already fixed to be 10 TeV by the thermal relic abundance [19], and such a large mass increases Λ_{LP}.

On the other hand, in cases of $n_\chi \geq 7$, the LP can exist well below the Planck scale. In Fig.4, we give numerical results Λ_{LP} as a function of $M_{\rm DM}$. Here, the two-loop results are shown by dashed lines. As is known, the one-loop Landau pole can be analytically solved as

$$\Lambda_{LP}|_{\text{1-loop}} = M_\chi \exp\left(\frac{8\pi^2}{\left(-\frac{19}{6}+\frac{1}{2}\frac{4}{3}S_n\right)g_2(M_\chi)^2}\right), \tag{27}$$

where S_n is the Dynkin index. From Fig.4, one can see that the two-loop effect is relatively important. As a result, we conclude that only the triplet and quintet real fermions can be DM candidates that is valid up to the Planck scale.

□ **Scalar extensions**

Let us next consider the SM with a new scalar X which is a n_X representation of the $SU(2)_L$ with a hypercharge Y_X. In this model, there are also new scalar couplings, and they also receive the renormalization effects. In particular, unlike the gauge couplings, these scalar couplings blow up even if they are zero at the weak scale because of the one-loop effects of the weak gauge bosons. Because nonzero initial values strengthen the RGE effects, we can obtain a conservative value of Λ_{LP} by putting their initial values zero at the weak scale.

The scalar potential of this model is generally given by

$$\begin{aligned} V =& -\mu^2 H^\dagger H + \lambda(H^\dagger H)^2 + M_X^2 X^\dagger X + \lambda_X |X^\dagger X|^2 \\ &+ \kappa|X^\dagger X||\Phi^\dagger\Phi| + \kappa'(X^\dagger T_X^a X)(\Phi^\dagger T_\Phi^a \Phi) \\ &+ \lambda_X'(X^\dagger T_X^a X)^2 + \lambda_X''(X^\dagger T_X^a T_X^b X)^2 + \cdots, \end{aligned} \tag{28}$$

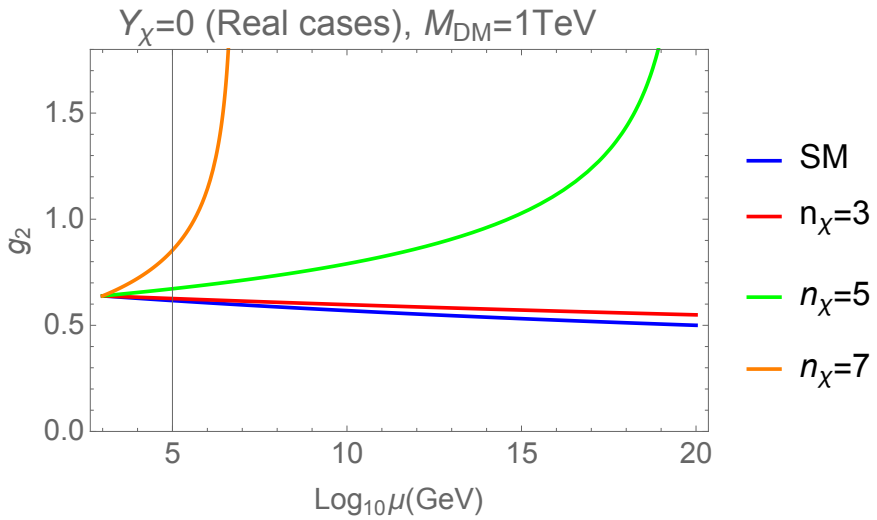

Figure 3: The runnings of g_2 based on two-loop RGEs. Candidates with $n_\chi \geq 5$ can hit the LP.

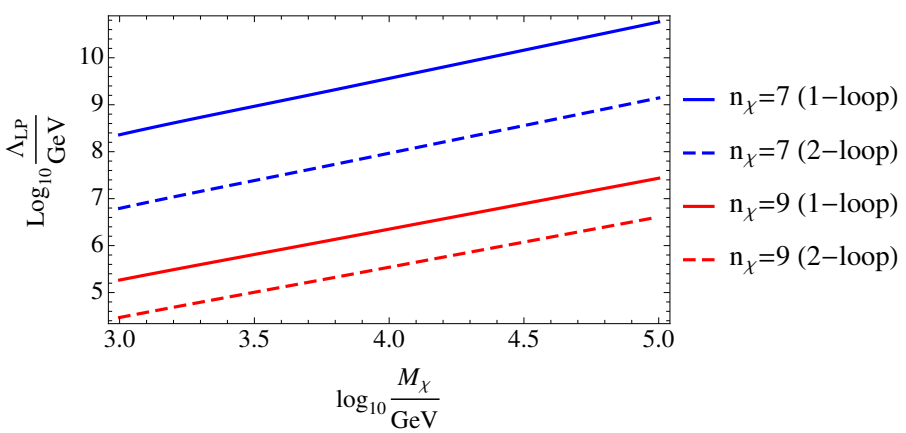

Figure 4: The scale Λ_{LP} of the Landau pole as a function of M_χ when $n_\chi = 7$ (blue) and 9 (red). Here, the two-loop results are represented by dashed lines.

(n_X, Y_X)	independent couplings	dim-4 extra couplings
$(4, 1/2)$	$\lambda, \kappa, \kappa', \lambda_X, \lambda'_X$	$H^{\dagger 2}X^2,\ HH^{\dagger 2}X$
$(4, 3/2)$	$\lambda, \kappa, \kappa', \lambda_X, \lambda'_X$	$H^{\dagger 3}X$
$(5, \text{real})$	$\lambda, \kappa, \lambda_X$	$\times$
$(5, 1)$	$\lambda, \kappa, \kappa', \lambda_X, \lambda'_X, \lambda''_X$	$\times$
$(5, 2)$	$\lambda, \kappa, \kappa', \lambda_X, \lambda'_X, \lambda''_X$	$\times$
$(6, 1/2)$	$\lambda, \kappa, \kappa', \lambda_X, \lambda'_X, \lambda''_X$	$H^{\dagger 2}X^2$
$(6, 3/2)$	$\lambda, \kappa, \kappa', \lambda_X, \lambda'_X, \lambda''_X$	$\times$
$(6, 5/2)$	$\lambda, \kappa, \kappa', \lambda_X, \lambda'_X, \lambda''_X$	$\times$
$(7, \text{real})$	$\lambda, \kappa, \lambda_X, \lambda''_X$	$\times$
$(7, 1)$	$\lambda, \kappa, \kappa', \lambda_X, \lambda'_X, \lambda''_X, \lambda'''_X$	$\times$
$(7, 2)$	$\lambda, \kappa, \kappa', \lambda_X, \lambda'_X, \lambda''_X, \lambda'''_X$	$\times$
$(7, 3)$	$\lambda, \kappa, \kappa', \lambda_X, \lambda'_X, \lambda''_X, \lambda'''_X$	$\times$

Table 2: The independent scalar couplings are listed. We also show the dimension four extra couplings which contribute to the beta functions.

where H is the SM Higgs doublet, X is a new scalar field, M_X is its mass parameter, and the $SU(2)_L$ generator for X is represented by $T^a_X (a = 1, 2, 3)$. Among the scalar quartic coupling constants, some of them are not independent each other depending on the electroweak charges of X. For quadruplets, extra coupling constants are allowed,

$$\lambda_{HH^{\dagger 2}X} HH^\dagger H^\dagger X = \lambda_{HH^{\dagger 2}X} H^i H^\dagger_j H^\dagger_k X^{i'jk} \epsilon_{ii'}, \tag{29}$$

$$\lambda_{H^{\dagger 2}X^2} H^{\dagger 2} X^2 = \lambda_{H^{\dagger 2}X^2} H^\dagger_i H^\dagger_j X^{ik\ell} X^{jk'\ell'} \epsilon_{kk'} \epsilon_{\ell\ell'}, \tag{30}$$

$$\lambda_{H^{\dagger 3}X} H^{\dagger 3} X = \lambda_{\Phi^{\dagger 3}X} H^\dagger_i H^\dagger_j H^\dagger_k X^{ijk}, \tag{31}$$

where we adopt the symmetric tensor notation, i.e., $(X^{111}, X^{112}, X^{122}, X^{222}) = (X^1, X^2/\sqrt{3}, X^3/\sqrt{3}, X^4)$ for $n_X = 4$. The former two coupling constants exist for $Y_X = 1/2$, while the last does for $Y_X = 3/2$. We summarize the independent coupling constants and the possible dimension four extra coupling constants of each model in Table 2.

Before showing our numerical results, let us understand how the LP appears in those models qualitatively. The one-loop RGEs of the above scalar couplings is typically given by

$$\frac{d\lambda_X}{dt} = a\lambda_X^2 + b\lambda_X g_i^2 + c g_i^4,\ \ a, c > 0 \tag{32}$$

where a, b and c are some constants. Thus, even if $\lambda_X = 0$ at the weak scale, it starts to increase by cg_i^4 term, and finally it diverges because of the first term. In Fig.5, we show the corresponding

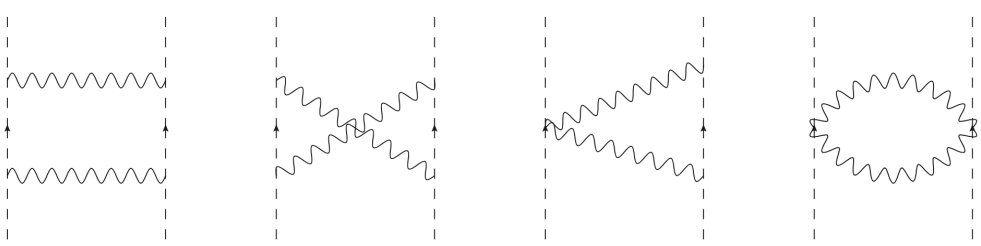

Figure 5: The Feynman diagrams that contribute the RGEs of the scalar quartic couplings as $const \times g_i^4$. From these contributions, the scalar couplings are inevitably induced by the RGEs.

Feynman diagrams. If the initial values of those scalar couplings are positive, Λ_{LP} decreases because they increase the beta functions. In other words, we can obtain the conservative value of $\Lambda_{\rm LP}$ by setting them to be zero:

$$\lambda_X(v_h) = \lambda_X^{'}(v_h) = \cdots = 0. \tag{33}$$

In our calculations, we do not consider the negative initial values because such values might contradict the vacuum stability. The one-loop RGEs of these models are shown in Appendix A. Note that the contributions from the new scalar X are taken into account for $\mu \geq M_X$.

In Fig. 6, we present the conservative scale of the LP as a function of M_X for each of the models .[3] From the top to the bottom, the results with a quadruplet ($Y_X = 1/2, 3/2$), a quintet ($Y_X = 0, 1, 2$), a sextet ($Y_X = 1/2, 3/2, 5/2$), and septet ($Y_X = 0, 1, 2, 3$) are respectively shown, where a real scalar condition is assumed for a field with $Y_X = 0$. Here, the $n_X \leq 3$ cases are not shown because they do not hit the LP below the Planck scale. The solid lines in each plot represent the numerical results, while the dashed lines show the approximated results obtained from the analytic study as we will discussed in the following. From these plots, one can see that the LP appears well before the Planck scale for $n_X \geq 4$. Therefore, the scalar minimal dark matter models with $n_X \geq 4$ are forbidden by perturbativity.

In Table.3, we also show the fitted results of Λ_{LP} as a function of M_X. One can see that they typically behave as

$$\Lambda_{LP} \propto M_X^{1+\epsilon},\ \epsilon \ll 1 \tag{34}$$

which is consistent with the typical behavior as in Eq.(15). Here, the difference ϵ originates in the runnings of the gauge couplings: In our cases, we use the RGEs of the scalar extension models from M_X, but use the SM RGEs from v_h to M_X. As a result, the beta functions of the scalar couplings

[3]By requiring the tree-level unitarity of $SU(2)_L$ gauge interactions, $n_X \leq 8(9)$ is obtained for a complex (real) scalar multiplet [106, 107].

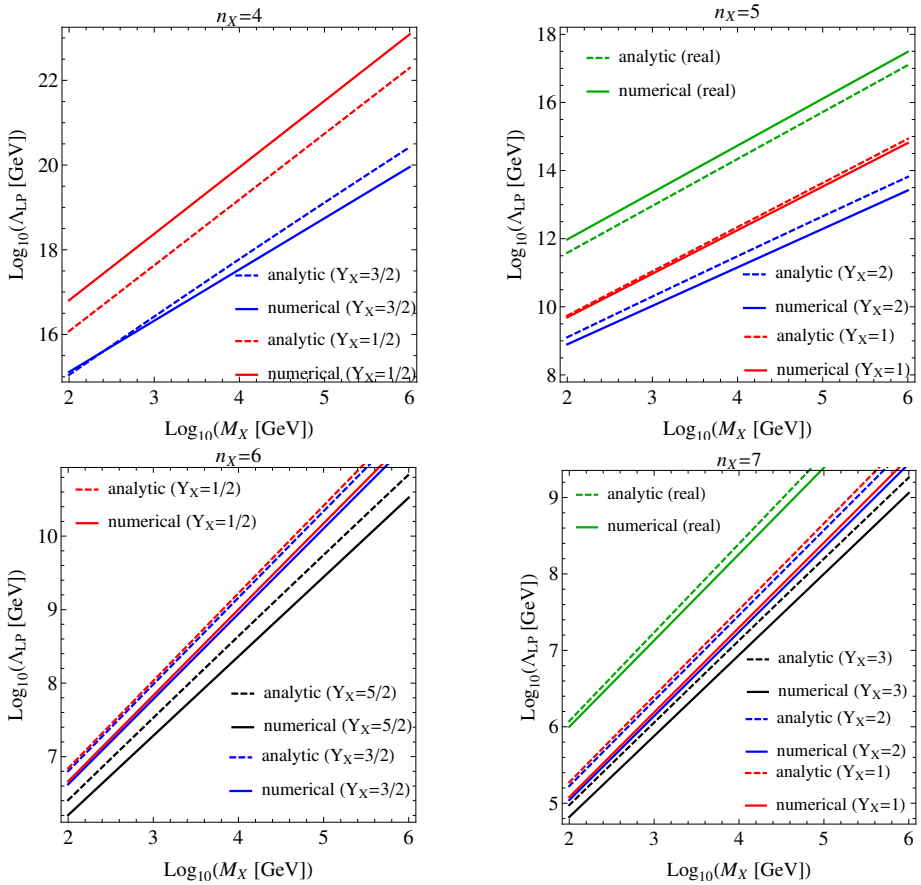

Figure 6: The solid and dashed lines correspond to the numerical results and the approximated results in Eq. (37).

at M_X slightly change when we change M_X because of the runnings of the gauge couplings from v_h to M_X.

Now, let us derive the analytical expression of Λ_{LP}. In the following we neglect the runnings of the gauge couplings, and treat them as constants. Then, by redefining the scalar couplings $\lambda'_X, \cdots$, we can obtain the favored RGEs such that g^4 terms only appear in one beta function. We call the new coupling constants $\lambda_X, \tilde{\lambda}'_X$, etc., among which only the beta function of λ_X contains g^4 term. Consequently, the RGEs are simplified as

$$\begin{aligned}\frac{d\lambda_X}{dt} &= \frac{1}{16\pi^2}(c_0 - c_1\lambda_X + c_2\lambda_X^2 + c_3\lambda_X\tilde{\lambda}'_X + c_4\tilde{\lambda}'^2_X),\\ \frac{d\tilde{\lambda}'_X}{dt} &= \frac{1}{16\pi^2}(-\tilde{c}'_1\lambda_X + \tilde{c}'_2\lambda_X^2 + \tilde{c}'_3\lambda_X\tilde{\lambda}'_X + \tilde{c}'_4\tilde{\lambda}'^2_X).\end{aligned} \tag{35}$$

(n_X, Y_X)	LP [GeV]	Λ_{g_Y} [GeV]	Λ_{g_2} [GeV]
$(4, 1/2)$	$6.4 \times 10^{16}\,(M_X/100\,\mathrm{GeV})^{1.57}$	1.2×10^{41}	–
$(4, 3/2)$	$1.3 \times 10^{15}\,(M_X/100\,\mathrm{GeV})^{1.21}$	3.1×10^{30}	–
$(5, \mathrm{real})$	$9.5 \times 10^{11}\,(M_X/100\,\mathrm{GeV})^{1.38}$	9.6×10^{42}	–
$(5, 1)$	$4.9 \times 10^{9}\,(M_X/100\,\mathrm{GeV})^{1.28}$	9.0×10^{34}	9.0×10^{488}
$(5, 2)$	$7.9 \times 10^{8}\,(M_X/100\,\mathrm{GeV})^{1.13}$	5.7×10^{22}	9.0×10^{488}
$(6, 1/2)$	$4.6 \times 10^{6}\,(M_X/100\,\mathrm{GeV})^{1.17}$	1.6×10^{40}	2.7×10^{32}
$(6, 3/2)$	$4.2 \times 10^{6}\,(M_X/100\,\mathrm{GeV})^{1.16}$	5.2×10^{26}	2.7×10^{32}
$(6, 5/2)$	$1.6 \times 10^{6}\,(M_X/100\,\mathrm{GeV})^{1.08}$	3.2×10^{16}	2.7×10^{32}
$(7, \mathrm{real})$	$1.0 \times 10^{6}\,(M_X/100\,\mathrm{GeV})^{1.13}$	9.6×10^{42}	1.3×10^{56}
$(7, 1)$	$1.2 \times 10^{5}\,(M_X/100\,\mathrm{GeV})^{1.11}$	3.6×10^{32}	1.4×10^{15}
$(7, 2)$	$1.1 \times 10^{5}\,(M_X/100\,\mathrm{GeV})^{1.10}$	2.2×10^{19}	1.4×10^{15}
$(7, 3)$	$6.6 \times 10^{4}\,(M_X/100\,\mathrm{GeV})^{1.06}$	1.2×10^{12}	1.4×10^{15}

Table 3: The fitted results of the scale of LPs with the initial condition Eq.(33). The positions of LP derived from one-loop beta function of the gauge couplings taking $M_X = 100\,\mathrm{GeV}$ are also given.

However, even if we set $\tilde{\lambda}'_X = 0$ at M_X, nonzero $\tilde{\lambda}'_X$ is induced by $\tilde{c}'_2$ term, which affects the running of λ_X through c_3 term.[4] Therefore, we redefine λ_X in order to cancel c_3 term. As a result, we have

$$\frac{d\tilde{\lambda}_X}{dt} = \frac{1}{16\pi^2}(\tilde{c}_0 - \tilde{c}_1\tilde{\lambda}_X + \tilde{c}_2\tilde{\lambda}_X^2), \tag{36}$$

taking $\tilde{\lambda}'_X = \cdots = 0$. This simplified differential equation can be solved analytically, and we obtain the analytical expression of Λ_{LP}:

$$\frac{\Lambda_{\mathrm{LP}}}{M_X} = \exp\left[\frac{16\pi^2}{\tilde{c}_2 d}\left\{\frac{\pi}{2} - \tan^{-1}\left[\frac{1}{d}\left(\tilde{\lambda}_X(M_X) - \frac{\tilde{c}_1}{2\tilde{c}_2}\right)\right]\right\}\right], \tag{37}$$

$$d = \sqrt{\frac{\tilde{c}_0}{\tilde{c}_2} - \frac{\tilde{c}_1^2}{4\tilde{c}_2^2}}. \tag{38}$$

The dashed lines in Fig.6 shows the approximated results by using Eq.(37), and they correctly reproduce the numerical results within order of magnitude.

In conclusion, we have shown that a new scalars which has $n_X \geq 4$ suffers from the LP bellow the Planck scale. As a result, the triplet real scalar remains as a DM candidate that is valid up to the Planck scale.

[4] We checked that the effect of c_4 term is smaller than that of c_3 term.

2.3 The Standard Model Criticality

In this subsection, we study the vacuum structure of the Higgs potential. In subsubsection 2.3.1, we briefly see the Higgs potential and its critical behavior in the SM. In subsubsection 2.3.2, we study the criticality in the minimal dark matter models. In particular, we just consider the triplet and quintet real fermions, and the triplet real scalar because they do not suffer the LP.

2.3.1 The criticality in the Standard Model

The one-loop effective potential of the SM Higgs is given by

$$V_{\rm eff}(\mu,\phi) = e^{4\Gamma(\mu)}\frac{\lambda(\mu)}{4}\phi^4 + V_{\rm 1loop}(\mu,\phi), \tag{39}$$

$$\begin{aligned} V_{\rm 1loop}(\mu,\phi) := e^{4\Gamma(\mu)}\Bigg\{ & -12\cdot\frac{M_t(\phi)^4}{64\pi^2}\left[\log\left(\frac{M_t(\phi)^2}{\mu^2}\right)-\frac{3}{2}+2\Gamma(\mu)\right] \\ & +6\cdot\frac{M_W(\phi)^4}{64\pi^2}\left[\log\left(\frac{M_W(\phi)^2}{\mu^2}\right)-\frac{5}{6}+2\Gamma(\mu)\right]+3\cdot\frac{M_Z(\phi)^4}{64\pi^2}\left[\log\left(\frac{M_Z(\phi)^2}{\mu^2}\right)-\frac{5}{6}+2\Gamma(\mu)\right]\Bigg\}, \end{aligned}$$

where

$$M_t(\phi) = \frac{y_t(\mu)}{\sqrt{2}}\phi \quad , \quad M_W(\phi) = \frac{g_2(\mu)}{2}\phi \ , \ M_Z(\phi) = \frac{\sqrt{g_2^2(\mu)+g_{\rm Y}^2(\mu)}}{2}\phi, \tag{40}$$

$$\Gamma(\mu) = \int_{M_t}^{\mu} d\ln\mu' \frac{1}{(4\pi)^2}\left(\frac{9}{4}g_2(\mu')^2+\frac{3}{4}g_Y(\mu')^2-3y_t(\mu')^2\right). \tag{41}$$

Here, μ is the renormalization scale, and all the running couplings are determined by Eqs.(16)-(21). From these equations, we can define the effective Higgs quartic coupling $\lambda_{\rm eff}(\mu)$ as

$$\begin{aligned} \lambda_{\rm eff}(\mu) &:= 4\frac{V_{\rm eff}(\mu,\mu)}{\phi^4} \\ &= \lambda(\mu) + \frac{e^{4\Gamma(\mu)}}{16\pi^2}\Bigg\{-3y_t(\mu)^4\left[\log\left(\frac{y_t(\mu)^2}{2}\right)-\frac{3}{2}+2\Gamma(\mu)\right] \\ &+\frac{3g_2(\mu)^4}{8}\left[\log\left(\frac{g_2(\mu)^2}{4}\right)-\frac{5}{6}+2\Gamma(\mu)\right]+\frac{(g_2(\mu)^2+g_Y(\mu))^2}{8}\left[\log\left(\frac{g_2(\mu)^2+g_Y(\mu)^2}{4}\right)-\frac{5}{6}+2\Gamma(\mu)\right]\Bigg\} \end{aligned} \tag{42}$$

where we have put $\mu=\phi$ in order to minimize the one-loop contributions. In the left panel in Fig.7, we numerically plot $\lambda_{\rm eff}(\mu)$. As for the initial values of the $\overline{\rm MS}$ SM couplings, we use the

results of [3]. Here, the blue band corresponds to the uncertainty of the pole mass of top quark [108]

$$M_t^{\rm pole} = 171.2 \pm 2.4 \text{ GeV}, \tag{43}$$

and the red contour corresponds to its center value. In the right panel, we also show the effective beta function

$$\beta_{\rm eff}(\mu) := \frac{d\lambda_{\rm eff}}{d\ln\mu}. \tag{44}$$

From these figures, one can see that both of them simultaneously approach zero around the Planck scale. In the potential language, this fact means that $V(\phi)$ and $dV(\phi)/d\phi$ simultaneously vanish around the Planck scale:

$$V(\phi) \sim 0,\ \frac{dV(\phi)}{d\phi} = \lambda_{\rm eff}(\mu)\phi^3 + \frac{1}{4}\beta_{\rm eff}(\mu)\phi^4 \sim 0. \tag{45}$$

We can actually satisfy Eq.(45) by tuning the top mass, and the corresponding Higgs potential is already shown in Fig. 2. Therefore, we can now conclude that *the Higgs potential in the SM can have another degenerate vacuum around the Planck scale.* [5]. In the next subsubsection, we examine whether this criticality holds in the minimal dark matter models.

2.3.2 The criticality in Minimal Dark Matter Models

Let us now study the Higgs potential in the minimal dark matter models. As mentioned before, it is sufficient to consider the triplet and quintet real fermions and the triplet real scalar because they do not suffer the LP. As well as the previous subsubsection, we use the effective Higgs self coupling $\lambda_{\rm eff}$ and its beta function $\beta_{\lambda_{\rm eff}}$ defined from the one-loop effective Higgs potential $V_{\rm eff}(\phi)$. Furthermore, we denote another degenerate vacuum as $\Lambda_{\rm MPP}$. Note that we regard the top mass M_t as a free parameter, and the Higgs mass is varied within [111]

$$M_h = 125.09 \pm 0.32\text{GeV}. \tag{47}$$

First, we consider a new fermion. For $n_\chi = 3$ and 5, the mass M_χ is determined by the thermal relic abundance [17, 18]:

$$M_\chi \simeq \begin{cases} 2.8 \text{ TeV} & (\text{for } n_\chi = 3), \\ 10 \text{ TeV} & (\text{for } n_\chi = 5). \end{cases} \tag{48}$$

[5] On the other hand, the recent analyses by ATLAS and CMS are

$$M_t = 173.34 \pm 0.76\text{GeV [109]}, \text{ and } M_t = 172.38 \pm 0.10 \pm 0.65\text{GeV [110]} \tag{46}$$

which are larger than the critical value. However, these values are measured by Monte Carlo simulation, and it is not so clear how we relate these values to $\overline{\rm MS}$ parameters. Therefore, we use Eq.(43) in this thesis.

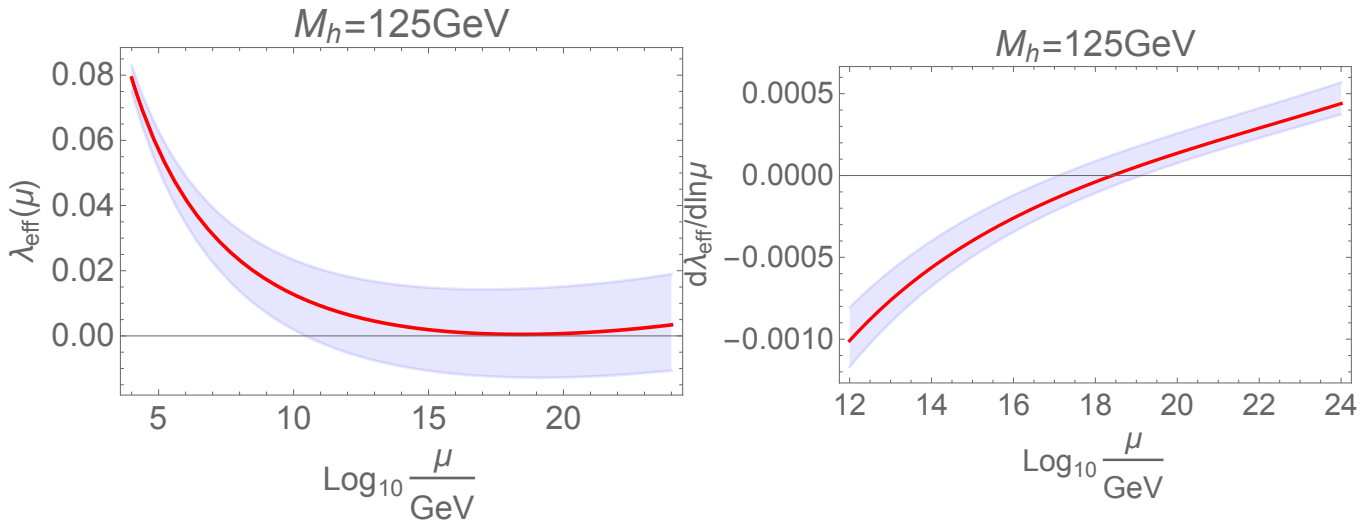

Figure 7: Left (Right): The running of the effective Higgs quartic coupling (beta function) $\lambda_{\rm eff}(\mu)$ ($\beta_{\rm eff}(\mu) := \frac{d\lambda_{\rm eff}}{d\ln\mu}$) is shown. Here, the blue band corresponds to the uncertainty of the pole mass of top quark Eq.(43).

As a result, M_t and $\Lambda_{\rm MPP}$ can be uniquely predicted by the criticality

$$V(\Lambda_{\rm MPP}) = \left.\frac{dV(\phi)}{d\phi}\right|_{\phi=\Lambda_{\rm MPP}} = 0, \tag{49}$$

because there is no additional free parameter. The numerical results are

$$\begin{aligned} &171.7\mathrm{GeV} \le M_t \le 172.0\mathrm{GeV}\ ,\ \ 2.5\times10^{16}\mathrm{GeV} \le \Lambda_{\rm MPP} \le 3.2\times10^{16}\mathrm{GeV}\ \ (\text{for } n_\chi = 3),\\ &174.8\mathrm{GeV} \le M_t \le 175.2\mathrm{GeV}\ ,\ \ 1.1\times10^{11}\mathrm{GeV} \le \Lambda_{\rm MPP} \le 1.2\times10^{11}\mathrm{GeV}\ \ (\text{for } n_\chi = 5), \end{aligned} \tag{50}$$

depending on $124.77\mathrm{GeV} \le M_h \le 125.41\mathrm{GeV}$.

In Fig. 8 (9), we present our analysis for the triplet (quintet) fermion case. Here, the upper panel shows the runnings of the SM parameters where $M_h = 125.09\mathrm{GeV}$, and M_t is correspondingly fixed so that the degeneration of vacua is realized. Note that we also show the SM running of g_2 by the dashed green line for comparison. Furthermore, in the lower panels, we show the corresponding $\lambda_{\rm eff}$ (left) and $V_{\rm eff}(\phi)$ (right). In these figures, the one-loop results are also shown. One can actually see that the potential and its derivative simultaneously become zero at a high energy scale. In particular, only the triplet can have the other vacuum near the Planck/String scale. We note that the two-loop effects are small.

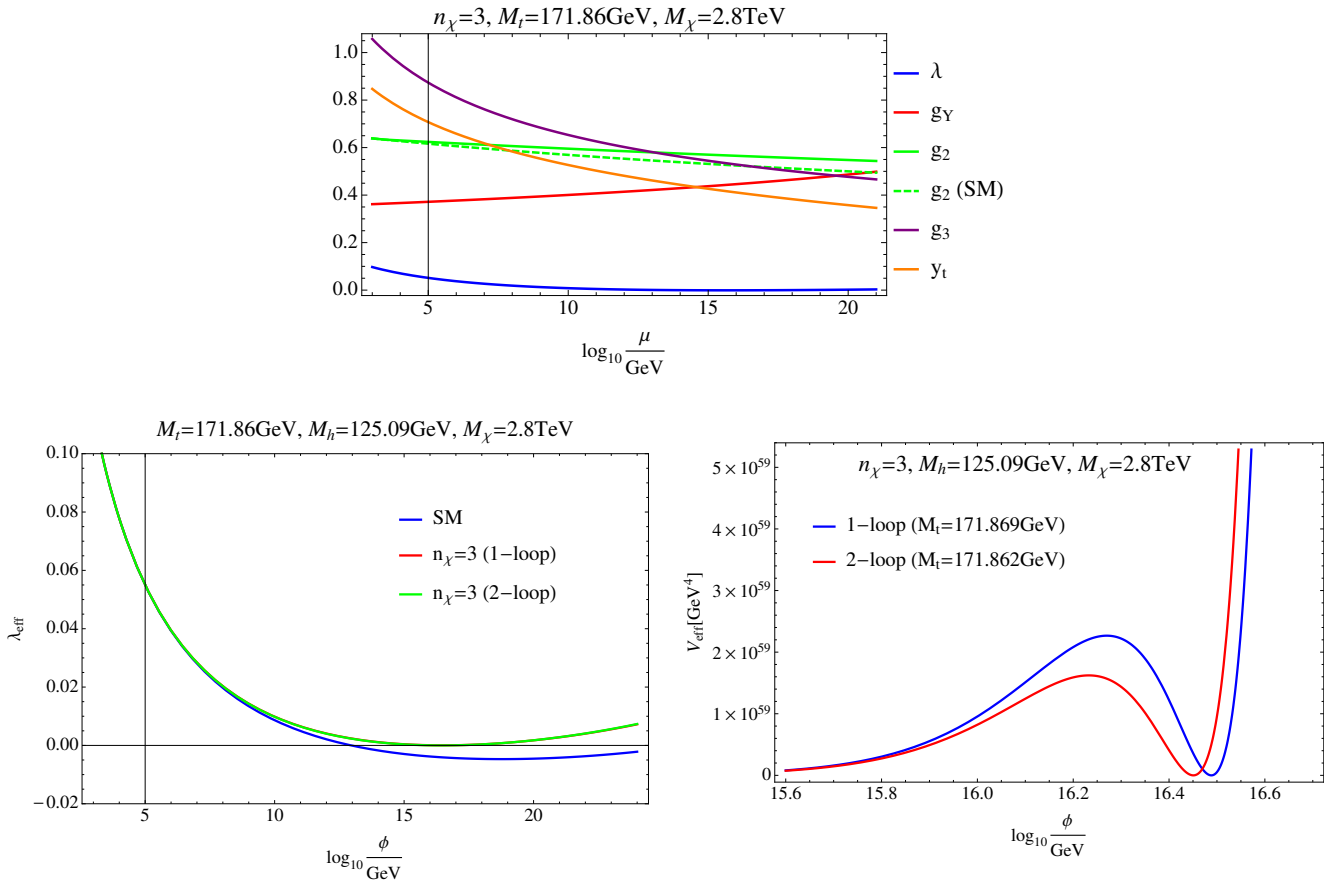

Figure 8: The analyses for the triplet Majorana fermion. Upper: The runnings of the SM couplings are shown. Here, the dashed green lines represent the SM running of g_2. Lower: The running of the effective Higgs self coupling λ_{eff} (left) and the one-loop effective Higgs potential $V_{\text{eff}}(\phi)$ (right).

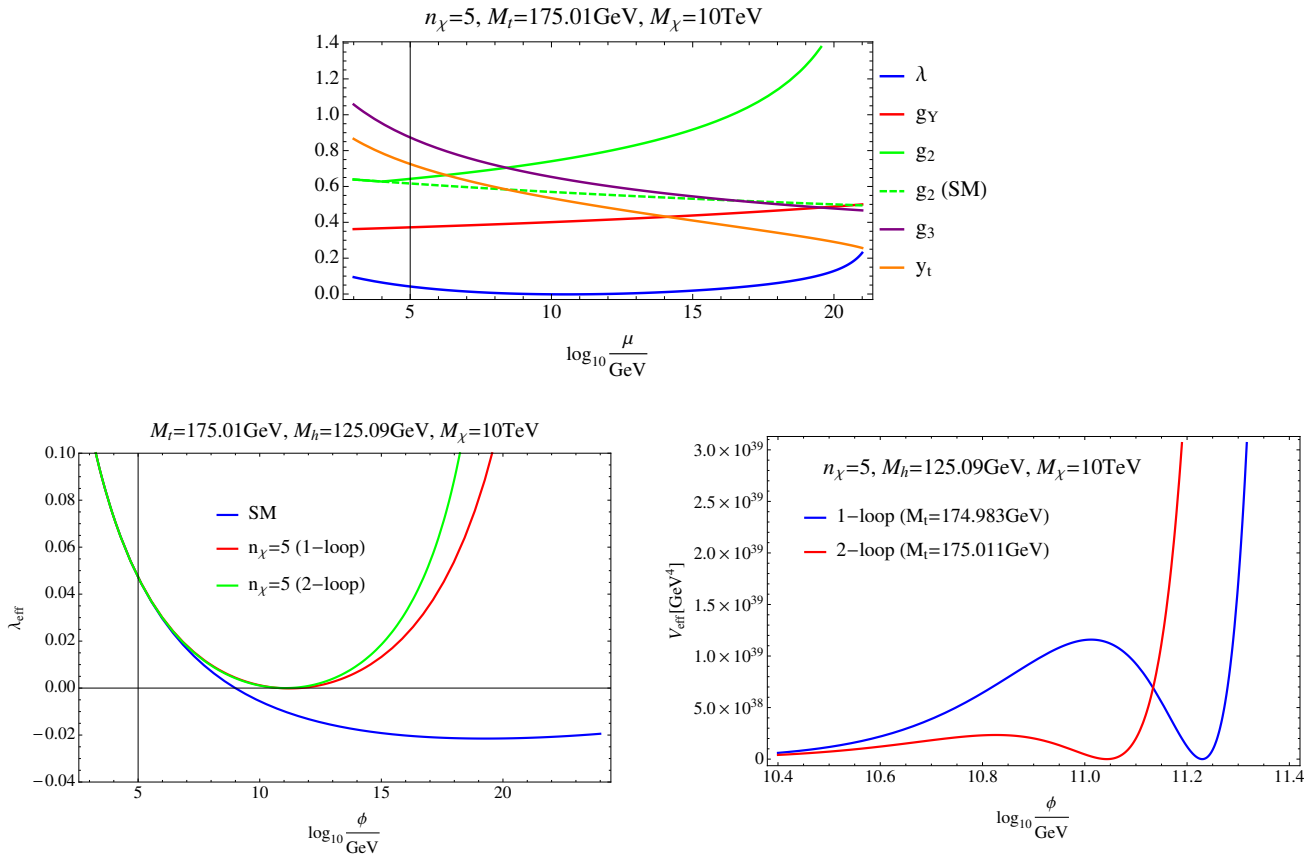

Figure 9: The analyses for the quintet Majorana fermion. Upper: The runnings of the SM couplings are shown. Here, the dashed green lines represent the SM running of g_2. Lower: The running of the effective Higgs self coupling λ_{eff} (left) and the one-loop effective Higgs potential $V_{\text{eff}}(\phi)$ (right).

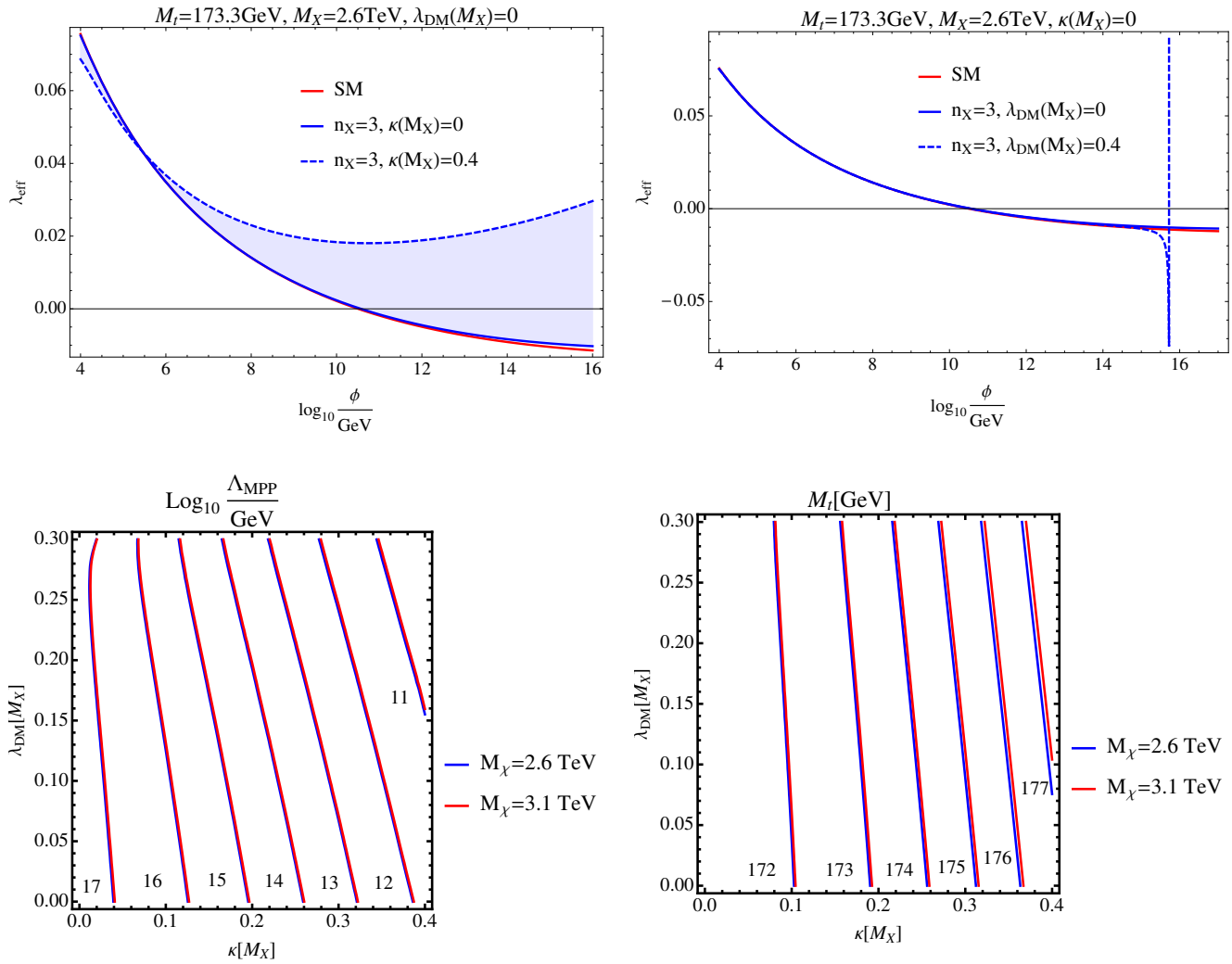

Figure 10: The analyses for the triplet real scalar. Upper: The running of $\lambda_{\rm eff}$ is shown. Here, the blue band of the left panel corresponds to the change of κ at $\mu = M_X$ from 0 to 0.4. Lower: $\Lambda_{\rm MPP}$ (left) and M_t (right) as a function of κ and λ_{DM} at $\mu = M_X$ are shown. The blue (red) contours correspond to $M_X = 2.6$ (3.1) TeV.

Now let us consider the triplet real scalar. In this case, the scalar potential is

$$V = -\frac{M_h^2}{2} H^\dagger H + \frac{M_{\rm DM}^2}{2} XX + \lambda \left(H^\dagger H\right)^2 + \lambda_{DM} \left(XX\right)^2 + \kappa \left(H^\dagger H\right) \left(XX\right). \tag{51}$$

Here, H is the SM Higgs doublet. The one-loop RGEs which are different from those of the SM are as follows :

$$\frac{dg_2}{dt} = -\frac{g_2^3}{(4\pi)^2} \frac{17}{6}, \tag{52}$$

$$\frac{d\lambda}{dt} = \frac{1}{16\pi^2} \left(\lambda \left(24\lambda - 9g_2^2 - 3g_Y^2 + 12y_t^2\right) + \frac{3}{2}\kappa^2 + \frac{3}{4} g_Y^2 g_2^2 + \frac{9}{8} g_2^4 + \frac{3}{8} g_Y^4 - 6y_t^4 \right), \tag{53}$$

$$\frac{d\lambda_{DM}}{dt} = \frac{1}{16\pi^2} \left(22\lambda_{DM}^2 + 2\kappa^2 - 24 g_2^2 \lambda_{DM} + 12 g_2^4\right), \tag{54}$$

$$\frac{d\kappa}{dt} = \frac{1}{16\pi^2} \left(4\kappa^2 + 12\kappa\lambda + 10\kappa\lambda_{DM} + 6y_t^2\kappa - \frac{33}{2} g_2^2 \kappa - \frac{3}{2} g_Y^2 \kappa + 6 g_2^4 \right). \tag{55}$$

Furthermore, there is an additional contribution to $V_{\rm eff}(\phi)$:

$$\Delta V_{\rm 1loop}(\phi) = \frac{3 m_{DM}(\phi)^4}{64\pi^2} \left(\ln \left(\frac{m_{DM}(\phi)^2}{\phi^2} \right) - \frac{3}{2} \right), \tag{56}$$

where

$$m_{DM}(\phi) = \sqrt{M_{\rm DM}^2 + \kappa(\phi) e^{2\Gamma(\phi)} \phi^2}. \tag{57}$$

In this case, the thermal abundance of X also depends on κ. Here we use

$$M_X = 2.6 \ \text{TeV and } 3.1 \ \text{TeV} \tag{58}$$

for our calculation [6]. $M_X = 2.6$ TeV and $M_X = 3.1$ TeV correspond to $\kappa = 0$ and $\kappa = 1$, respectively [18]. The upper panels of Fig.10 show the runnings of $\lambda_{\rm eff}$ when $M_X = 2.6$ TeV. Here, the blue band of the left panel corresponds to the change of κ at $\mu = M_X$ from 0 to 0.4. In the case of $\lambda_{DM}(M_X) = 0.4$ of the right panel, the rapid increase of $\lambda_{\rm eff}$ around 10^{16} GeV is due to the Landau pole of λ_{DM}. Namely, λ_{DM} becomes infinity below M_{pl}. The lower left (right) panel of Fig.3 shows the contour plot of $\Lambda_{\rm MPP}$ (M_t) as a function of λ_{DM} and κ at $\mu = M_X$. The blue (red) contours correspond to $M_X = 2.6$ (3.1) TeV. One can see that $\Lambda_{\rm MPP}$ is close to the Planck/String scale when $\kappa(M_X) \lesssim 0.1$ and $M_t \lesssim 172$GeV.

[6]The mass of a new scalar, of course, suffers from fine-tuning problem. However, we simply take Eq.(58) as the dark matter mass because our motivation is to distinguish the minimal dark matter models in the context of the SM criticality.

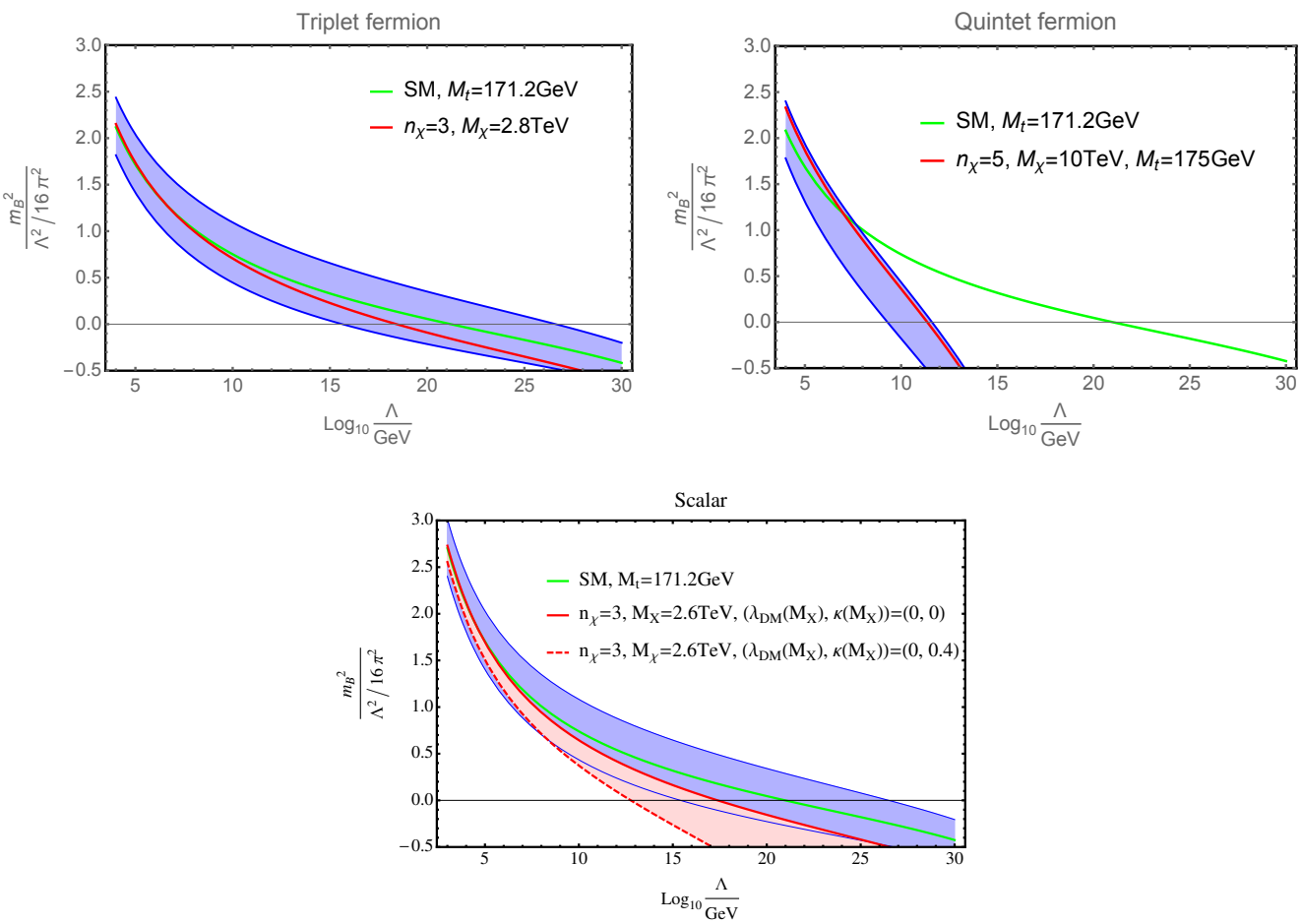

Figure 11: The bare Higgs mass $\frac{m_B^2}{16\pi^2\Lambda^2}$ as a function of a cut-off scale Λ. Upper left (right) shows the triplet (quintet) fermion case, and lower corresponds to the triplet scalar. Here the blue bands (red band) correspond(s) to the 2σ deviation from $M_t = 171.2$ GeV (the change of κ at $\mu = M_X$ from 0 to 0.4).

□ **Bare Higgs mass**

So far, we have not seriously considered the Higgs mass term at a high energy scale. However, from the point of view of the Planck/String scale physics, it is quite important because it quadratically diverges as a function of cutoff scale Λ. Therefore, it is meaningful to consider how the existence of a new particle changes the behavior of the bare Higgs mass m_B as a function of Λ [7]. In particular, the vanishing bare mass is so-called Veltman condition [112], and it suggests a new symmetry such as supersymmetry at the cutoff Λ. Of course, from the point of view of low energy physics, such a vanishing just seems to be accidental and to require fine-tuning at the Planck scale. Investigating the reason is beyond the scope of this section, but we hope that $m_B^2 = 0$ comes from some mechanism related to the physics at the Planck scale [31].

Now let us examine m_B as a function of Λ. See [6] for the evaluation of m_B in the SM. Here, let us focus on the triplet and quintet fermions, and the triplet real scalar at one-loop level. For the fermions, m_B is given by

$$\frac{m_B^2|_{\text{1-loop}}}{\Lambda^2/16\pi^2} = -\left(6\lambda + \frac{3}{4}g_Y^2 + \frac{9}{4}g_2^2 - 6y_t^2\right), \tag{59}$$

where the couplings are evaluated at $\mu = \Lambda$. On the other hand, for the triplet real scalar, $m_B^2|_{\text{1-loop}}$ becomes

$$\frac{m_B^2|_{\text{1-loop}}}{\Lambda^2/16\pi^2} = -\left(6\lambda + \frac{3}{4}g_Y^2 + \frac{9}{4}g_2^2 - 6y_t^2 + \frac{3}{2}\kappa\right). \tag{60}$$

The upper left (right) panel of Fig.11 shows m_B as a function of Λ when a new particle is the triplet (quintet) Majorana fermion. Here, the green contour is the SM prediction when $M_t = 171.2$ GeV, and the blue band corresponds to the 2σ deviation from it [108]:

$$M_t = 171.2 \pm 4.8 \ \text{GeV} \quad (95\%\text{CL}). \tag{61}$$

In the lower panel, we show m_B in the case of the triplet real scalar. Here, we change κ at $\mu = M_X$ from 0 to 0.4, and they are represented by a red band. Depending on the values of M_t and κ, one can see that the scale at which m_B becomes zero quite changes. One can see that m_B can take zero around Gut or string scale [8] in both of the triplet cases while the quintet case gives

[7] Within field theory, the quadratic divergence does not appear after the renormalization. However, it can have the physical meaning if we consider the scale around the Planck/string one, because, in principle, such a mass term can be calculable from more fundamental theory such as string scale. In this paper, we assume that the physics around the Planck scale is described by string theory, which is the cutoff theory whose universal cutoff scale is given by the string scale. This is why we take the universal cutoff in the calculation of m_B^2. See [6] for the detail.

[8] In order to obtain the correct electroweak symmetry breaking, we need to add small negative mass term to the Higgs potential, which is much small than Λ^2. However, in the case of the $SU(2)_L$ triplet scalar, it may be possible to realize the electroweak symmetry breaking by the Coleman-Weinberg mechanism. See Appendix D in [26] for the details.

slightly lower vanishing scale $\sim 10^{13}$GeV due to the rapid running of the gauge coupling g_2. In addition to the vanishing λ at around the Planck/String scale, this fact may suggest that the bare mass also vanishes around that scale, and it might be an indication of a new symmetry such as supersymmetry at the Planck/String scale.

3 Leptogenesis

In this section, we discuss the baryon (lepton) asymmetry of the universe, and study how it can be generated in the thermal history of the universe. In subsection 3.1, we briefly summarize the theoretical foundations of leptogenesis and ordinary thermal leptogenesis scenario. Readers who are familiar to this topic can skip this subsection. In subsection 3.2, we propose a new leptogenesis scenario at the reheating era by assuming the existence of a heavy inflaton.

3.1 Theoretical foundations and ordinary thermal leptogenesis

Before studying our new scenario, let us briefly summarize the ordinary thermal leptogenesis scenario in addition to some theoretical foundations. See [48] for the detail analyses.

In order to generate the baryon or lepton asymmetry, we must satisfy the following three condition (Sakharov's Conditions) simultaneously in some stage of the history of the universe:

Sakharov's three Conditions

- *Existence of baryon (lepton) number violating interaction*
- *Violation of C and CP*
- *Departure from thermal equilibrium*

The first one is obvious because we cannot have asymmetry if all interactions of a theory conserve lepton (baryon) number. The second one is a little non-trivial. As an example, let us consider a typical lepton-number violating process

$$X + Y \to Z + W, \tag{62}$$

where X, Y, Z and W represent some particles having lepton (baryon) number. We denote the change of the lepton (baryon) number by $\Delta L(B)$ in this process. By considering the charge conjugation of this interaction, we have

$$X^C + Y^C \to Z^C + W^C, \tag{63}$$

where the lepton (baryon) number changes by $-\Delta L(B)$. Thus, if a theory is completely C-invariant, these two interactions occurs at the same reaction rate, and the asymmetry never appears. This also applies to CP transformation. We can also understand the third reason from Eq.(62): If a system is thermal equilibrium, the inverse process $X + Y \leftarrow Z + W$ also has the same reaction rate, and both of them cancel each other. We can also show this conclusion in more sophisticated manner: Let $\hat{H}$ a Hamiltonian of a system, and $\hat{B}$ the number operator of baryons.Then,

$$\begin{aligned}\langle \hat{B} \rangle :&= \mathrm{Tr}\left(e^{-\beta \hat{H}} \hat{B}\right) \\ &= \mathrm{Tr}\left(e^{-\beta \hat{H}} (CPT)(CPT)^{-1} \hat{B} (CPT)(CPT)^{-1}\right) \\ &= \mathrm{Tr}\left(e^{-\beta \hat{H}} (CPT)^{-1} \hat{B} (CPT)\right) = -\langle \hat{B} \rangle, \ \therefore \ \langle \hat{B} \rangle = 0, \end{aligned} \tag{64}$$

where we have assume that $\hat{H}$ is invariant by the CPT transformation. In the SM without right handed neutrinos, these conditions can be theoretically satisfied: (i) The baryon or lepton number violation process is given by the Sphaleron process (ii) The SM is a chiral gauge theory, so C is apparently violated, and the violation of CP is given by the CKM phase (iii) The universe can be out of equilibrium if the electroweak phase transition becomes first order. In order to realize it, the Higgs mass must be $M_h \lesssim 80$GeV. However, we already know that M_h is 125GeV, so the baryogengesis in the SM is unfortunately impossible, and we must consider new mechanism.

Among various possibilities [41, 42, 43, 44, 45, 46, 47, 48], the thermal leptogenesis [43, 48] in the SM with heavy Majorana neutrinos attracts much attention because of its simplicity and phenomenological aspects related with neutrino sector. The Lagrangian of the leptonic sector is given by

$$\mathcal{L}_{lep} = \bar{L}_j i \not{D} L_j + \bar{e}_{Rj} i \not{D} l_{Rj} + \bar{N}_{Rj} i \not{\partial} N_{Rj} - \frac{1}{2} M_{Rij} \bar{N}^C_{Ri} N_{Rj} + y_{lij} \bar{e}_{Rj} (L_j)_a H^{\dagger a} + y_{\nu ij} \bar{N}_{Rj} (L_j)_a H_b \epsilon^{ab} + \text{h.c}, \tag{65}$$

where $i, j = 1, 2, 3$ are the family-number indices, and $a, b = 1, 2$ represent the indices of the fundamental representation of $SU(2)_L$. In the following, we choose a basis in which M_{Rij} and y_{lij} are simultaneously diagonalized. In this basis, $y_{\nu ij}$ is complex, and contains six CP-phases [9]. (Three phases can be absorbed into L_i's.) Note that the sixth term in Eq.(65) violates the lepton number because N_R has zero lepton number, while L_i has one. In this model, the lepton

[9] In low-energy picture, the effective Lagrangian of the lepton sector is

$$\mathcal{L}_{\text{eff}} = \bar{l}_{Lj} i \not{D} l_{Lj} + \bar{e}_{Rj} i \not{D} l_{Rj} + y_{lij} \bar{e}_{Rj} (l_{Lj})_a H^{\dagger a} + \frac{y^T_{\nu ik} y_{\nu kj}}{M_{Rk}} (l_{Li})_a (l_{Lj})_c H_b H_d \epsilon^{ab} \epsilon^{cd} + \text{h.c.} \tag{66}$$

Thus, the coupling between Higgs and lepton is given by the symmetric one $y^T_{\nu ik} y_{\nu kj} / M_{Rk}$, and it contains three CP-phases among the original six CP-phases. It is difficult to relate these phases [48].

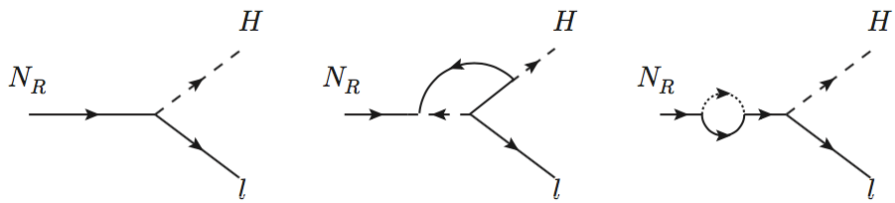

Figure 12: The decay of heavy Majorana neutrino. The left figure shows the tree level diagram, and the middle and right figures show the one loop level diagrams. We must take all of them into consideration for the calculation of the decay rate $\Gamma(N \to L(\bar{L})H(\bar{H}))$. As a result, we can obtain a small difference between $\Gamma(N \to LH)$ and $\Gamma(N \to \bar{L}\bar{H})$.

asymmetry is generated as follows: At the early stage of the universe where $T \gg M_{Ri}$, all the particles are thermal equilibrium. However, when T becomes around M_R, the Majorana neutrinos decouple from the thermal bath, and they start to decay into the SM leptons and Higgs through the sixth term in Eq.(65). Here, the above mentioned CP phases have no effect on this decay process at tree level, however, they actually contribute if we also consider one-loop diagram. See Fig.12 for example. As a result, the lepton asymmetry appears by the decay of right handed neutrinos. Finally, this lepton asymmetry is converted to baryons through the Sphaleron process. In the case that the heavy Majorana masses are hierarchical, $M_{R2,3} \gg M_{R1}$, the amount of baryon asymmetry can be estimated as [43, 48]

$$\eta_B = -d \times \epsilon_1 \times \kappa_f, \tag{67}$$

where $d \sim 10^{-2}$ is just a numerical factor determined by the Sphaleron process and the photon productions between leptogenesis era and the recombination,

$$\epsilon_1 := \frac{\Gamma(N_1 \to L + H) - \Gamma(N_1 \to \bar{L} + \bar{H})}{\Gamma(N_1 \to L + H) + \Gamma(N_1 \to \bar{L} + \bar{H})} \simeq \frac{1}{16\pi^2 (y_\nu y_\nu^\dagger)_{11}} \sum_i \frac{M_{R1}}{M_{Ri}} \mathrm{Im}\left((y_\nu y_\nu^\dagger)_{i1}\right) \tag{68}$$

is the CP asymmetry factor, and κ_f is called the *efficiency factor* which does not depend on the CP asymmetry, but contains the information of scattering and decaying processes. Therefore, in order to determine it, we must solve the Boltzmann equations. Following the detail analyses [113, 48], we can obtain enough baryon asymmetry for wide range of values of M_{R1}:

$$\mathcal{O}(10^9\mathrm{GeV}) \lesssim M_{R1} \lesssim \mathcal{O}(10^{16}\mathrm{GeV}), \tag{69}$$

from which we can roughly obtain the lower bound of the reheating temperature

$$\mathcal{O}(10^9\mathrm{GeV}) \lesssim M_{R1} \lesssim T_R. \tag{70}$$

However, under the assumption of the usual seesaw mechanism, M_{R1} should be larger than $\mathcal{O}(10^{15})$GeV, and it is usually difficult to obtain such a high reheating temperature. In the following subsection, we propose a new leptogenesis scenario in order to overcome this problem.

3.2 Leptogenesis at the reheating era

Let us now propose a new leptogenesis scenario at the reheating era. In addition to the SM particles, we assume the existence of a heavy inflaton ϕ which can decay into the SM particles. Note that we do not need specific information of the inflaton potential because our discussion concentrates on the reheating era after the inflation. In general, the decay of the inflaton can also have an origin of CP-violation, however, we first assume that there is no CP-violation and asymmetry in the inflaton sector. In this case, we can attribute the origin of CP violation to the higher dimensional operators in the SM. (See Eq.(71).) We call this contribution *the first contribution*. On the other hand, we call the contribution originated in the inflaton decay *the secound contribution*. We will discuss the secound contribution after examining the first contribution.

□ **<u>First contribution</u> (There is no CP violation in inflaton decay)**
We consider the effective Lagrangian of the SM with dimension 5 and 6 operators [117]:

$$\mathcal{L}_{\rm eff} = \mathcal{L}_{\rm SM} + \frac{1}{\Lambda_1}\lambda_{1,ij}(L_i)_a(L_j)_c H_b H_d \epsilon^{ab}\epsilon^{cd} + \frac{1}{\Lambda_2^2}\lambda_{2,ijkl}(\bar{L}_i\gamma^\mu L_j)(\bar{L}_k\gamma_\mu L_l) + \text{h.c.} \tag{71}$$

where the second term corresponds to the fourth term in Eq.(66). Here, we do not assume a specific model, and treat the couplings $\lambda_{1,ij}/\Lambda_1$, $\lambda_{2,ijkl}//\Lambda_2^2$ as free parameters. In this sense, our discussion is model independent. Of course, we can always discuss leptogenesis in a specific model by rewriting $\lambda_{1,ij}/\Lambda_1$ and $\lambda_{2,ijkl}//\Lambda_2^2$ as functions of the couplings of the model. See [52] for example. Note that the above effective picture is valid when the mass of a new particle is smaller than the reheating temperature T_R. Before going into detail calculations, let us here give a qualitative explanation of our scenario:

1. From the end of the inflation, the inflaton starts to decay into the SM particles. These particles are highly relativistic, but not yet thermalized. Therefore, the scatterings of these particles are inevitably out of equilibrium, which corresponds to one of the Sakharov's conditions. Note that the thermalization process also occurs simultaneously.

2. Among the various scatterings, the processes $LL \to HH$ and $\bar{L}\bar{L} \to \bar{H}\bar{H}$ through the second and third terms in Eq.(71) violate the lepton number and CP symmetry. In particular, the

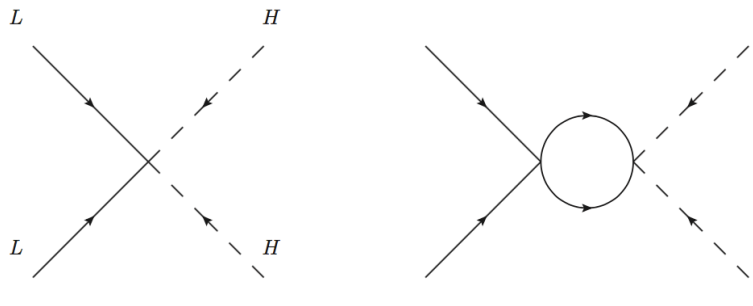

Figure 13: Tree (left) and one-loop (right) Feynman diagrams that violate the lepton numbers. The one-loop diagram depends on $\lambda_{2,ijkl}$ that contains CP phases.

CP phases comes from $\lambda_{2,ijkl}$ which exits in one-loop diagram. See Fig.13 and the following discussion for the details.

3. After the completion of the reheating, the lepton number is fixed, and it is converted to the baryon number by the Sphaleron process:

$$n_B = \frac{28}{79} n_{-L} \tag{72}$$

We summarize the derivation of this equality in Appendix B.

Let us now evaluate the amount of the lepton asymmetry. We first show the result:

$$\eta_B \sim \frac{n_{\rm inf}}{s} \times \sum_i \epsilon_i {\rm Br}_i \times \frac{\Gamma_{\not{L}}}{\Gamma_{\rm brem}} \bigg|_{T=T_R} \tag{73}$$

The meaning of each of the factors is as follows: $n_{\rm inf}$ is the number density of the inflaton which can be solved as a function of T_R by equating the energy density of the inflaton $m_{\rm inf} n_{\rm inf}$ with that of the radiation $3sT/4$ when the reheating is completed:

$$\frac{n_{\rm inf}}{s} \simeq \frac{3}{4} \frac{T_R}{m_{\rm inf}}. \tag{74}$$

ϵ_i represents the efficiency

$$\epsilon_i := 2\, \frac{\sigma_{\bar{L}_i \bar{L}_i \to HH} - \sigma_{L_i L_i \to \bar{H}\bar{H}}}{\sigma_{\bar{L}_i \bar{L}_i \to HH} + \sigma_{L_i L_i \to \bar{H}\bar{H}}}, \tag{75}$$

where σ represents the cross section of each of the processes. Note that the imaginary part of $\lambda_{2,ijkl}$ becomes relevant in ϵ_i due to the interference between the tree and one-loop diagrams. After the

straightforward calculation, we obtain

$$\epsilon_i \simeq \sum_j \frac{1}{2\pi} \frac{12 m_{\rm inf} T_R}{\Lambda_2^2} \frac{\lambda_{1,jj} {\rm Im}(\lambda_{2,ij})}{\lambda_{1,ii}}, \tag{76}$$

where $\lambda_{2,ij} := \lambda_{2,ijij}$, and Λ_1 dependence is canceled between the numerator and the denominator. ${\rm Br}_i$ denotes the branching ratio of the inflaton to $L_i \bar{L}_i$. Note that the lepton asymmetry vanishes in the case that ${\rm Br}_i$'s satisfy ${\rm Br}_1 = {\rm Br}_2 = {\rm Br}_3$ [10]. In the following, we simply assume ${\rm Br} := {\rm Br}_1 \neq 0,\ {\rm Br}_2 = {\rm Br}_3 = 0$ [11]. Finally, $\Gamma_{\not{L},i}$ represents the interaction rate of the lepton violation process,

$$\Gamma_{\not{L},i} = n_{\rm thermal} \langle \sigma v \rangle \simeq \frac{11}{4\pi^3} \zeta(3) \frac{m_{i,\nu}^2}{v^4} T_R^3, \tag{78}$$

where T_R^3 comes from the number density of the thermal plasma $n_{\rm thermal}$. On the other hand, $\Gamma_{\rm brems}$ is the interaction rate of the thermalization process without the lepton number violation,

$$\Gamma_{\rm brems} \sim \alpha_2^2 T_R \sqrt{\frac{T_R}{m_{\rm inf}}}. \tag{79}$$

Here, α_2 is the $SU(2)_L$ structure constant. If we naively estimate the bremsstrahlung diagram with t-channel gauge boson exchange, we have $\alpha_2^2 T_R$. However, because the emission process continues until their energy becomes comparable with thermal bath, the interference among the emission processes should be taken into account. This interference effect suppresses the thermalization process, which is represented by $\sqrt{T_R/m_{\rm inf}}$, and called Landau-Pomeranchuk-Migdal effect [118, 119, 120, 121]. The leptons produced by the inflaton experience both of the lepton-number violating process and the thermalization process, so if the latter is more rapid than the former, we can not obtain the enough lepton asymmetry. In this sense, $\Gamma_{\not{L}}/\Gamma_{\rm brems}$ corresponds to the probability that the lepton number violating process occurs during the time interval $\Delta t = 1/\Gamma_{\rm brems}$, which is the typical time scale the high energy leptons lose their energy. Note that this statement is valid if the Hubble parameter is sufficiently smaller than $\Gamma_{\rm brems}$. In this case, the high energy leptons mainly lose their energy by bremsstrahlung process. On the other hand, if the Hubble parameter is larger than the $\Gamma_{\rm brems}$, the leptons mainly lose their energies by the redshift, and the probability is given

[10] In this case, Eq.(73) is proportional to

$$\sum_{i,j} \lambda_{1,ii} \lambda_{1,jj} {\rm Im} \lambda_{2,ij} = \frac{1}{2} \sum_{i,j} \lambda_{1,ii} \lambda_{1,jj} \left(\lambda_{2,ijij} - \lambda_{2,ijij}^* \right). \tag{77}$$

However, by including the h.c term and redefining λ_2 in Eq.(71), we can show $\lambda_{2,ijij} = \lambda_{2,jiji}^*$. Thus, Eq.(77) vanishes.

[11] We also assume a vanishing branching ratio of the inflaton to HH for simplicity. It would be interesting to investigate our scenario with general decay modes.

by $\Gamma_{\not{L}}/H$. Our scenario corresponds to the former case because

$$\Gamma_{\rm brems}/H \sim \frac{\alpha_2^2 M_{pl}}{\sqrt{T_R m_{\rm inf}}} \gg 1, \tag{80}$$

is satisfied for typical values of parameters. (See Eq.(82)). Here, note that we have used Eq.(79) and

$$H \sim \frac{T_R^2}{\sqrt{3} M_{pl}}, \tag{81}$$

at the reheating. .

By substituting those quantities into Eq.(73), we obtain

$$\frac{n_B}{s} \simeq 8.7 \times 10^{-11} \left(\frac{4 \times 10^{-4}}{\alpha_2^2}\right) \left(\frac{m_{\rm inf}}{2 \times 10^{13}\,{\rm GeV}}\right)^{\frac{1}{2}} \left(\frac{T_R}{3 \times 10^{11}\,{\rm GeV}}\right)^{\frac{7}{2}} \times \left(\frac{m_\nu}{0.1\,{\rm eV}}\right)^2 \left(\frac{10^{15}\,{\rm GeV}}{\Lambda_2}\right)^2, \tag{82}$$

from which we can see that the observed baryon asymmetry can be successfully generated within reasonable values of the parameters. In particular, we can obtain enough asymmetry even if $T_R \ll 10^{15}$GeV, and this fact is a desirable feature to various inflation scenarios because it is usually difficult to obtain the high reheating temperature.

Here we comment on the possible washout effect. The interaction rate of the washout process is similar to Eq.(78):

$$\Gamma_{\rm wash} \simeq \frac{11}{4\pi^3} \zeta(3) \frac{\sum m_\nu^2}{v^4} T^3. \tag{83}$$

From this, one can conclude that the strong wash out is avoided if T_R is sufficiently small [12]. We emphasize that this washout process is collision between the particles in thermal plasma while Eq. (78) corresponds to the scattering between leptons in the thermal plasma and ones from inflaton decay.

In order to confirm the above estimation, let us now solve the following Boltzmann equations

[12] When the reheating is completed, the ratio $\Gamma_{\rm wash}/H$ is

$$\Gamma_{\rm wash}/H \sim \frac{T_R M_{pl}}{\Lambda_1^2}. \tag{84}$$

If we take $T_R = 3 \times 10^{11}$ GeV as a successful example, the ratio is small enough to ignore the washout effect. Note that this does not mean that the lepton number violation process does not occur. As clarified in footnote 5, since $\Gamma_{\rm brems} \gg H$, the asymmetry is roughly proportional to $\Gamma_{\not{L}}/\Gamma_{\rm brems}$, which can be large enough to realize the observed baryon asymmetry.

numerically: [13]

$$
\begin{aligned}
H^2 &= \frac{1}{3M_{pl}^2}\left(\rho_{\rm inf} + \frac{\pi^2 g_*}{30}T^4 + \frac{m_{\rm inf}}{2}n_l\right), \\
\dot{\rho}_R + 4H\rho_R &= (1-{\rm Br})\Gamma_{\rm inf}\,\rho_{\rm inf} + \frac{m_{\rm inf}}{2}n_l\left(\Gamma_{\rm brems} + H\right), \\
\dot{n}_L + 3Hn_L &= \Gamma_{\not{L}} 2\epsilon\, n_l - \Gamma_{\rm wash} n_L, \\
\dot{n}_l + 3Hn_l &= \frac{\Gamma_{\rm inf}\,\rho_{\rm inf}}{m_{\rm inf}}{\rm Br} - n_l(\Gamma_{\rm brems} + H), \\
\rho_{\rm inf} &= \Lambda_{\rm inf}^4\left(\frac{a(t=t_{\rm end})}{a}\right)^3 e^{-\Gamma_{\rm inf}t}.
\end{aligned}
\tag{85}
$$

Here, dot represents the derivative respect to time t, a is the scale factor, $H := \dot{a}/a$ is the Hubble expansion rate, $\rho_{\rm inf}$ is the energy density of the inflaton, g_* is the effective degrees of freedom of the SM, T is the temperature of radiation, $\rho_R = \pi^2 g_* T^4/30$ is the energy density of radiation, n_l is the number density of the left handed lepton produced by the decay of the inflaton, $\Gamma_{\rm inf}$ is the decay rate of the inflaton which is related to the reheating temperature as $T_R \sim \sqrt{M_{pl}\Gamma_{\rm inf}}$, $\Lambda_{\rm inf}^4$ is the energy density at the end of the inflation, $t_{\rm end}$ is the time when inflation ends. In Fig. 14, we show the contours which correspond to the observed baryon asymmetry Eq.(3) as functions of $m_{\rm inf}$ and T_R. Here, the solid and dashed contours correspond to $\Lambda_2 = 10^{14}\,{\rm GeV}$ and $\Lambda_2 = 10^{15}\,{\rm GeV}$ respectively, and the red and blue contours represent ${\rm Br} = 1$ and 0.1. From these plots, one can actually see that the analytical estimation Eq.(82) correctly produces the numerical values within an order of magnitude.

□ **<u>Second contribution</u> (CP violation originates in inflaton decay)**

Now let us consider the possibility that the CP violation originates in the inflaton decay. As a concrete example, we consider the following Lagrangian [14]:

$$
\mathcal{L}_{\rm eff} = \mathcal{L}_{\rm SM} + \frac{1}{\Lambda_1}\lambda_{1,ij}(L_i)_a(L_j)_c H_b H_d \epsilon^{ab}\epsilon^{cd} + \frac{1}{\Lambda_3^2}\lambda_{3,ijkl}(\bar{L}_i\gamma^\mu L_j)(\bar{E}_k\gamma_\mu E_l) + \frac{1}{M}y_{ij}\phi\bar{L}_i H E_j + {\rm h.c} - \frac{m_{\rm inf}^2}{2}\phi^2.
\tag{86}
$$

[13] We include the effect of redshift as last terms in the right hand side in the second and fourth equations. The leptons produced by the inflaton are highly relativistic, and lose their energy by thermalization process or redshift due to the cosmic expansion. Although the effect of redshift is not important in practice since $\Gamma_{\rm brems} > H$ for typical parameters, we include it for completeness.

[14] Another possibility is to consider the models where the inflaton has same charge as the SM Higgs field. Then, the inflaton can decay into right and left lepton pairs by dimension-4 operator, which can become main channel if we take $\mathcal{O}(1)$ coupling. Although such a coupling often threatens the flatness of inflaton potential, it is known that the inflation is possible by introducing non-minimal coupling between gravity and the inflaton sector [123, 37]. In this case, however, more careful study is needed because we must also consider the preheating of the Higgs field.

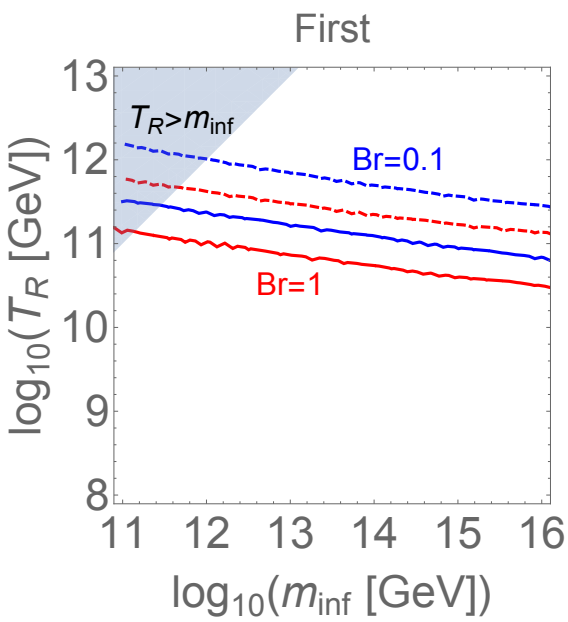

Figure 14: The contours where the first contribution (Eq.(85)) can explain the observed baryon asymmetry. Here we take $\Lambda_{\rm inf} = 10^{15}$GeV, $\sum_j \lambda_{1,jj}{\rm Im}(\lambda_{2,1j}) = 2$ and $m_\nu = 0.1\,$eV. Note that the normalization of a can be chosen freely, and we take $a(t = t_{\rm end}) = 1$. We numerically confirmed that the asymmetry is mainly produced at the time where the reheating is completed, $t \sim \Gamma_{\rm inf}^{-1}$. Therefore, the result is insensitive to $\Lambda_{\rm inf}$ as long as $T_R \lesssim \Lambda_{\rm inf}$. The solid and dashed lines correspond to $\Lambda_2 = 10^{14}\,$GeV and $\Lambda_2 = 10^{15}\,$GeV, respectively. The red and blue lines represent Br $= 1$ and 0.1. In the blue region, because $T_R > m_{\rm inf}$, we need more careful study of the reheating, which is beyond scope of this paper.

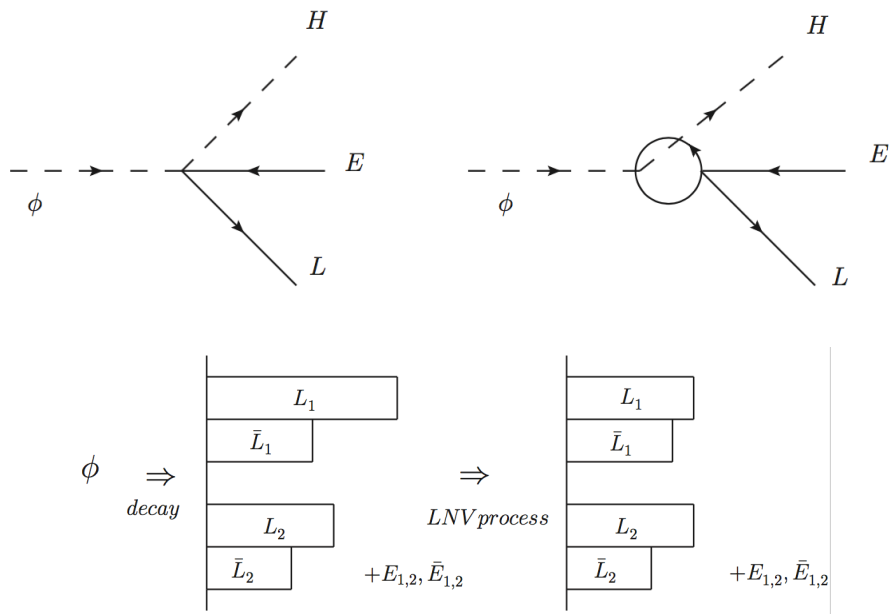

Figure 15: Upper: Tree (left) and one-loop (right) Feynman diagrams of the inflaton decay. The one-loop diagram depends on $\lambda_{3,ijkl}$ that contains CP phases. Lower: Schematic figure that represents the numbers of the left handed leptons produced by the inflaton. Because $\Gamma(\phi \to \bar{H} L_i \bar{E}_j)$ and $\Gamma(\phi \to H \bar{L}_i E_j)$ are different at one-loop level, we can have asymmetry between L_i and $\bar{L}_i$. (Note that the total lepton number produced by the inflaton is zero including the right handed leptons.) As long as $\lambda_{1,ii}$'s are different for each flavors, we obtain the lepton asymmetry. In this figure, we show two flavor case, and choose $\lambda_{1,22} = 0$ for simplicity.

where M is some scale, and we have assumed that the potential of ϕ is well approximated by its mass term. In the following argument, we choose such a basis that $\lambda_{1,ij}$'s are diagonal. Note that $\lambda_{3,ijkl}$ and y_{ij} are generally complex in this basis. Therefore, we can obtain an asymmetry between the left and right leptons by the decay of an inflaton See Fig. 15 for example. Here, we show the two flavor case for simplicity. In the upper panel, we show the tree (left) and one-loop (left) diagrams of the inflaton decay. In this process, the asymmetry between L_i's and E_i's appears, and this asymmetry can be also interpreted as the asymmetry between flavors.

Succeedingly, the lepton number is violated by the dimension-5 operator [15] because the only

[15]The second contribution is different from the leptogenesis by the inflaton decay [114, 115, 116] with the strong washout, in which heavy Majorana neutrinos, produced by the inflaton decay, give both of lepton number and CP violations. In this case, the lepton number violating SM scattering just decreases the total number of asymmetry. On the contrary, in our scenario, the decay of heavy inflatons only provides the CP violation, and the lepton

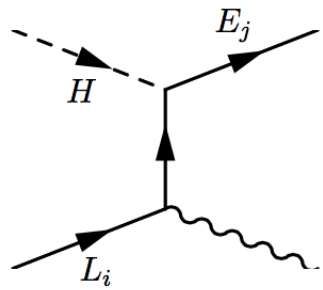

Figure 16: The washout process of lepton flavor asymmetry. If the interaction rate of this process is faster than that of the lepton number violation process, we can not obtain enough asymmetry.

left handed leptons feel lepton number violation. By assuming that $\lambda_{1,11}$ is larger than $\lambda_{1,22}$ and $\lambda_{1,33}$, the net lepton asymmetry is approximately given by

$$\frac{n_L}{s} \sim \frac{n_{\rm inf}}{s} \sum_{i=1,2,3} 2\epsilon_{1,i}\, {\rm Br}_{1i} \frac{\Gamma_{\not{L},1}}{\Gamma_{\rm LF}}, \tag{87}$$

where ${\rm Br}_{ij}$ is the branching ratio of the inflaton to $HL_i\bar{E}_j$, $\epsilon_{i,j}$ is

$$\begin{aligned} \epsilon_{i,j} &:= \frac{\Gamma(\phi \to \bar{H} L_i \bar{E}_j) - \Gamma(\phi \to H \bar{L}_i E_j)}{\Gamma_{\rm inf}} \\ &\simeq \frac{1}{8\pi} \frac{m_{\rm inf}^2}{\Lambda_3^2} \sum_{k,l} \frac{{\rm Im}(y_{ij}^* y_{kl} \lambda_{3,iklj})}{|y_{ij}|^2}, \end{aligned} \tag{88}$$

and $\Gamma_{\rm LF}$ is the interaction rate of the washout process of the asymmetry between the left and right leptons,

$$\Gamma_{\rm LF} \sim \alpha_2 \alpha_{y_l} T_R, \tag{89}$$

see also Fig. 16 . Here α_{y_l} is the structure constant of the charged lepton Yukawa. Then, we obtain

$$\begin{aligned} \frac{n_B}{s} \simeq & 8.7 \times 10^{-11} \left(\frac{2\times 10^{-2}}{\alpha_2}\right) \left(\frac{8\times 10^{-6}}{\alpha_{y_l}}\right) \left(\frac{m_{\rm inf}}{2\times 10^{13}\,{\rm GeV}}\right) \left(\frac{T_R}{4\times 10^{10}\,{\rm GeV}}\right)^3 \\ & \times \left(\frac{m_\nu}{0.1\,{\rm eV}}\right)^2 \left(\frac{10^{15}\,{\rm GeV}}{\Lambda_3}\right)^2 \left(\frac{\sum_{i=1,2,3} {\rm Br}_{1i}}{1}\right) \left(\frac{\sum {\rm Im}(y_{1i}^* y_{kl} \lambda_{3,1kli})/|y_{1i}|^2}{1}\right). \end{aligned} \tag{90}$$

asymmetry is produced by the scattering between these SM particles.

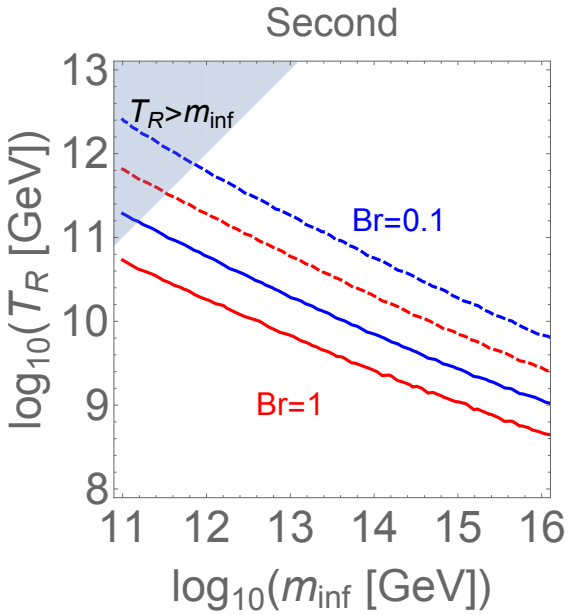

Figure 17: The contours where the second contribution (Eq.(85)) can explain the observed baryon asymmetry. Here we take $\Lambda_{\rm inf} = 10^{15}$GeV, $\sum {\rm Im}(y^*_{1i} y_{kl} \lambda_{2,1ikl})/|y_{1i}|^2 = 1$ and assume $\lambda^2_{1,11} \gg \lambda^2_{1,22}, \lambda^2_{1,33}$. The solid and dashed lines correspond to $\Lambda_2 = 10^{14}$ GeV and $\Lambda_2 = 10^{15}$ GeV, respectively. The red and blue lines represent Br = 1 and 0.1. In the blue region, because $T_R > m_{\rm inf}$, we need more careful study of the reheating, which is beyond scope of this paper.

In this case, the Boltzmann equations are the same as Eq. (85) except for the third line. Instead of it, we have

$$\dot{n}_L + 3Hn_L = -\sum_j 2\Gamma_{\not{L},j} n_{Lj} - \Gamma_{\rm wash} n_L, \tag{91}$$

$$\dot{n}_{L1} - \dot{n}_{Lj} + 3H(n_{L1} - n_{Lj}) = \frac{\Gamma_{\rm inf}\,\rho_{\rm inf}}{m_{\rm inf}} {\rm Br}_{1j}\, 2\epsilon_{1,j} - (n_{L1} - n_{Lj})\Gamma_{\rm LF}, \quad (j = 2, 3) \tag{92}$$

where n_{Li} is the lepton number asymmetry of L_i. In Fig. 17, we show contours which realize the observed baryon asymmetry. Here, the parameters are chosen in the same way as Fig.14 except for y_{ij}, $\lambda_{3,ijkl}$ and Λ_3. As a benchmark, we here choose $\Lambda_3 = 10^{15}$GeV which is a favorable value from the analytic estimation Eq.(90). One can see that the numerical estimations match Eq.(90) within an order of magnitude. In order to check whether this is true or not, the model dependent analysis is needed. See [52] for example.

□ Summary and Discussion

In this section, we have proposed a new leptogenesis scenario at the reheating era. We have assumed the existence of an inflaton that can decay into the SM particles, which leads to the reheating of the universe. During this era, the produced leptons are inievetabelly out of equilibrium, and its asymmetry can be successfully produced by using the dimension 5 and 6 operators in the SM (Eqs.(71)(86)). As one can see from the analytical estimations Eqs.(82)(90), our scenarios can successfully explain the observed asymmetry even at the lower reheating temperature $T_R \lesssim 10^{15}$GeV as long as the inflaton mass is greater than 10^{13}GeV. Because our study is based on the effective Lagrangians, this mechanism can be applicable to various extensions of the SM model.

For example, in the case of type-I seesaw, the dimension-5 and dimension-6 operators are generated by integrating out the right handed neutrino:

$$\frac{\lambda_{1,ij}}{\Lambda_1} \simeq (y_\nu m_N^{-1} y_\nu^T)^i_j, \qquad \frac{\lambda_{2,ijkl}}{\Lambda_2^2} \simeq (y_\nu y_\nu^\dagger)^i_j (y_\nu y_\nu^\dagger)^k_l \frac{1}{16\pi^2 m_N^2}, \tag{93}$$

where y_ν is the neutrino Yukawa coupling and m_N is the typical mass of right handed neutrinos. We can see that the value of Λ_2 is $\mathcal{O}(10^{15})$ GeV due to the one-loop suppression by right handed neutrinos. Of course we can have different Λ_2 for other seesaw models, and they are discussed in [52] in detail. As for the dimension-6 operator suppressed by Λ_3, it can be generated at the tree level, e.g., if the second Higgs doublet heavier than the electroweak scale is added in addition to the SM Higgs doublet.

Before concluding this section, a few comments are needed. First, although we have not considered in this paper, if the right handed neutrino is lighter than the inflaton, it can be produced by the scattering between the SM particles. It might be interesting to investigate whether we can obtain enough asymmetry even in this situation. Second, our scenario goes well with the high scale inflation model. In the case of the quadratic chaotic inflation [124], we have $m_{\rm inf} \simeq 2 \times 10^{13}$ GeV. In this case, from Eq.(90), one can see that the observed baryon asymmetry is explained if the inflaton couples with the SM particles by the dimension-5 operator as $\Gamma_{\rm inf} \simeq \frac{1}{8\pi}\frac{m_{\rm inf}^3}{M^2}\frac{1}{100}$, where $M \sim 10^{15\text{–}16}$ GeV. Because this scale is close to the Gut or string scale, it might be also interesting to consider its origin from more fundamental physics point of view. Finally, in relation with the Higgs inflation, it is also interesting to explore whether our mechanism can be applicable even in this case.

4 Theoretical Approaches to the Naturalness Problem

In this section, we discuss a few theoretical approaches to the naturalness problem. In particular, we seek for solution or mechanism without assuming new particle or symmetry. As discussed in Introduction, such an approach is motivated by "*desert scenario*" suggested by the recent experiments. Because our following discussion is somewhat long, let us here give a short summary:

As a first candidate, we consider the Froggatt-Nielsen mechanism (FNM) [56, 57, 58, 59]. This mechanism assumes micro-canonical partition function in QFT, and argue that the couplings of QFT is dynamically determined in the same way as the temperature in statistical mechanics. Then, authors in [56] showed that the SM criticality can be explained by this mechanism. Note that an origin of this micro-canonical picture is yet unclear. In Appendix C, we present one possibility of such an origin.

As a second candidate, we study the Coleman's theory [66]. The original Coleman's argument was based on the Euclidean wormhole theory at the Planck scale: Because wormholes mix various states of universes having various values of the couplings, they become dynamical in the Euclidean path integral. Then, as for the cosmological constant (CC) Λ, Coleman actually showed that the partition function in the pure de Sitter universe has a strong peak at $\Lambda = 0$. However, this result is quite doubtful because the Euclidean formulation of gravity is not well defined. After 23 years later, the Minkowski version was finally formulated [60, 61, 62, 63, 64, 31, 65], and it was shown that this theory can also solve other natulraness problems in addition to the CCP. In this thesis, we study the Minkowski theory in detail, and discuss possible solutions for a few naturalness problems. In the following discussion, we do not use " Coleman's theory" because, in our present understating, it can be also obtained from different physics such as the matrix model [79]. In this sense, the Coleman's theory now becomes a broad concept than the original one. Instead, we use a terminology "multi-local theory (MLT)" in the following discussion. In Appendix C, we actually present a possible derivation of the MLT from the matrix model.

The following discussion is organized as follows. In subsection 4.1, we first reconsider the FNM as an origin of fine-tunings. In subsection 4.2-4.5, we study the MLT, and show that a few naturalness problems, the Strong CP problem and the CCP, can be solved by it, including the SM criticality. At a first glance, it seems that the MLT has nothing to do with the FNM, however, we will see that both of them are actually equivalent in the sense that their path integrals have the same forms .

4.1 Froggatt-Nielsen mechanism

□**Statistical mechanics**

Let us first review how temperature is determined in statistical mechanics. In ordinary QFT, a system is completely described by the canonical-like partition function:

$$Z^{(\mathrm{QFT})}(\lambda) = \int \mathcal{D}\phi \ \exp\left(iS\right), \tag{94}$$

where S is a given action, and λ represents a coupling in S. The corresponding quantity in statistical mechanics is the canonical distribution:

$$Z_{\mathrm{C}}^{(\mathrm{Statistical})}(\beta) = \sum_n \exp\left(-\beta E_n\right), \tag{95}$$

where $\beta = 1/T$ is the inverse temperature, and E_n's are the energy eigenvalues. On the other hand, it is known that this distribution is equivalent to the micro-canonical distribution [16]

$$Z_{\mathrm{MC}}^{(\mathrm{Statistical})}(E) = i\pi \sum_n \delta(E_n - E) \tag{96}$$

in the thermodynamic limit. Here, we give a brief proof. When the space volume $V_3 \to \infty$, the canonical distribution can be written as

$$Z_{\mathrm{C}}^{(\mathrm{Statistical})} = \int_0^\infty dE \ \frac{d\Omega(E)}{dE} e^{-\beta E} \sim -\beta V_3 \int_0^\infty d\epsilon \ \exp\left(V_3(s-\beta\epsilon)\right) \sim \beta V_3 \exp\left(V_3(s-\beta\epsilon)\right)\Big|_{\epsilon=\epsilon^*}, \tag{97}$$

where $\Omega(E)$ is the number of states, $S(E) = \log\Omega(E)$ is the entropy, s is its density, ϵ is the energy density, and ϵ^* is the solution of $ds/d\epsilon = \beta$. Note that we have done a partial integration in the second equality. Thus, the free energy is given by

$$F(\beta) = -\frac{1}{\beta}\log Z_{\mathrm{C}}^{(\mathrm{Statistical})} \sim \frac{V_3}{\beta}(\beta\epsilon^* - s(\epsilon^*)) = \underset{E}{\mathrm{Min}}\left(E - TS(E)\right) \tag{98}$$

This shows that the free energy determined by the canonical distribution is thermodynamically equivalent to the entropy defined by the micro-canonical distribution. From the microscopic point of view, the micro-canonical distribution is more fundamental because there is no thermodynamical quantity in Eq.(96). In this picture, the temperature T is dynamically determined by the following

[16] Here, the overall coefficient $i\pi$ is just a convention.

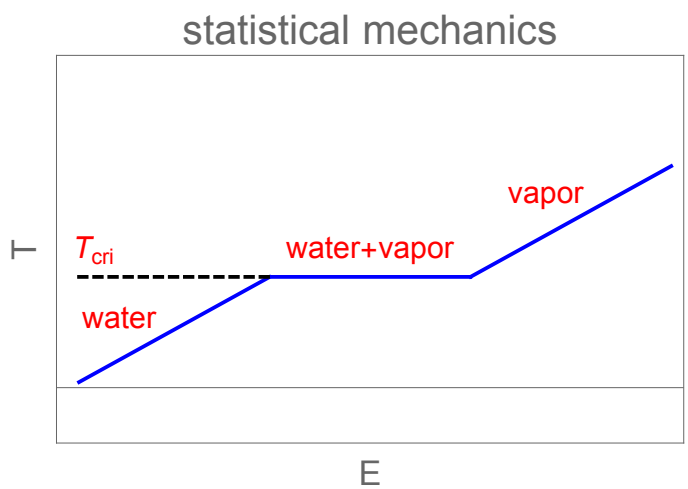

Figure 18: The blue contour shows $T^*(E)$ determined by the micro-canonical distribution. For example, consider water heated by external environment. While the phase transition occurs, $T^*(E)$ does not change.

way: Eq.(96) can be rewritten as

$$
\begin{aligned}
&= \sum_n \left[\frac{1}{E_n - E} - P\left(\frac{1}{E_n - E} \right) \right] \\
&= \int_0^\infty d\beta \ \sum_n \exp\left(-\beta(E_n - E)\right) - \sum_n P\left(\frac{1}{E_n - E} \right) \\
&\simeq \int_0^\infty d\beta \ Z_{\mathrm{C}}^{(\mathrm{Statistical})}(\beta) e^{\beta E} = \int_0^\infty d\beta \ \exp\left(-\beta(F(\beta) - E)\right), \qquad (99)
\end{aligned}
$$

where P represents the Cauchy principal value, and $F(\beta)$ is the free energy. In the thermodynamic limit, this integral is dominated by a point $\beta^*(E) = 1/T^*(E)$ at which the exponent of Eq.(99) satisfies

$$
\frac{\partial}{\partial \beta} \left(\beta F(\beta) \right) \Big|_{\beta = \beta^*} - E = 0 \ \leftrightarrow \ \langle H \rangle_{\mathrm{C}} = E, \qquad (100)
$$

where H is the Hamiltonian of the system, and $\langle \ \rangle_{\mathrm{C}}$ represents the average by the canonical distribution. Thus, T is dynamically fixed so that the average of H by the canonical distribution becomes E, and it depends on E. Of course, the explicit form of $T^*(E)$ depends on properties of a system. A typical example is a system that experiences phase transition like water. See Fig.18 for example. When different phases coexist, $T^*(E) = T_{\mathrm{cri}}$ does not change until the system gains enough energy. From the naturalness point of view, this fact indicates that T is most likely to be fixed at the critical value T_{cri} because the probability of E being chosen to be in the interval is

biggest. In the following, we will apply the above argument to QFT, and see that the coupling in QFT corresponds to T in statistical mechanics.

□**Micro-canonical QFT**

Here, without considering its origin, let us adopt a micro-canonical partition function even in QFT:

$$Z_{\rm MC}^{\rm (QFT)} = \int \mathcal{D}\phi \ \prod_i \delta(S_i - I_i), \tag{101}$$

where S_i's are the ordinary local actions in QFT, and I_i's are their arbitrary values. Note that we have chosen actions as fixing quantities in order to maintain the Lorentz (diffeomorphism) invariance, and that I_i's correspond to E in statistical mechanics. In principle, S_i's should be determined from microscopic physics such as string theory, however, we now assume that all the low-energy (renormalizable) actions are included in S_i's. Rewriting the delta functions in Eq.(101) as the Fourier forms, we obtain

$$\begin{aligned} Z_{\rm MC}^{\rm (QFT)} &= \int \mathcal{D}\phi \ \int \cdots \int \left(\prod_i d\lambda_i \right) \ \exp\left(i \sum_i \lambda_i (S_i - I_i) \right) \\ &= \int \cdots \int \left(\prod_i d\lambda_i \right) \ Z^{\rm (QFT)}(\overrightarrow{\lambda}) = \int \cdots \int \left(\prod_i d\lambda_i \right) \ \exp\left(-iV_4 \rho(\overrightarrow{\lambda}) \right), \end{aligned} \tag{102}$$

where $\rho(\overrightarrow{\lambda})$ is the vacuum energy density determined by $Z^{\rm (QFT)}(\overrightarrow{\lambda})$. One can see that λ_i's play roles of the couplings. Thus, if there is a point $\overrightarrow{\lambda}_0$ that strongly dominates in the above integration, we have

$$\sim Z^{\rm (QFT)}(\overrightarrow{\lambda}_0), \tag{103}$$

and this is the ordinary partition function where $\overrightarrow{\lambda}$ is fixed to $\overrightarrow{\lambda}_0$. Here, because of the exponential factors in Eq.(102), such a dominant point is naively given by the saddle point of $\rho(\overrightarrow{\lambda})$ [17]:

$$\frac{\partial \rho(\overrightarrow{\lambda})}{\partial \lambda_i} = \frac{\int \mathcal{D}\phi \ (S_i - I_i) \exp\left(i \sum_j \lambda_j (S_j - I_j) \right)}{Z^{\rm (QFT)}(\overrightarrow{\lambda})} = \langle S_i \rangle - I_i = 0, \tag{104}$$

where $\langle \ \rangle$ is the expectation value in QFT. In [56], Froggatt and Nielsen showed that, for a wide range of values of I_i's, the above saddle point corresponds to the coexisting phase of the Higgs vacua as in statistical mechanics. As one of examples, let us choose the Higgs quartic term $S_H = \int d^4x \ \left(H^\dagger H\right)^2$ as S_i, and confirm their argument. Because the Higgs potential can have two minima

[17] Of course, it is possible that a system can not satisfy Eq.(104) for any value of I_i. In this case, we must carefully study the coupling dependence of $\rho(\overrightarrow{\lambda})$. See [64] for example. When a saddle point exits, the fluctuation of the coupling is roughly given by $\mathcal{O}\left(((\rho''(\lambda) V_4)^{-1/2} \right)$.

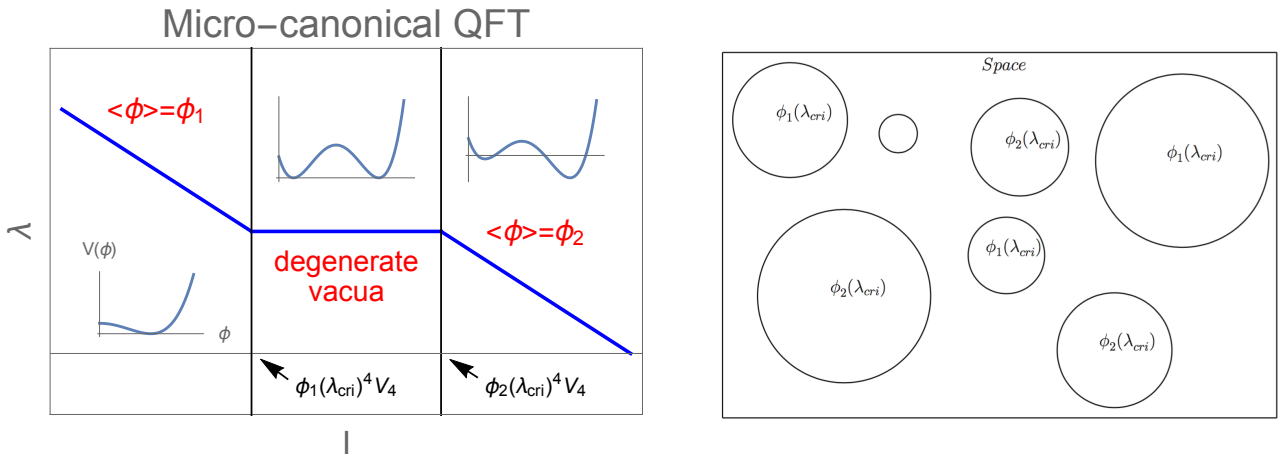

Figure 19: Left: The fixed Higgs quartic coupling λ as a function of I_H. As well as the statistical mechanics, there is a finite interval $\phi_1(\lambda_{\rm cri})^4 V_4 \leq I_H \leq \phi_2(\lambda_{\rm cri})^4 V_4$ where the phase coexisting is realized. Right: The coexisting of the Higgs vacua when $\phi_1(\lambda_{\rm cri})^4 V_4 \leq I_H \leq \phi_2(\lambda_{\rm cri})^4 V_4$.

depending on the couplings in the SM, we denote the small (large) vacuum expectation value as $\phi_1(\lambda)$ ($\phi_2(\lambda)$) in the following discussion. Furthermore, we represent the critical Higgs quartic coupling where the two vacua degenerate as $\lambda_{\rm cri}$. When $I_H \leq \phi_1(\lambda_{\rm cri})^4 V_4$ (V_4 : spacetime volume), the Higgs quartic coupling λ is fixed at the point $\lambda^*(I_H)$ ($\geq \lambda_{\rm cri}$) so that $\phi_1(\lambda)$ satisfies Eq.(104):

$$\langle S_H \rangle = \phi_1(\lambda^*(I_H))^4 V_4 = I_H. \tag{105}$$

In the left panel in Fig.19, we show $\lambda^*(I_H)$ by a blue contour. Note that $\phi_1(\lambda)$ is the true vacuum in the this case. As we increase I_H, $\lambda^*(I_H)$ decreases in order to satisfy Eq.(105). When I_H becomes $\phi_1(\lambda_{\rm cri})^4 V_4$, namely, $\lambda^*(I_H)$ becomes $\lambda_{\rm cri}$, the system undergoes the first order phase transition. At a first glance, it seems difficult to find the solution of Eq.(104) because $\langle S_H \rangle$ changes discretely at this point. However, even if $I_H > \phi_1(\lambda_{\rm cri})^4 V_4$, the universe can actually satisfy Eq.(104) by keeping the coexisting of two vacua over the whole space:

$$\langle S_H \rangle = (x\phi_1(\lambda_{\rm cri}) + (1-x)\phi_2(\lambda_{\rm cri}))^4 \times V_4 = I_H, \tag{106}$$

where x represents the ratio of one vacuum to the other vacuum, and it is easily determined by solving Eq.(106). In other words, the symbol $\langle \cdots \rangle$ also includes the average over the space. See the right panel in Fig.19 for example. This shows a typical distribution of the Higgs vacua when the coexisting is realized. Thus, when $\phi_2(\lambda_{\rm cri})^4 V_4 > I_H > \phi_1(\lambda_{\rm cri})^4 V_4$, the system always experiences the coexisting phase, and λ is fixed at $\lambda_{\rm cri}$. (See again the left panel in Fig.19.) This result is

completely the same as the temperature in statistical mechanics. Finally, when $I_H \geq \phi_2(\lambda_{\rm cri})^4$, λ is fixed to $\lambda^*(I_H)$ in the same way as the $I_H \leq \phi_1(\lambda_{\rm cri})^4$ case. As a result, as long as we start from the micro-canonical partition function, the state of a system is most likely the coexisting phase, and a coupling is fixed at the critical value. In this sense, the FNM gives us a fine-tuning mechanism in QFT [18].

4.2 Multi-local theory and the naturalness problem

In this subsection, we discuss the MLT and possible solutions for the naturalness problem based on it.

4.2.1 Coleman's first idea

First, let us briefly look at the Coleman's first idea [66]. He started from Euclidean gravity:

$$Z = \sum_{topology} \int_{\mathcal{M}} \mathcal{D}g \int \phi \exp\left(-S_E\right), \tag{107}$$

where S_E is the Euclidean action of Einstein gravity and matter, and $\mathcal{M}$ represents a spacetime. This theory generally has various classical solutions. Among them, the solutions satisfying

$$g^{\mu\nu}(x) \underset{l_p \ll |x|}{\rightarrow} \delta^{\mu\nu}, \ l_p : \text{Planck length} \tag{108}$$

are called *wormhole solutions*. From this definition, one can see that the typical length of wormhole is $\mathcal{O}(l_p)$. Of course, Einstein gravity also has classical solution with large scale, namely, universe. From the former point of view, the latter seems to be nearly flat, so we can generalize Eq.(108) as

$$g^{\mu\nu}(x) \underset{l_p \ll |x|}{\rightarrow} \tilde{g}^{\mu\nu}(x), \tag{109}$$

where $\tilde{g}^{\mu\nu}(x)$ represents the metric of the universe. In other words, a general classical solution is given by the spacetime having universe(s) and wormholes:

$$\mathcal{M} = \mathcal{M}_U \otimes \mathcal{M}_W, \tag{110}$$

where $\mathcal{M}_U$ ($\mathcal{M}_W$) represents the universe(s) (wormholes). See Fig.20 for example. Because we

[18] The numerical value of the critical value, of course, depends on values of other couplings. For example, in the case of the Higgs quartic coupling, $\lambda_{\rm cri}$ is given by 0.12 if the top mass is around 171GeV. As we mentioned in Section 2, this value is slightly smaller than the recent analyses based on Monte Carlo simulations: $M_t = 173.34 \pm 0.27 \pm 0.71$GeV [125] and $M_t = 172.44 \pm 0.13 \pm 0.47$GeV [126].

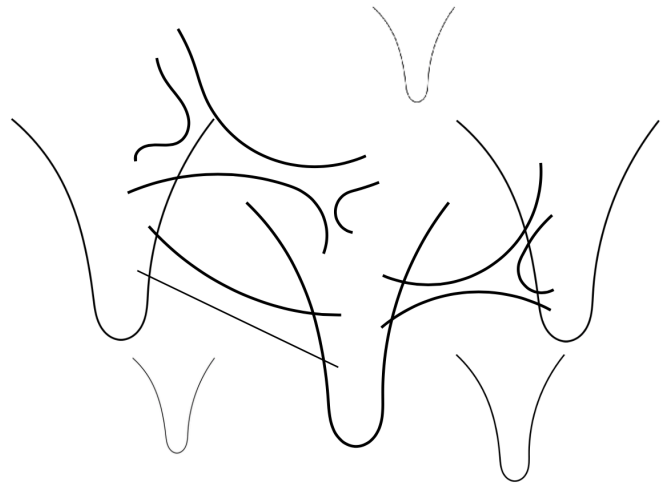

Figure 20: Universes and wormholes. After integrating out the wormhole configurations, only universes remain.

are living in the universe, it is reasonable to integrate metric and matter on the wormhole. For example, if we consider the universe(s) with a wormhole, its path integral becomes

$$Z_1 = \int_{\mathcal{M}_U \otimes \mathcal{M}_W} \mathcal{D}g \int \mathcal{D}\phi \exp\left(-S_E|_{\mathcal{M}_U} - S_E|_{\mathcal{M}_W}\right) \tag{111}$$

$$\simeq \int_{\mathcal{M}_U} \mathcal{D}\tilde{g} \int \mathcal{D}\tilde{\phi} \exp\left(-S_E|_{\mathcal{M}_U}\right) e^{-S_E^{(cl)}} F(\tilde{g}^{\mu\nu}, \tilde{\phi}), \tag{112}$$

where $S_E^{(cl)}$ is the classical action of a wormhole solution, and

$$F(\tilde{g}^{\mu\nu}, \tilde{\phi}) = \int_{\mathcal{M}_W} \mathcal{D}\delta g \int \mathcal{D}\delta\phi \exp\left[\int d^dx \left(- \frac{\delta^2 S_E|_{\mathcal{M}_W}}{\delta g \delta g}\bigg|_{\text{classical}} \delta g \delta g - 2\frac{\delta^2 S_E|_{\mathcal{M}_W}}{\delta g \delta \phi}\bigg|_{\text{classical}} \delta g \delta \phi - \frac{\delta^2 S_E|_{\mathcal{M}_W}}{\delta \phi \delta \phi}\bigg|_{\text{classical}} \delta\phi\delta\phi\right)\right] \tag{113}$$

represents the integration of the fluctuation on $\mathcal{M}_W$. Because the end of a wormhole can be freely attached to any place of the universe(s), F is typically given by

$$= c_{ij} \int d^dx \int d^dy \; \mathcal{O}_i(x)\mathcal{O}_j(y), \tag{114}$$

where c_{ij} is a constant, and $\mathcal{O}_i(x)$ is a local operator determined by $\tilde{g}^{\mu\nu}$ and $\tilde{\phi}$, and we have assumed that there is no relation between two ends of a wormhole. Thus, we obtain

$$Z_1 \sim \int_{\mathcal{M}_U} \mathcal{D}\tilde{g} \int \mathcal{D}\tilde{\phi} \exp\left(-S_E|_{\mathcal{M}_U}\right) e^{-S_E^{(cl)}} \times c_{ij} \int d^dx \int d^dy\ \mathcal{O}_i(x)\mathcal{O}_j(y). \tag{115}$$

In the following, we simply denote $\tilde{g}^{\mu\nu}$, $\tilde{\phi}$ and $S_E|_{\mathcal{M}_U}$ as $g^{\mu\nu}$, ϕ and S_E respectively. As well as the instanton calculation in QCD [67], we must sum up all the wormhole configurations in order to correctly take their effects into account:

$$\begin{aligned} Z &\sim \sum_{n=0}^{\infty} \int_{\mathcal{M}_U} \mathcal{D}g \int \mathcal{D}\phi \exp\left(-S_E\right) \frac{1}{n!} \left(e^{-S_E^{(cl)}} \times \int d^dx \int d^dy\ \mathcal{O}_i(x)\mathcal{O}_j(y) \right)^n \\ &= \int_{\mathcal{M}_U} \mathcal{D}g \int \mathcal{D}\phi \exp\left(-S_E + e^{-S_E^{(cl)}} c_{ij} \int d^dx \int d^dy\ \mathcal{O}_i(x)\mathcal{O}_j(y) \right) \\ &:= \int_{\mathcal{M}_U} \mathcal{D}g \int \mathcal{D}\phi \exp\left(-S_E + \sum_{i,j} \tilde{c}_{ij} S_E^i S_E^j \right), \end{aligned} \tag{116}$$

where S_E^i represents an ordinary local action. This result shows that the action of the universe(s) becomes multi-local due to the wormhole effects. In the following, we assume that the original action S_E is also included among S^i's. At a first glance, this theory seems to be difficult to handle, however, by regarding the integrand of Eq.(116) as a function of S^i's and doing the Laplace transform, we obtain

$$\begin{aligned} Z &\sim \int \prod_i d\lambda_i\ f(\{\lambda_i\}) \int_{\mathcal{M}_U} \mathcal{D}g \int \mathcal{D}\phi \exp\left(-\sum_i \lambda_i S_E^i \right), \\ &= \int \prod_i d\lambda_i\ f(\{\lambda_i\}) Z^{(\mathrm{QFT})}(\{\lambda_i\}) \end{aligned} \tag{117}$$

where $f(\{\lambda_i\})$ is the Laplace coefficient, and $Z^{(\mathrm{QFT})}(\{\lambda_i\})$ represents the ordinary path integral in QFT where the couplings are $\{\lambda_i\}$. This result means that the couplings in QFT become dynamical due to the wormhole effects, and Coleman argued that they are fixed at the point where the integrand in Eq.(117) strongly dominates. For example, by assuming pure gravity system having a positive cosmological constant, he claimed that it is fixed to zero because the partition function is classically given by

$$Z = \int d\Lambda Z(\Lambda) \simeq \int d\Lambda\ e^{const \times \frac{M_{pl}^2}{\Lambda}}, \tag{118}$$

which has a peak at $\Lambda = 0$ [19]. However, because the Euclidean path integral of gravity is not well defined, the above argument can drastically change if we take the quantum effects into account. Therefore, in order to obtain well defined quantities, the Minkowski formulation is inevitably needed. In the following section, we will discuss such a formulation, and see that it actually does work.

We can also repeat the above argument from the point of view of the baby universes [66, 68] as follows. This point of view is quite instinctive compared with the above wormhole discussion. Besides, we can formulate the Minkowski version. Instead of using the multi-local action, the wormhole effect can be expressed by introducing operators $\hat{a}_i$ and $\hat{a}_i^\dagger$ that describe the creation and annihilation of a baby universe. (See the right figure in Fig.21 for example.) Namely, we assume that the action of the universe is created by these operators:

$$S_C = \sum_i (\hat{a}_i + \hat{a}_i^\dagger) S_i. \tag{121}$$

Note that there is no relation between S_i and $\hat{a}_i$ ($\hat{a}_i^\dagger$), so they are commutative each other. In particular, the Hamiltonian of the universe also commutes $(\hat{a}_i, \hat{a}_i^\dagger)$. Therefore, $\hat{a}_i + \hat{a}_i^\dagger$'s become conserved quantities from the point of view of the universe. Thus, for each set of their eigenvalues, Eq.(121) becomes an ordinary local action for the universe:

$$S_C = \sum_i \lambda_i S_i \text{ for eigenstates of } \hat{a}_i + \hat{a}_i^\dagger\text{'s} \tag{122}$$

So the total Hamiltonian of the system consisting of the universe and baby universes is given by

$$\hat{H}_{\text{tot}} = \int d\overrightarrow{\lambda} |\overrightarrow{\lambda}\rangle\langle\overrightarrow{\lambda}| \otimes \hat{H}(\overrightarrow{\lambda}), \tag{123}$$

where $\{|\overrightarrow{\lambda}\rangle\}$ is the complete set of the Fock space of the baby universes:

$$1 = \int d\overrightarrow{\lambda} |\overrightarrow{\lambda}\rangle\langle\overrightarrow{\lambda}| \quad , \quad \left(\hat{a}_i + \hat{a}_i^\dagger\right) |\overrightarrow{\lambda}\rangle = \lambda_i |\overrightarrow{\lambda}\rangle, \tag{124}$$

[19] In the original paper [66], Coleman also assumed the multiverse. In that case, by summing up all the universes, the partition function becomes

$$Z = \int \prod_i d\lambda_i \; f(\{\lambda_i\}) \sum_{N=0}^{\infty} \frac{1}{N!} Z^{(\text{QFT})}(\{\lambda_i\})^N \tag{119}$$

$$= \int \prod_i d\lambda_i \; f(\{\lambda_i\}) \exp\left(Z^{(\text{QFT})}(\{\lambda_i\})\right). \tag{120}$$

So, the peak at $\Lambda = 0$ becomes more and more strong.

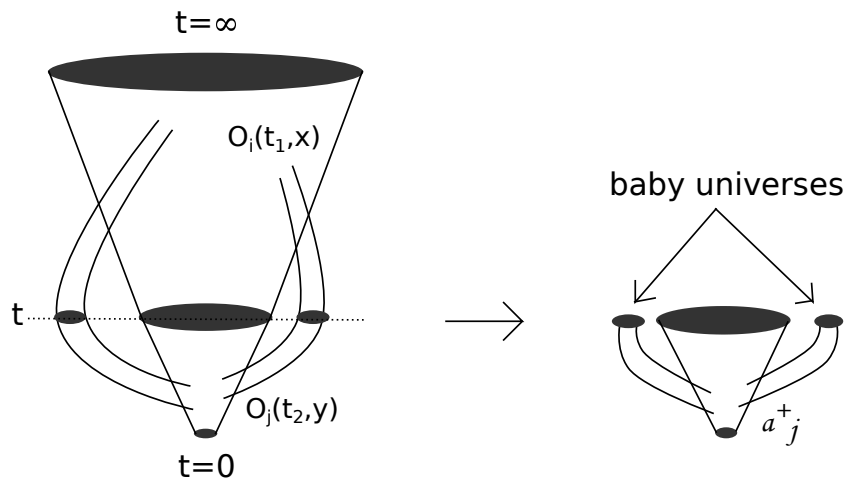

Figure 21: Universe and baby universes. Here, we show wormholes having two legs for simplicity. In the left figure, we show the whole spacetime in which the partition function is defined. In the right figure, we present the universe at a finite time. Typical, there are many baby universes in addition to the universe.

and $\hat{H}(\overrightarrow{\lambda})$ is the Hamiltonian for the universe that corresponds to the action $\sum_i \lambda_i S_i$. Then, for the initial state $|i\rangle = |i\rangle_{\text{baby}} \otimes |i\rangle_{\text{universe}}$, the wave function at t is given by

$$e^{-i\hat{H}_{\text{tot}}t}|i\rangle = \int d\overrightarrow{\lambda}|\overrightarrow{\lambda}\rangle\langle\overrightarrow{\lambda}|i\rangle_{\text{baby}} \otimes T\exp\left(-it\hat{H}(\overrightarrow{\lambda})\right)|i\rangle_{\text{universe}}. \tag{125}$$

Thus, by considering the $t \to +\infty$ limit, and multiplying a final state $\langle f| := {}_{\text{baby}}\langle f| \otimes {}_{\text{universe}}\langle f|$ to Eq.(125), we obtain

$$\begin{aligned} Z &= \lim_{t\to\infty}\int d\overrightarrow{\lambda}\,{}_{\text{baby}}\langle f|\overrightarrow{\lambda}\rangle\langle\overrightarrow{\lambda}|i\rangle_{\text{baby}} \times {}_{\text{universe}}\langle f|T\exp\left(-it\hat{H}(\overrightarrow{\lambda})\right)|i\rangle_{\text{universe}} \\ &= \int d\overrightarrow{\lambda} f(\overrightarrow{\lambda}) Z^{(\text{QFT})}(\{\lambda_i\}), \end{aligned} \tag{126}$$

which is the same as Eq.(117) except for that Eq.(126) is formulated in Minkowski signature. The above argument is the derivation of the MLT from the point of view of the baby universe. Note that the weight function $f(\overrightarrow{\lambda})$ is not important in the following discussion because we will consider general initial and final states of baby universes. Namely, we do not consider such a special case that $|i\rangle_{\text{baby}}$ or $|f\rangle_{\text{baby}}$ is $|\overrightarrow{\lambda}'\rangle$ in the following discussion.

4.2.2 Minkowski version

Our starting point is the partition function that has Minkowski signature and a multi-local action:

$$Z = \int \mathcal{D}\phi \exp\left(i\left(\sum_i c_i S_i + \sum_{i,j} c_{i,j} S_i S_j + \sum_{i,j,k} c_{i,j,k} S_i S_j S_k + \cdots\right)\right), \tag{127}$$

where S_i is a local action with Minkowski signature, and we have dropped gravity for simplicity. By expressing the integrand as a Fourier transform

$$\exp\left(i\left(\sum_i c_i S_i + \sum_{i,j} c_{i,j} S_i S_j + \sum_{i,j,k} c_{i,j,k} S_i S_j S_k + \cdots\right)\right) = \int d\overrightarrow{\lambda} f(\overrightarrow{\lambda}) \exp\left(i \sum_i \lambda_i S_i\right), \tag{128}$$

we can rewrite the partition function as

$$\begin{aligned} Z &= \int d\overrightarrow{\lambda} f(\overrightarrow{\lambda}) \int \mathcal{D}\phi \exp\left(i \sum_i \lambda_i S_i\right) \\ &= \int d\overrightarrow{\lambda} f(\overrightarrow{\lambda}) \lim_{T\to+\infty} \langle f | T \exp\left(-i2\hat{H}(\overrightarrow{\lambda})T\right) | i\rangle, \end{aligned} \tag{129}$$

where $\hat{H}(\lambda)$ is the Hamiltonian of a system, and $|i\rangle$ ($|f\rangle$) represents an initial (final) state. For now, we simply assume the usual $i\epsilon$ prescription. The cosmological justification of this procedure is discussed in Appendix D. In this case, Eq.(129) can be examined as

$$Z \simeq \int d\overrightarrow{\lambda} f(\overrightarrow{\lambda}) \exp\left(-iV_4 \rho(\overrightarrow{\lambda})\right), \tag{130}$$

where $\rho(\overrightarrow{\lambda})$ is the vacuum energy, and V_4 is the spacetime volume. This result is completely the same as Eq.(102) except that Eq.(102) includes the arbitrary parameters I_k's. In this sense, the Froggatt-Nielsen mechanism and the MLT predict the same fine-tuning mechanism though the predicted values of the couplings might be different. In the following sections, we actually see that the Strong CP problem, the SM criticality and the CCP can be solved based on Eq.(130).

Let us here mention a generalization of the above argument. Although we have assumed Eq.(127) as our starting point, our mechanism does not change even if we start from more general partition function

$$\tilde{Z} = \int \mathcal{D}\phi \; F(S_0, S_1, \cdots), \tag{131}$$

where $F(S_0, S_1, \cdots)$ is an ordinary function of S_i's. This is because it can be also rewritten like Eq.(129) by doing the Fourier transform. In other words, our mechanism does not depend on a specific form of the fundamental partition function as long as it is an ordinary function of S_i's.

4.3 Strong CP problem

In the QCD Lagrangian, there exists a CP violating topological term

$$S_\theta := \frac{\theta}{16\pi^2}\int d^4x F^a_{\mu\nu}\tilde{F}^{a\mu\nu}, \tag{132}$$

where θ is a dimensionless coupling, and it is expected to be $\mathcal{O}(1)$. However, its experimental bounds are quite strong [127, 128]:

$$\theta < 10^{-9}, \tag{133}$$

This is the so-called "strong CP problem". We can naturally solve this problem as follows.

From the argument of the previous section, the partition function is given by

$$Z \sim \int_0^{2\pi} d\theta f(\theta)\exp\left(-i\varepsilon(\theta)V_4\right) \tag{134}$$

where

$$\varepsilon(\theta) \sim \Lambda^4_{\rm QCD}\cos\theta \tag{135}$$

is the energy density of the θ vacuum (see [67] for example). Because V_4 is quite large, and $f(\theta)$ is an ordinary function of θ, we can approximate this integration around the saddle points [20]:

$$Z \sim \sqrt{\frac{1}{V_4\Lambda^4_{\rm QCD}}}\left[f(0)e^{-i\varepsilon(0)V_4} + f(\pi)e^{-i\varepsilon(\pi)V_4}\right]. \tag{136}$$

This shows that the partition function is strongly dominated by $\theta = 0$ and $\theta = \pi$ worlds, as in the many world interpretation. Therefore, the probability that we live in $\theta = 0$ world is now given by 1/2.

4.4 The SM criticality

In this section, we show another derivation of the SM criticality based on our formulation. Here, we consider a general potential $V(\phi, \lambda)$ of a scalar field ϕ having two minima at $\phi_1(\lambda)$ and $\phi_2(\lambda)$, where we take $\phi_1(\lambda) < \phi_2(\lambda)$. Here, λ is one of the coupling constants of the theory. Without loss of generality, we can assume that two minima become degenerate when λ is equal to zero, and that the signature of λ is chosen as

$$\begin{aligned} V(\phi_1(\lambda),\lambda) &< V(\phi_2(\lambda),\lambda) \qquad \text{for } \lambda > 0, \\ V(\phi_1(\lambda),\lambda) &> V(\phi_2(\lambda),\lambda) \qquad \text{for } \lambda < 0. \end{aligned} \tag{137}$$

[20] Here, we assume general initial and final states as the boundary states. However, if we consider a specific state such as the n vacuum $|n\rangle$ that has a finite winding number n, the exponent of the integrand in Eq.(134) becomes stationary at the point where $\sin\theta \sim n/\left(\Lambda^4_{\rm QCD}V_4\right)$.

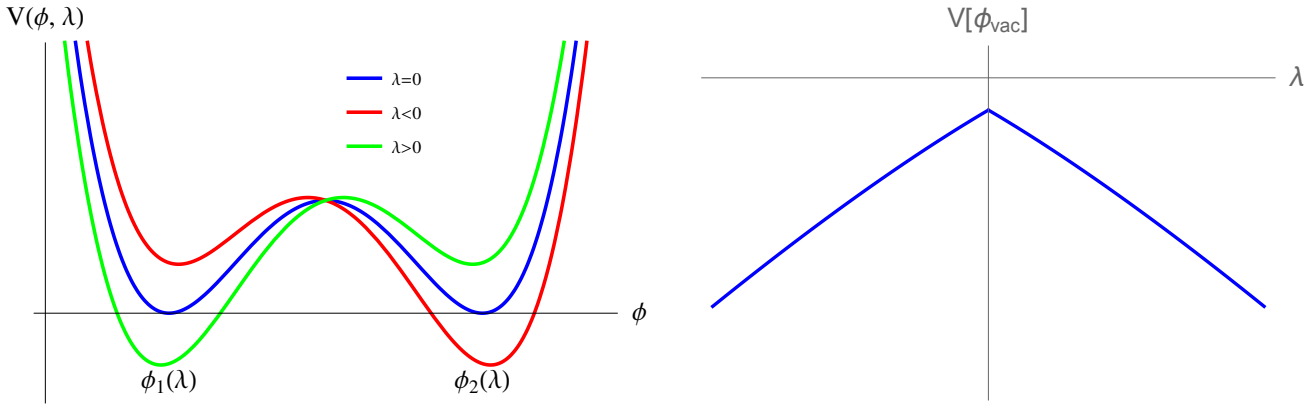

Figure 22: Left:Schematic behavior of $V(\phi, \lambda)$. The blue line corresponds to $\lambda = 0$, and the green (red) line corresponds to $\lambda > 0$ (< 0). Right: A typical behavior of the vacuum energy. $\lambda = 0$ corresponds to a non-anlytic point.

See Fig.22 for example. Then, the true vacuum expectation value $\phi_{\rm vac}(\lambda)$ and the vacuum energy density $\varepsilon(\lambda)$ are given by

$$\phi_{\rm vac}(\lambda) = \begin{cases} \phi_2(\lambda) & \text{for } \lambda < 0 \\ \phi_1(\lambda) & \text{for } \lambda > 0 \end{cases} \quad , \quad \varepsilon(\lambda) = \begin{cases} V(\phi_2(\lambda)) & \text{for } \lambda < 0 \\ V(\phi_1(\lambda)) & \text{for } \lambda > 0. \end{cases} \tag{138}$$

In this situation, we want to know a dominant point of the partition function:

$$Z = \int d\lambda f(\lambda) \exp\left(-i\varepsilon(\lambda) V_4\right). \tag{139}$$

We assume that $V(\phi_1(\lambda))$ and $V(\phi_2(\lambda))$ are monotonic functions of λ in $\lambda > 0$ and $\lambda < 0$ respectively, and that their derivatives are not equal at $\lambda = 0$. In this case, we can use the following mathematical formula:

Mathematical Formula

If $g(\lambda)$ is smooth and monotonic in the $\lambda > 0$ region, and $g'(0) \neq 0$, we have

$$e^{ikg(\lambda)}\theta(\lambda) \underset{k\to\infty}{\sim} \frac{i}{k}\left(\frac{dg}{d\lambda}\right)^{-1} e^{ikg(0)}\delta(\lambda), \tag{140}$$

where $\theta(\lambda)$ is a step function.
(Proof)
By multiplying a test function $F(\lambda)$ with finite support to $e^{ikg(\lambda)}$, and integrating from 0 to ∞, we obtain

$$\begin{aligned}\int_0^\infty d\lambda e^{ig(\lambda)k}F(\lambda) &= \int_{g(0)}^\infty dg\ \left(\frac{dg}{d\lambda}\right)^{-1} e^{ikg}F(\lambda=\lambda(g)) \\ &= \left[\frac{e^{ikg}}{ik}\left(\frac{dg}{d\lambda}\right)^{-1} F(\lambda(g))\right]_{g(0)}^\infty + \mathcal{O}\left(\frac{1}{k^2}\right) \\ &= \frac{i}{k}\left(\frac{dg}{d\lambda}\right)^{-1} e^{ikg(0)}F(\lambda)\Big|_{\lambda=0} + \mathcal{O}\left(\frac{1}{k^2}\right),\end{aligned} \tag{141}$$

Thus, one can see that Eq.(140) holds in the $k \to \infty$ limit.

By using this formula for $\lambda > 0$ and $\lambda < 0$ respectively, we obtain

$$e^{-i\varepsilon(\lambda)V_4} \sim -\frac{ie^{-i\varepsilon(0)V_4}}{V_4} \times \left[\left(\frac{V(\phi_1(\lambda))}{d\lambda}\right)^{-1}\Bigg|_{0+} - \left(\frac{V(\phi_2(\lambda))}{d\lambda}\right)^{-1}\Bigg|_{0-}\right]\delta(\lambda). \tag{142}$$

By substituting this into Eq.(139), the partition function can be approximated as

$$Z \sim \frac{f(0)}{V_4} \times e^{-i\varepsilon(0)V_4}, \tag{143}$$

which shows that the degrease vacua are favorable from the point of view of the MLT. Although we have just focused on one of the couplings, the above argument can be easily generalized to many couplings as long as the potential depends on them monotonically in each of the vacua. In this sense, the degeneration of vacua is one of general predictions from the MLT.

4.5 Cosmological constant problem

In order to discuss the fine-tuning of the cosmological constant, we must take gravity into consideration. In particular, it is known that our universe is well described by the Friedman universe, so we must consider the universe's expansion and its quantum mechanical effects. Furthermore, we

must also take care of the sign of the cosmological constant because the final state of the universe seriously depends on it. In the following discussion, we assume the positive cosmological constant because we are now living in such an universe. The detail formulation including gravity is discussed in Appendix E. For our present purpose, however, it is sufficient to consider the effective action for the radius a because only the vacuum energy is relevant:

$$Z = \int_0^\infty dT \int_0^\infty d\Lambda f(\Lambda) \langle a_\infty | e^{-i\hat{H}(\Lambda)T} | \epsilon \rangle, \tag{144}$$

where the effective Hamiltonian $\hat{H}(\Lambda)$ is

$$\hat{H}(\Lambda) = -\frac{\hat{p}_a^2}{2\hat{a}M_{pl}^2} + \frac{\hat{a}^3 \rho(\hat{a})}{6} \ , \ \rho(\hat{a}) = \Lambda + \rho_{MR}(\hat{a}), \tag{145}$$

Here, $\rho_{MR}(\hat{a})$ stands for the energy density of the matter and radiation, and we have simply assumed that the universe started from the state $|\epsilon\rangle$ with a tiny radius ϵ, and will evolve to the state $|a_\infty\rangle$ with a huge radius a_∞. One can see that $-\hat{a}^4\rho(\hat{a})$ plays the roll of a potential of the radius of the universe. By inserting the complete set

$$1 = \int_{-\infty}^{+\infty} dE |E;\Lambda\rangle\langle E;\Lambda| \ , \ \hat{H}(\Lambda)|E;\Lambda\rangle = E|E;\Lambda\rangle \tag{146}$$

into Eq.(144), we obtain

$$\begin{aligned} Z &= \int_0^\infty d\Lambda f(\Lambda) \int_0^\infty dt \int_{-\infty}^{+\infty} dE\, e^{-iEt} \langle a_\infty | E;\Lambda\rangle\langle E;\Lambda|\epsilon\rangle \\ &= \int_0^\infty d\Lambda f(\Lambda) \left(\pi \langle a_\infty | 0;\Lambda\rangle\langle 0;\Lambda|\epsilon\rangle + PV \int_{-\infty}^{+\infty} \frac{dE}{E} \langle a_\infty | E;\Lambda\rangle\langle E;\Lambda|\epsilon\rangle \right), \end{aligned} \tag{147}$$

where $|0;\Lambda\rangle$ is the zero-energy eigenstate, and PV represents the principal value. Here, we have used the following identity [21]:

$$\lim_{t\to+\infty} \frac{e^{-iEt}-1}{-iE} = \pi\delta(E) + PV\frac{1}{E}. \tag{148}$$

[21] The derivation is as follows: We can neglect e^{-iEt} by introducing the adiabatic factor $E \to E - i\epsilon$. Thus, by multiplying a smooth test function $F(E)$ with finite support to the left hand side, and integrating over E, we have

$$\int_{-\infty}^{\infty} dE \frac{-1}{-i\,(E-i\epsilon)} F(E) = \pi F(i\epsilon) - PV \int_{-\infty}^{\infty} dE \frac{F(E)}{E-i\epsilon}.$$

Therefore, in the $\epsilon \to 0$ limit, we obtain Eq.(148). Here, note that, if we also include the negative region in the time integral, we obtain the delta function $2\pi\delta(E)$ instead of Eq.(148). This leads to the ordinary Wheeler-Dewitt state $|0;\Lambda\rangle$.

The second term in Eq.(147) comes from the fact that we have chosen $t = 0$ as the beginning of the universe. However, because the universe is well described classically by the Friedman equation $\hat{H}(\Lambda) = 0$, we expect that only the first term in Eq.(147) is relevant. In Appendix F, we actually check this by using the WKB approximation. As a result, Eq.(147) can be approximated by

$$Z \sim \int_0^\infty d\Lambda f(\Lambda) \langle a_\infty | 0; \Lambda \rangle \langle 0; \Lambda | \epsilon \rangle. \tag{149}$$

Let us now evaluate $\langle a|0;\Lambda\rangle$ by using the WKB approximation. The Wheeler-Dewitt wave function is given by [62]

$$\langle a|0;\Lambda\rangle = M_{pl}\sqrt{\frac{a}{p_{cl}}} \exp\left(i\int^a da'\, p_{cl}(a')\right), \;\; p_{cl}(a) := M_{pl}a^2\sqrt{\frac{\rho(a)}{3}}, \tag{150}$$

where $p_{cl}(a)$ is the classical momentum. For simplicity, we consider the matter dominated universe:

$$\rho(a) = \Lambda + \frac{M}{a^3} := \Lambda + \rho_M(a), \tag{151}$$

where M is the total energy of the matter. Then, the exponent in Eq.(150) becomes

$$\begin{aligned}\int_{a_M}^a da'\, p_{cl}(a') &= \frac{M_{pl}}{3^{\frac{3}{2}}}\left(a^3\sqrt{\rho(a)} - a_M^3\sqrt{\rho(a_M)} + \frac{M}{\sqrt{\Lambda}}\log\left[\frac{a^{\frac{3}{2}}(\Lambda+\sqrt{\Lambda\rho(a)})}{a_M^{\frac{3}{2}}(\Lambda+\sqrt{\Lambda\rho(a_M)})}\right]\right) \\ &:= \frac{M_{pl}a^3}{3^{\frac{3}{2}}} g(\Lambda, a),\end{aligned} \tag{152}$$

where a_M is the radius of the universe at the time when the matter dominated era starts. $g(\Lambda, a)$ is a smooth and monotonic function of Λ, which satisfies

$$\begin{aligned} g(0,a) =& 2\left(\sqrt{\rho_M(a)} - \left(\frac{a_M}{a}\right)^3\sqrt{\rho_M(a_M)}\right) \;\; , \;\; \lim_{a\to\infty} g(\Lambda, a) = \sqrt{\Lambda}, \\ \left.\frac{dg(\Lambda,a)}{d\Lambda}\right|_{\Lambda=0} =& \frac{1}{3}\left(\frac{1}{\sqrt{\rho_M(a)}} - \left(\frac{a_M}{a}\right)^3\frac{1}{\sqrt{\rho_M(a_M)}}\right). \end{aligned} \tag{153}$$

Thus, by substituting Eq.(152) to Eq.(150), and using Eq.(140), we obtain

$$\begin{aligned}\langle a|0;\Lambda\rangle &\underset{a\to\infty}{\sim} \frac{3^{\frac{3}{2}}i}{M_{pl}a^3}\left(\frac{dg(\Lambda,a)}{d\Lambda}\right)^{-1}\Bigg|_{\Lambda=0} M_{pl}\sqrt{\frac{a}{p_{cl}(a)}}\exp\left(i\frac{M_{pl}a^3}{3^{\frac{3}{2}}}g(0,a)\right)\delta(\Lambda) \\ &= \frac{3^{\frac{3}{2}}i}{M_{pl}a^3}\left(\frac{dg(\Lambda,a)}{d\Lambda}\right)^{-1}\Bigg|_{\Lambda=0}\delta(\Lambda)\langle a|0;0\rangle,\end{aligned} \tag{154}$$

where $|0;0\rangle$ is the zero energy eigenstate with $\Lambda = 0$. By substituting this to Eq.(149), we have

$$\begin{aligned} Z &\sim \frac{1}{a_\infty^3}\left(\frac{dg(\Lambda, a_\infty)}{d\Lambda}\right)^{-1}\Bigg|_{\Lambda=0} \langle a_\infty|0;0\rangle\langle 0;0|\epsilon\rangle \\ &\sim \frac{1}{a_\infty^3}\left(\frac{dg(\Lambda, a_\infty)}{d\Lambda}\right)^{-1}\Bigg|_{\Lambda=0} \int_0^\infty dt \langle a_\infty|e^{-i\hat{H}(0)t}|\epsilon\rangle. \end{aligned} \tag{155}$$

This shows that Λ is fixed to zero as long as we concentrate on its positive region. However, this is inconsistent with the cosmological observation [**?**], which supports the small but non-zero Λ.

□**Can multiverse give a nonzero cosmological constant ?**

In order to save this situation, let us now consider the effect of multiverse. In this case, in addition to the summation of wormholes, we must also sum up all of universes. This can be done as follows:

$$Z_M := \sum_{N=0}^{\infty} \int dg \frac{f(g)}{N!} Z_u(g)^N = \int dg f(g) \exp\left(Z_u(g)\right), \tag{156}$$

where g is a coupling constant, and $Z_u(g)$ is the partition function of a single universe, and we have assumed that all the universes are copies of our universe. Eq.(156) indicates a new possibility to fix the parameter g: Even if $Z_u(g)$ itself does not have a strong peak, g can be fixed at a point g^* where $Z_u(g)$ becomes stationary. Namely, by expanding $Z_u(g)$ around the saddle point, we have

$$Z_u(g) = Z_u(g^*) + \frac{1}{2}\frac{d^2 Z_u}{dg^2}\Bigg|_{g=g^*} (g-g^*)^2 + \mathcal{O}\left((g-g^*)^3\right). \tag{157}$$

Here, by using the path integral expression

$$Z_U(g) = \int \mathcal{D}\phi e^{igS_g + \cdots} \times \psi_f^* \psi_i, \tag{158}$$

the coefficient of the second term can be written as the expectation value of the local action S_g

$$\begin{aligned} \frac{d^2 Z_u}{dg^2}\Bigg|_{g=g^*} &= -\int \mathcal{D}\phi e^{ig^* S_{g^*} + \cdots} S_{g^*}^2 \times \psi_f^* \psi_i \\ &:= -\langle \hat{S}_{g^*}^2 \rangle Z_u(g^*). \end{aligned} \tag{159}$$

Therefore, in the multiverse picture Eq.(156), the fluctuation of g around g^* is given by

$$\Delta g \sim \left(\frac{d^2 Z_u}{dg^2}\right)^{-\frac{1}{2}}\Bigg|_{g=g^*} = \frac{1}{\sqrt{\langle \hat{S}_{g^*}^2 \rangle Z_u(g^*)}}, \tag{160}$$

where $\langle \hat{S}^2_{g^*}$ is typically given by

$$\begin{aligned}\langle \hat{S}^2_{g^*} \rangle &= \int d^4x \int d^4y \langle \underbrace{\hat{\mathcal{O}}_{g^*}(x)\hat{\mathcal{O}}_{g^*}(y)}_{\text{contract}} \rangle \\ &= \int d^4x \int d^4y W(x-y) \\ &= V_4 \int d^4x W(x) \sim V_4 M_{pl}^4. \end{aligned} \tag{161}$$

Here, we have assumed that the cut-off scale is M_{pl}, and that $\int d^4x W(x) \sim M_{pl}^4$ by the dimensional analysis. Thus, one can see that Δg is of order $(V_4 M_{pl}^4 Z_u(g^*))^{-\frac{1}{2}}$. Thus, because the quantum correction to the vacuum energy is typically given as

$$\rho \sim M_{pl}^4 g, \tag{162}$$

we obtain the fluctuation of the vacuum energy density:

$$\Delta\rho \sim M_{pl}^4 \Delta g \sim \frac{M_{pl}^4}{\sqrt{V_4 M_{pl}^4 Z_u(g^*)}} \sim \frac{M_{pl}^2 H_0^2}{\sqrt{Z_u(g^*)}}, \tag{163}$$

where we have replaced V_4 with H_0^{-4}. Thus, if $Z_u(g^*)$ is $\mathcal{O}(1)$, this fluctuation is consistent with the observed value. Although the normalization of the partition function is a subtle problem, this result is itself interesting in that small coupling constant can be explained as a fluctuation in the multiverse partition function.

5 Origin of Gravity

In this section, we discuss the matrix model as an origin of gravity. In particular, we study the IIB matrix model [69] with matters, and interpret it as the noncommutative (NC) $U(1)$ gauge theory. Remarkably, we will see that all the matters couple with the $U(1)$ gauge field, and this coupling is given by the form of the metric because of the noncommutativity [88, 89, 90]. Then, we study whether this model can actually describe usual gravity by calculating the scattering amplitude of the NC $U(1)$ gauge field. The following discussion is organized as follows. In subsection 5.1, we review the IIB matrix model and its NC field interpretation. In subsection 5.2, we consider a matter in a NC background, and calculate the scattering amplitude. This section is based on the paper [100].

5.1 Noncommutative field theory from the matrix model

Here, we review the IIB matrix model and NC field theory. See also [85]. The action of the IIB matrix model is given by

$$S_{\rm IIB} = \frac{1}{g^2\Lambda^4}{\rm Tr}\left(\frac{1}{4}[\hat{X}^a,\hat{X}^b][\hat{X}^c,\hat{X}^d]\eta_{ac}\eta_{bd} + \frac{1}{2}\hat{\bar{\Psi}}\Gamma^a[\hat{X}^b,\hat{\Psi}]\eta_{ab}\right), \tag{164}$$

where a, b, c, and d are the ten dimensional Lorentz indices, $\hat{X}^a$ and $\hat{\Psi}$ are a ten dimensional vector and a Majorana spinor respectively, and they are also $N\times N$ hermitian matrices. Here, we have chosen the momentum interpretation of matrix, so $\hat{X}^a$ and $\hat{\Psi}$ have dimension 1 and 3/2 respcetevelly. Eq.(164) has the manifest $SO(9,1)$ and $U(N)$ invariances. In the following, we drop the second term for simplicity. In this case, the classical equation of motion is given by

$$\left[\hat{X}^b,\left[\hat{X}_b,\hat{X}_a\right]\right] = 0. \tag{165}$$

There are various solutions of this equation. For example, we can consider consider the diagonalized matrices:

$$\hat{P}^\mu = diag(p_1^\mu,\cdots,p_N^\mu) \text{ for } \mu = 1,2,\cdots,d, \tag{166}$$

$$\hat{P}^a = 0 \text{ for } a = d+1,\cdots,10. \tag{167}$$

From the fluctuation around this solution $\hat{A}^\mu = \hat{X}^\mu - \hat{P}^\mu$, we define a $U(N)$ gauge field as

$$A^\mu(x) := e^{-i\hat{P}_\mu x^\mu}\hat{A}^\mu e^{i\hat{P}_\mu x^\mu}, \tag{168}$$

from which we can obtain

$$[\hat{P}_\nu, A^\mu(x)] = e^{-i\hat{P}_\mu x^\mu}[\hat{P}_\nu,\hat{A}^\mu]e^{i\hat{P}_\mu x^\mu} = i\partial_\nu A^\mu(x). \tag{169}$$

Thus, we can rewrite the first term of Eq.(**??**) explicitly as

$$\begin{aligned}
S_B &= \frac{1}{g^2}{\rm Tr}\left(\frac{1}{4}[\hat{P}^a+\hat{A}^a,\hat{P}^b+\hat{A}^b][\hat{P}_a+\hat{A}_a,\hat{P}_b+\hat{A}_b]\right)\\
&= \frac{1}{g^2}{\rm Tr}\left(\frac{1}{4}[\hat{P}^\mu+A^\mu(x),\hat{P}^\nu+A^\nu(x)][\hat{P}_\mu+A_\mu(x),\hat{P}_\nu+A_\nu(x)]\right)\\
&= \frac{1}{4g^2}{\rm Tr}\left((i\partial^\mu A^\nu(x) - i\partial^\nu A^\mu(x) + [A^\mu(x),A^\nu(x)])^2\right)\\
&= -\frac{1}{4g^2}\int d^dx\ F^{\mu\nu}(x)F_{\mu\nu}(x),
\end{aligned} \tag{170}$$

where $F^{\mu\nu}(x) = \partial^\mu A^\nu(x) - \partial^\nu A^\mu(x) - i[A^\mu(x), A^\nu(x)]$ is the ordinary field strength of the $U(N)$ gauge field, and we have assumed the large N limit. This result shows that the matrix model expanded around the classical solution Eq.(167) is equivalent to the $U(N)$ gauge theory in the large N limit. This is one of the examples of the large N reduction [82, 83, 84]. In this sense, the matrix model contains the spacetime and the degrees of freedom of gauge field simultaneously.

Now, let us consider a little non-trivial classical solution. This is given by

$$\begin{aligned} &[\hat{p}_\mu, \hat{p}_\nu] = i\Lambda_{\rm NC}^2 \times \tilde{\theta}_{\mu\nu}\mathbf{1} \quad (\mu, \nu = 1, \cdots, d), \\ &\hat{p}_i = 0 \quad (i = d+1, \cdots, 10), \end{aligned} \tag{171}$$

where where $\tilde{\theta}_{\mu\nu}$ is an antisymmetric dimensionless constant, and $\Lambda_{\rm NC}$ is a NC scale. By denoting the inverse matrix of $\Lambda_{\rm NC}^2\tilde{\theta}_{\mu\nu}$ as $\Lambda_{\rm NC}^{-2}\theta^{\mu\nu}$ and defining the conjugate matrices $\hat{x}^\mu := \Lambda_{\rm NC}^{-2}\theta^{\mu\nu}\hat{p}_\nu$, they satisfies

$$[\hat{x}^\mu, \hat{p}_\nu] = i\delta^\mu_\nu \times \hat{\mathbf{1}}. \tag{172}$$

This shows that we can interpret the classical matrices as the operators that act on functions on $\mathbf{R}^d$. Furthermore, we can easily show the following identities:

$$\left[\hat{p}_\mu, \exp\left(-ik_\nu\hat{x}^\nu\right)\right] = k_\mu, \tag{173}$$

$$\exp\left(-iq_\mu\hat{x}^\mu\right)\exp\left(-ik_\nu\hat{x}^\nu\right) = \exp\left(-i(q_\mu + k_\mu)\hat{x}^\mu\right)\exp\left(-\frac{i}{2}\Lambda_{\rm NC}^{-2}\theta^{\mu\nu}q_\mu k_\nu\right), \tag{174}$$

$$\mathrm{Tr}\left(\exp\left(-ik_\nu\hat{x}^\nu\right)\right) = (2\pi)^{d/2}\sqrt{det\tilde{\theta}} \times \Lambda_{\rm NC}^d \times \delta^{(d)}(k) \tag{175}$$

The first one indicates that $\exp\left(-ik_\nu\hat{x}^\nu\right)$ behaves as an eigenoperator of $\hat{p}_\mu$. Therefore, as well as ordinary functions, we can Fourier decompose the fluctuation $\hat{A}_\mu = \hat{X}_\mu - \hat{p}_\mu$ as

$$\hat{A}_\mu = \sum_k \tilde{a}_\mu(k)\exp\left(-ik_\nu\hat{x}^\nu\right), \ \tilde{a}_\mu(k)^* = \tilde{a}_\mu(-k), \tag{176}$$

where we can choose the degrees of freedom of k_μ's so that they coincide with that of $\hat{A}^\mu$. Under this decomposition, the product of two matrices is given by

$$\begin{aligned} \hat{a}\cdot\hat{b} &= \sum_{k,q}\tilde{a}(k)\tilde{b}(k)\exp\left(-ik_\nu\hat{x}^\nu\right)\exp\left(-iq_\nu\hat{x}^\nu\right) \\ &= \sum_{k,q}\tilde{a}(k)\tilde{b}(k)\exp\left(-i(k_\nu + q_\nu)\hat{x}^\nu\right)\exp\left(-\frac{i}{2}\Lambda_{\rm NC}^{-2}\theta^{\mu\nu}k_\mu q_\nu\right). \end{aligned} \tag{177}$$

From Eqs.(175), (176) and (177), we can read a map from a matrix to a function:

$$\hat{A}_\mu \ \to \ A_\mu(x) = \sum_k \tilde{a}_\mu(k) \exp\left(-ik_\nu x^\nu\right), \ \tilde{a}_\mu(k)^* = \tilde{a}_\mu(-k), \tag{178}$$

$$\mathrm{Tr}() \ \to \ (2\pi)^{d/2}\sqrt{det\tilde{\theta}} \int d^d x \ , \tag{179}$$

$$\hat{a}\cdot\hat{b} \ \to \ a(x)\star b(x) := \exp\left(\frac{i}{2}\Lambda_{\mathrm{NC}}^{-2}\theta^{\mu\nu}\partial_\mu^{(y)}\partial_\nu^{(z)}\right) a(y)b(z)\Big|_{y=z=x}. \tag{180}$$

Namely, the matrix model expanded around the classical solution Eq.(171) gives the ordinary local gauge field $A_\mu(x)$ where the product of functions is defined by Eq.(180), and this is called the Moyal product. Field theory that has such a non-trivial product is generally called NC field theory.

By using the above correspondences, we can evaluate the IIB action in the large N limit as

$$\begin{aligned} S_B &= -\mathrm{Tr}\left(\frac{(2\pi)^2}{4\Lambda^4}[\hat{p}_\mu + \hat{A}_\mu, \hat{p}_\nu + \hat{A}_\nu][\hat{p}^\mu + \hat{A}^\mu, \hat{p}^\nu + \hat{A}^\nu]\right) \\ &= \frac{\Lambda_{\mathrm{NC}}^4}{\Lambda^4}\left\{\frac{1}{4}N\tilde{\theta}^{\mu\nu}\tilde{\theta}_{\mu\nu} + \frac{1}{4}\int d^4x\sqrt{|\tilde{\theta}|}\left(\delta^{\mu\nu}\delta^{\alpha\beta}F_{\mu\alpha}F_{\nu\beta}\right)_\star\right\}, \end{aligned} \tag{181}$$

where $F_{\mu\nu} = \partial_\mu A_\nu - \partial_\nu A_\mu + i\left[A_\mu, A_\nu\right]_\star$ is the field strength of A_μ on the NC spacetime. This action has the NC gauge symmetry

$$\delta A_\mu(x) = \partial_\mu\Lambda(x) + i[A_\mu(x), \Lambda(x)]_\star. \tag{182}$$

Of course, the above NC gauge theory becomes the commutative $U(1)$ gauge theory if we take $\theta \to 0$. In conclusion, we have obtained the NC $U(1)$ gauge theory from the IIB matrix model expanded around the background Eq.(171). In the next subsection, we discuss its relation with gravity.

5.2 Emergent gravity from NC $U(1)$ gauge theory

□**Metric from the NC $U(1)$ gauge field**

In this subsection, based on the argument of the previous section, we discuss the NC interpretation of the IIB matrix model with matters and the emergent gravity from it. We start from the following action:

$$\begin{aligned} S &= S_B + S_\Phi \\ &= -\mathrm{Tr}\left(\frac{(2\pi)^2}{4\Lambda^4}\delta^{ac}\delta^{bd}[\hat{X}_a, \hat{X}_b][\hat{X}_c, \hat{X}_d]\right) - \frac{(2\pi)^2}{g^2\Lambda^4}\mathrm{Tr}\left(\frac{1}{2}\delta^{ab}[\hat{X}_a, \hat{\Phi}][\hat{X}_b, \hat{\Phi}]\right), \quad (a, b = 1, \cdots, 10) \end{aligned} \tag{183}$$

where S_B is the bosonic part of the IIB matrix model, Λ represents a cut-off scale, and $\hat{X}_a$ and $\hat{\Phi}$ are $N \times N$ hermitian matrices. Note that δ^{ab} stands for the ten-dimensional flat metric. We want to study fluctuations around a specific background $\hat{p}_a$'s which are determined by the classical equation of motion:

$$\left[\hat{X}^b, \left[\hat{X}_b, \hat{X}_a\right]\right] + \left[\hat{\Phi}, \left[\hat{X}_a, \hat{\Phi}\right]\right] = 0. \tag{184}$$

Among the various solutions, we consider the following one that gives the four dimensional NC spacetime:

$$\begin{aligned} &[\hat{p}_\mu, \hat{p}_\nu] = i\Lambda_{\rm NC}^2 \times \tilde{\theta}_{\mu\nu}\mathbf{1} \quad (\mu, \nu = 1, \cdots, 4), \\ &\hat{p}_i = 0 \quad (i = 5, \cdots, 10), \ \Phi = 0 \end{aligned} \tag{185}$$

where $\tilde{\theta}_{\mu\nu}$ is an antisymmetric dimensionless constant, and $\Lambda_{\rm NC}$ is a NC scale. By considering the fluctuation $\hat{A}_\mu := \hat{p}_\mu - \hat{X}_\mu$ around the solution, and using the results of the previous section, we obtain

$$\begin{aligned} S &= -{\rm Tr}\left(\frac{(2\pi)^2}{4\Lambda^4}\delta^{\mu\alpha}\delta^{\nu\beta}[\hat{p}_\mu + \hat{A}_\mu, \hat{p}_\nu + \hat{A}_\nu][\hat{p}_\alpha + \hat{A}_\alpha, \hat{p}_\beta + \hat{A}_\beta]\right) - \frac{(2\pi)^2}{g^2\Lambda^4}{\rm Tr}\left(\frac{1}{2}\delta^{\mu\nu}[\hat{p}_\mu + \hat{A}_\mu, \hat{\Phi}][\hat{p}_\nu + \hat{A}_\nu, \hat{\Phi}]\right) \\ &= \frac{\Lambda_{\rm NC}^4}{\Lambda^4}\Bigg\{\frac{1}{4}N\tilde{\theta}^{\mu\nu}\tilde{\theta}_{\mu\nu} + \frac{1}{4}\int d^4x\,\sqrt{|\tilde{\theta}|}\,\left(\delta^{\mu\nu}\delta^{\alpha\beta}F_{\mu\alpha}F_{\nu\beta}\right)_\star \\ &\qquad + \frac{1}{2g^2}\int d^4x\,\sqrt{|\tilde{\theta}|}\delta^{\mu\nu}\Big(\left(\partial_\mu\Phi - i[A_\mu, \Phi]\right)\left(\partial_\nu\Phi - i[A_\nu, \Phi]\right)\Big)_\star\Bigg\}, \end{aligned} \tag{186}$$

where we have neglected the fluctuation of $\hat{X}_i$'s $(i = 5, \cdots 10,)$ for simplicity. Note that we can always eliminate $|\tilde{\theta}|^{1/2}$ by the field redefinition $\Phi \to (\Lambda^2/\Lambda_{\rm NC}^2)|\tilde{\theta}|^{-1/4}\Phi$ in the last term of Eq.(186). A notable feature of this action is that even real scalar couples with the gauge field A_μ because of the noncommutativity. Although we have just shown a scalar case, this is also true even in fermion case. In this sense, the NC $U(1)$ gauge field couples with all the matters, and this property reminds us gravity. In particular, it was also argued that A_μ can be interpreted as the fluctuation of the four dimensional spacetime metric in the semi-classical limit [88, 89, 90]. Here, 'semi-classical' means that we should keep the lowest order terms in $\Lambda_{\rm NC}^{-2}\theta^{\mu\nu}$, and neglect higher order terms. In this approximation, noncommutativity gets switched off, and the commutator turns into the Poisson bracket as

$$[f, g]_\star \sim i\{f, g\}, \quad \{f, g\} \equiv \Lambda_{\rm NC}^{-2} \times \theta^{\mu\nu}\partial_\mu f\partial_\nu g. \tag{187}$$

Then, Eq.(186) now becomes

$$S\Big|_{\rm semi} = \frac{\Lambda_{\rm NC}^4}{4\Lambda^4}\int d^4x\,\sqrt{|\tilde{\theta}|}\,(\sqrt{|G|}G^{\mu\nu})\tilde{\theta}_{\mu\alpha}\tilde{\theta}_{\nu\beta}(\sqrt{|G|}G^{\alpha\beta}) + \int d^4x\,\frac{1}{2g^2}\sqrt{|G|}G^{\mu\nu}\partial_\mu\Phi\partial_\nu\Phi, \tag{188}$$

where

$$\sqrt{|G|}G^{\mu\nu} = \delta^{\mu\nu} + \Lambda_{\rm NC}^{-2} \times (\theta^{\alpha\mu}\partial_\alpha A^\nu + \theta^{\alpha\nu}\partial_\alpha A^\mu) + \Lambda_{\rm NC}^{-4} \times \mathcal{O}(A^2), \tag{189}$$

with $(\theta\cdot\theta)^{\mu\nu} = \theta^{\mu\alpha}\theta^{\nu\beta}\delta_{\alpha\beta}$. From this we can read the fluctuation of the metric $h^{\mu\nu} = -(G^{\mu\nu} - \delta^{\mu\nu})$ as

$$h^{\mu\nu} = \Lambda_{\rm NC}^{-2} \times \left(\theta^{\mu\alpha}\partial_\alpha A^\nu + \theta^{\nu\alpha}\partial_\alpha A^\mu + \frac{1}{2}\delta^{\mu\nu}\theta^{\alpha\beta}F_{\alpha\beta}\right) + \Lambda_{\rm NC}^{-4} \times \mathcal{O}(A^2) \tag{190}$$

In the following analysis, we investigate the dynamics of A_μ which is quadratic in the effective action. In this sense, the $\mathcal{O}(A^2)$ terms in $h^{\mu\nu}$ are not necessarily as long as we the action at the linearized level because such terms give higher order contributions. On the other hand, the $\mathcal{O}(A^2)$ terms in $h^{\mu\nu}$ are necessarily if we concentrate on the cosmological constant term

$$\Lambda \int d^4x\ \sqrt{g} = \Lambda V_4 + \Lambda \frac{1}{2}\int d^4x\ h. \tag{191}$$

at the liberalized level. This term actually appears in the one-loop effective action. See the following discussion for the detail calculations. From the above equations, one can actually see that Φ couples to A_μ in the covariant way, and that A_μ can be interpreted as the fluctuation of the metric. On the other hand, as for the bosonic part of IIB matrix model, its semi-classical action cannot be written in a covariant way. (See the first term in Eq.(188).) Although this is a big problem in the present formulation of emergent gravity, we simply drop the term in the following discussion.

□**Action for the NC $U(1)$ gauge field**

If we drop the original IIB action, we have no action for the NC $U(1)$ gauge field $A_\mu(x)$. It was claimed that it is given by the induced EH action by considering the one-loop effective action of A_μ in the semi-classical limit [93] [22]. By calculating the scalar one-loop diagrams (Fig.23), we obtain the effective action of A_μ as a NC field theory [93] [23]:

[22] Here, note that there exist two ways of obtaining such a semi-classical limit: One is to take the semi-classical limit after calculating the one-loop effective action as a NC field theory. The other is to take first the semi-classical limit at the tree-level action, and calculate the effective action as an ordinary field theory. However, we have checked that both of the approaches produce the same result.

[23] In this reference, calculation was done by adding the mass term for the scalar as a regulator, and then taking the massless limit. Furthermore, the following replacement is used as a regularization of the loop integral:

$$\int \frac{d^4p}{(2\pi)^4}\frac{f(p)}{[p^2+\triangle^2]^2} \to -\int_0^\infty d\alpha\alpha \int \frac{d^4p}{(2\pi)^4} f(p) e^{-\alpha(p^2+\triangle^2)-1/(\alpha\Lambda^2)}. \tag{192}$$

Therefore, to maintain the consistency, we also use this regularization scheme in the following calculation.

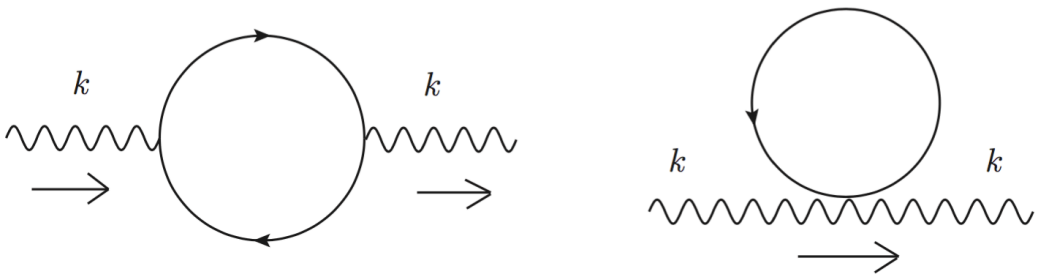

Figure 23: One-loop diagrams needed for the computation of the effective action of the NC $U(1)$ gauge field.

$$e^{-\Gamma_\Phi} = \int \mathcal{D}\Phi e^{-S}\Big|_{\text{1-loop without IIB action'}} \tag{193}$$

$$\begin{aligned}\Gamma_\Phi = &-\frac{1}{32\pi^2 g^2}\int \frac{d^4p}{(2\pi)^4}\Bigg[-\frac{1}{6}F_{\mu\nu}(p)F^{\mu\nu}(-p)\log\left(\frac{\Lambda^2}{\Lambda_{\text{eff}}^2}\right)\\ &+\frac{1}{4}\theta^{\mu\nu}F_{\mu\nu}(p)\theta^{\lambda\rho}F_{\lambda\rho}(-p)\left(\Lambda_{\text{eff}}^4-\frac{1}{6}p^2\Lambda_{\text{eff}}^2+\frac{(p^2)^2}{1800}\left(47-30\log\left(\frac{p^2}{\Lambda_{\text{eff}}^2}\right)\right)\right)\Bigg],\end{aligned} \tag{194}$$

where $\Lambda_{\text{eff}}^{-2} = \Lambda^{-2} + \tilde{p}^2/(4\Lambda_{\text{NC}}^4)$, $\tilde{p}^\mu = \theta^{\mu\nu}p_\nu$, and Λ is the cutoff momentum for loop integral. We suppose $\tilde{p}^2$ and p^2 are the same scale, since $\theta^{\mu\nu}$ is dimentionless and expected to be $O(1)$. When we focus on the IR regime,

$$\frac{p^2\Lambda^2}{\Lambda_{\text{NC}}^4} < 1, \tag{195}$$

Eq.(194) can be expanded as

$$\begin{aligned}\Gamma_\Phi \sim &-\frac{1}{32\pi^2 g^2}\int \frac{d^4p}{(2\pi^4)}\Bigg[\frac{\Lambda^4}{4\Lambda_{\text{NC}}^4}\theta^{\mu\nu}F_{\mu\nu}(p)\theta^{\lambda\rho}F_{\lambda\rho}(-p)-\frac{\Lambda^4}{\Lambda_{\text{NC}}^4}\frac{\Lambda^2}{8\Lambda_{\text{NC}}^4}\tilde{p}^2\theta^{\mu\nu}F_{\mu\nu}(p)\theta^{\lambda\rho}F_{\lambda\rho}(-p)\\ &-\frac{\Lambda^2}{24\Lambda_{\text{NC}}^4}\left(F^{\mu\nu}(p)F_{\mu\nu}(-p)\tilde{p}^2+\theta^{\mu\nu}F_{\mu\nu}(p)\theta^{\lambda\rho}F_{\lambda\rho}(-p)p^2\right)\Bigg]\\ =&-\frac{1}{32\pi^2 g^2}\int d^4x\Bigg[\frac{\Lambda^4}{4\Lambda_{\text{NC}}^4}\theta^{\mu\nu}F_{\mu\nu}\theta^{\lambda\rho}F_{\lambda\rho}+\frac{\Lambda^4}{\Lambda_{\text{NC}}^4}\frac{\Lambda^2}{8\Lambda_{\text{NC}}^4}\theta^{\mu\nu}F_{\mu\nu}(\partial\circ\partial)\theta^{\lambda\rho}F_{\lambda\rho}\\ &+\frac{\Lambda^2}{24\Lambda_{\text{NC}}^4}\left(F^{\mu\nu}\partial\circ\partial F_{\mu\nu}+\theta^{\mu\nu}F_{\mu\nu}\Box\theta^{\lambda\rho}F_{\lambda\rho}\right)\Bigg],\end{aligned} \tag{196}$$

where $\partial \circ \partial = (\theta \cdot \theta)^{\mu\nu}\partial_\mu\partial_\nu$, and $\Box = \delta^{\mu\nu}\partial_\mu\partial_\nu$. This result should be compared with the EH action with the cosmological constant term where the metric is given by Eq.(190):

$$\begin{aligned} S_G &= \frac{1}{16\pi^2}\int d^4x\sqrt{|G|}\left(-\frac{1}{2}\Lambda^4 - \frac{\Lambda^2}{12}R[G]\right) \\ &\sim -\frac{1}{32\pi^2 g^2}\int d^4x\left[\frac{\Lambda^4}{4\Lambda_{\rm NC}^4}\theta^{\mu\nu}F_{\mu\nu}\theta^{\lambda\rho}F_{\lambda\rho} + \frac{\Lambda^2}{24\Lambda_{\rm NC}^4}F^{\mu\nu}\partial\circ\partial F_{\mu\nu}\right], \end{aligned} \tag{197}$$

where we have extracted the quadratic part in A_μ and rescaled it as $A_\mu \to A_\mu/g$. From Eq.(197), one can see that the terms $\theta^{\mu\nu}F_{\mu\nu}\Box\theta^{\lambda\rho}F_{\lambda\rho}$ and $\theta^{\mu\nu}F_{\mu\nu}(\partial\circ\partial)\theta^{\lambda\rho}F_{\lambda\rho}$ in Eq.(196) are absent in Eq.(197). The latter is, however, a higher-order term in $(\Lambda/\Lambda_{\rm NC})^4$. Therefore, we can neglect this term because we now consider the lowest order of $\Lambda_{\rm NC}$. On the other hand, we can not neglect the former term. This mismatch between Eq.(196) and Eq.(197) originates in the path-integral measure: In the NC theory, it is induced from the flat metric originated in the matrix model:

$$||\delta\Phi||^2 = \int d^4x\ \delta\Phi(x)^2, \tag{198}$$

and this apparently violates the diffeomorphism invariance [24]. In spite of this mismatch, the similarity between Eq.(196) and Eq.(197) is impressive, and it is meaningful to study whether the NC $U(1)$ gauge theory can actually describe the real gravity. In the following, we in particular consider the amplitude of the graviton exchange between two scalars.

□**Scattering amplitude in NC $U(1)$ gauge theory**

In order to confirm this emergent gravity scenario, let us first compute the two-body scattering amplitude of scalar particles exchanging the $U(1)$ gauge field whose action is given by Eq.(196). In the following discussion, we put $32\pi^2 g^2 = 1$ for simplicity, and drop the first term in Eq.(196) because it corresponds to the cosmological constant term, which we assume to be canceled by some mechanism. Adding a gauge fixing term and rewriting them in terms of A_μ, we have

$$\begin{aligned} &\Gamma_\Phi\big|_{O(\Lambda^2)\text{ without CC term}} + \frac{1}{\alpha}\int\frac{d^4p}{(2\pi)^4}\frac{\Lambda^2}{12\Lambda_{\rm NC}^4}\tilde{p}^2 p^\mu A_\mu(p)p^\nu A_\nu(-p) \\ &\qquad = \frac{\Lambda^2}{12\Lambda_{\rm NC}^4}\int\frac{d^4p}{(2\pi)^4}A^\mu(p)\left[\tilde{p}^2\left(p^2\delta_{\mu\nu} - \left(1-\frac{1}{\alpha}\right)p^\mu p^\nu\right) + 2p^2\tilde{p}^\mu\tilde{p}^\nu\right]A^\nu(-p), \end{aligned} \tag{199}$$

where α represents the gauge freedom. From this, one can read off the propagator of A_μ as

$$D_{\mu\nu}(p) = \frac{6\Lambda_{\rm NC}^4}{\Lambda^2}\frac{1}{\tilde{p}^2p^2}\left[\delta_{\mu\nu} - (1-\alpha)\frac{p_\mu p_\nu}{p^2} - \frac{2}{3}\frac{\tilde{p}_\mu\tilde{p}_\nu}{\tilde{p}^2}\right]. \tag{200}$$

[24] If we use the diffeomorphism transformation, which is not realized in the NC $U(1)$ gauge theory, we can make $h^{\mu\nu}$ traceless in the leading-order in A_μ. In such coordinates, the 1-loop effective action indeed matches the EH action. See Appendix in [100] for the details.

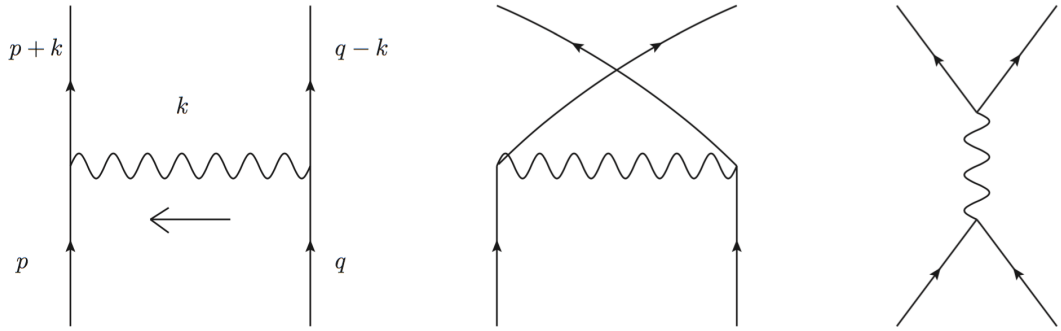

Figure 24: A scattering of test particles exchanging the $U(1)$ filed or graviton. In the former case, we read its propagator from the one-loop effective action Eq.(196).

In the following discussion, we take the Feynman gauge $\alpha = 1$. Furthermore, we can read the interaction between Φ and A_μ from Eqs.(188) and (189) as

$$\mathcal{L}_{\rm Int} = \Lambda_{\rm NC}^{-2} \times \theta^{\alpha\mu}\partial_\alpha A^\nu \partial_\mu \Phi \partial_\nu \Phi \tag{201}$$

from which we can read the vertex as

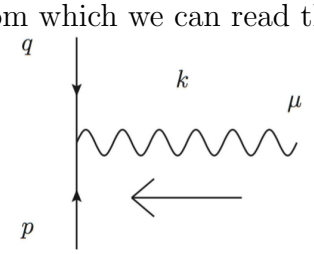

$$= i\Lambda_{\rm NC}^{-2} \times \left[p^\mu (q\cdot\tilde{k}) + q^\mu (p\cdot\tilde{k}) \right]. \tag{202}$$

We can now compute the two-body scattering amplitude. Their Feynman diagrams are shown in Fig.24. By straightforward calculations, we obtain

$$\mathcal{M}_A = \frac{6}{\Lambda^2}\frac{1}{k^2}\frac{(p\cdot\tilde{k})(q\cdot\tilde{k})}{\tilde{k}^2}\left[(4p\cdot q + k^2) - \frac{8}{3}\frac{(p\cdot\tilde{k})(q\cdot\tilde{k})}{\tilde{k}^2}\right] + (s \text{ channel}) + (u \text{ channel}). \tag{203}$$

where we have used the on-shell conditions for the scalar

$$p^2 = q^2 = 0, \quad (p+k)^2 = p^2, \quad (q-k)^2 = q^2, \tag{204}$$

This should be compared with the scattering amplitude calculated from the ordinary gravity system:

$$
\begin{aligned}
S =& S_G + S_{\rm gf} + S_\Phi, && (205)\\
S_G =& \frac{1}{2G_{\rm N}} \int d^4x \sqrt{|(\delta+h)|} R[\delta+h]\Big|_{\text{quadratic part in } h}, \\
=& \int d^4x \left[\frac{1}{8}\partial_\lambda h_{\mu\nu}\partial^\lambda h^{\mu\nu} - \frac{1}{4}\partial^\mu h_{\mu\nu}\partial_\lambda h^{\lambda\nu} + \frac{1}{4}\partial^\mu h_{\mu\nu}\partial^\nu h - \frac{1}{8}\partial_\mu h \partial^\mu h \right], && (206)\\
S_{\rm gf} =& \frac{1}{4}\int d^4x \left(\partial^\nu h_{\mu\nu} - \frac{1}{2}\partial_\mu h\right)\left(\partial^\lambda h^\mu{}_\lambda - \frac{1}{2}\partial^\mu h\right), && (207)\\
S_\Phi =& \int d^4x \sqrt{|(\delta+h)|}\left[\frac{1}{2}(\delta^{\mu\nu} - h^{\mu\nu})\partial_\mu\Phi\partial_\nu\Phi\right]\Big|_{\text{0th and 1st order of } h} \\
=& \int d^4x \left[\frac{1}{2}\partial_\mu\Phi\partial^\mu\Phi - \frac{1}{2}h^{\mu\nu}\partial_\mu\Phi\partial_\nu\Phi + \frac{1}{4}h\partial_\mu\Phi\partial^\mu\Phi\right], && (208)
\end{aligned}
$$

where the graviton is gauge-fixed in the de Donder gauge (harmonic gauge) which leads to the following propagator of graviton:

$$
D^{(h)}_{\mu\nu\lambda\rho}(k) = \frac{2}{k^2}(\delta_{\mu\lambda}\delta_{\nu\rho} + \delta_{\mu\rho}\delta_{\nu\lambda} - \delta_{\mu\nu}\delta_{\lambda\rho}). \tag{209}
$$

Then, we obtain

$$
\mathcal{M}_G = 2G_{\rm N}\left(\frac{2(p\cdot q)^2}{k^2} + p\cdot q\right) + (s\leftrightarrow t) + (t\leftrightarrow u) = -G_N\left(\frac{su}{t} + \frac{tu}{s} + \frac{ts}{u}\right), \tag{210}
$$

where s, t and u are the Mandelstam variables. This does not match Eq.(203) although both of them lead to the inverse-square law. In particular, Eq.(203) explicitly depends on the noncommutativity $\theta^{\mu\nu}$. Thus, this quantity generally depends on a choice of the background solution. This seems to be unphysical, and we need some mechanism to eliminate or average $\theta^{\mu\nu}$.

□**Averaging $\theta^{\mu\nu}$ and discussion**

Because $\theta^{\mu\nu}$ is a moduli parameter which specifies the classical solution of the matrix model, it seems to be is natural to take a kind of average over it. As an example, let us consider the average over the direction of $\theta^{\mu\nu}$ with its absolute value being fixed:

$$
(\theta\cdot\theta)^{\mu\nu} = \delta^{\mu\nu}, \tag{211}
$$

which is invariant under the Lorentz transformation

$$
\theta^{\mu\nu} \to \theta^{\mu\nu}_M = M^\mu{}_\alpha M^\nu{}_\beta \theta^{\alpha\beta}, \tag{212}
$$

where $M^{\mu}_{\ \alpha}$ is an element of $SO(4)$. Thus, we can average over the direction of $\theta^{\mu\nu}$, and this procedure yields the Lorentz covariant quantities:

$$\begin{aligned}
\int_{SO(4)} dM\ \theta^{\mu\nu}_M \theta^{\lambda\rho}_M &= \frac{1}{3}(\delta^{\mu\lambda}\delta^{\nu\rho} - \delta^{\mu\rho}\delta^{\nu\lambda}) \equiv \frac{1}{3}\Delta^{\mu\nu\lambda\rho}, \\
\int_{SO(4)} dM\ \theta^{\mu\nu}_M \theta^{\lambda\rho}_M \theta^{\alpha\beta}_M \theta^{\gamma\delta}_M &= -\frac{1}{27}(\Delta^{\mu\nu\lambda\rho}\Delta^{\alpha\beta\gamma\delta} + \Delta^{\mu\nu\alpha\beta}\Delta^{\lambda\rho\gamma\delta} + \Delta^{\mu\nu\gamma\delta}\Delta^{\lambda\rho\alpha\beta}) \\
&\quad + \frac{1}{9}\big((\delta^{\nu\lambda}\delta^{\rho\alpha}\delta^{\beta\gamma}\delta^{\delta\mu} + \delta^{\nu\alpha}\delta^{\beta\gamma}\delta^{\delta\lambda}\delta^{\rho\mu} + \delta^{\nu\gamma}\delta^{\delta\lambda}\delta^{\rho\alpha}\delta^{\beta\mu}) + [\mu\nu][\lambda\rho][\alpha\beta][\gamma\delta]\big),
\end{aligned} \tag{213}$$

where dM denotes the Haar measure of $SO(4)$, and $[\mu\nu][\lambda\rho][\alpha\beta][\gamma\delta]$ represents the antisymmetrized terms of the first one with respect to the superscripts in each of the brackets. Here the coefficients in the RHS of Eq.(213) are determined so that they are consistent with Eq.(211). By taking such an average, Eq.(203) now becomes

$$\mathcal{M}_A = \frac{2}{\Lambda^2}\left[\frac{52}{27}\frac{1}{k^2}2(p\cdot q)^2 + \frac{14}{27}p\cdot q + \frac{1}{36}k^2\right] + (s \leftrightarrow t) + (t \leftrightarrow u) = -\frac{52}{27\Lambda^2}\left(\frac{su}{t} + \frac{tu}{s} + \frac{st}{u}\right), \tag{214}$$

which correctly reproduces Eq.(210).

Therefore, we have shown that, if $\theta^{\mu\nu}$ is appropriately averaged as Eq.(213), the scattering amplitude in the induced gravity scenario coincides with that of the ordinary gravity. In this sense, the emergent gravity scenario is still alive. The question is the meaning and validity of averaging $\theta^{\mu\nu}$. In our analysis, we first calculated the amplitude with a fixed $\theta^{\mu\nu}$ and then averaged over its direction. On the other hand, turning back to the matrix model, $\theta^{\mu\nu}$ is determined by the commutator of matrices, and the path integral over them naturally includes the integration over $\theta^{\mu\nu}$ as a fundamental variable. In the language of NC field theory, this implies that $\theta^{\mu\nu}$ could have independent fluctuation, and that the average over $\theta^{\mu\nu}$ corresponds to the integral over $\theta^{\mu\nu}$:

$$Z = \int d\theta f(\theta) \int \mathcal{D}A \int \mathcal{D}\Phi \exp\left(-S\right), \tag{215}$$

where $f(\theta)$ is some weight function. Here, note that the original IIB action already has the gaussian weight if we choose the coordinate interpretation:

$$S_B\Big|_{\text{classical}} = -\frac{\Lambda^4}{4}\mathrm{Tr}\left([\hat{p}^\mu, \hat{p}^\nu][\hat{p}_\mu, \hat{p}_\nu]\right) = \frac{\Lambda^4}{4\Lambda^4_{\text{NC}}}\theta^{\mu\nu}\theta_{\mu\nu}, \tag{216}$$

and this is apparently invariant under $SO(4)$. Thus, our procedure Eq.(213) seems to be natural as long as we start from the IIB matrix model. Of course, in order to justify this picture, we need to

check whether the above average Eq.(213) can produce the correct results even in other scattering processes of gravity. Besides, we also need to find an origin of diffeomorphism symmetry in this emergent gravity scenario.

Naively, all the discrepancies between the NC $U(1)$ gauge theory and gravity seem to be originated in the mismatch of the off-shell degrees of freedom. Therefore, it might be interesting to consider a new matrix model such that $\theta^{\mu\nu}$ becomes dynamical quantity because it has six independent components. In addition to the gauge field, they can cover the enough degrees of freedom of graviton. Of course, we can also consider a new matrix model or novel interpretation of matrix variables in which gravity does not necessarily come from the noncommutativity [80][96].

6 Summary

In this thesis, we have investigated various problems of the SM together with their relations to the Planck/String scale physics. In Section 2, we have focused on DM, and studied perturbativity and the criticality of the minimal dark matter models. As a result, we have found that only the triplet Majorana fermion and real scalar can satisfy both of them. This fact also shows the usefulness of these method to constrain various models. In Section 3, we have proposed a new leptogenesis scenario at the reheating era by assuming an existence of an inflaton. Unlike the ordinary thermal leptogenesis, our mechanism can realize the enough baryon asymmetry even if the reheating temperature is well below 10^{15}GeV. Thus, this can be an promising alternative of leptogenesis. In Section 4, we have considered the naturalness problem from the point of view of the multi-local theory. By formulating the Minkowski version of the Coleman's theory, we have shown that the Strong CP problem, the SM criticality, and the CCP can be solved by it. It is quite surprising that a few naturalness problems can be solved by one mechanism. In Section 5, we have studied the matrix model and its possible relation to gravity. We have seen that all the matters couple with the NC $U(1)$ gauge field in the same way as graviton, and that their two body scattering amplitude coincides with that of the usual graviton exchange if we take an appropriate average of the NC background. More careful study is needed in order to justify our procedure.

Acknowledgement

I first really thank my supervisor Prof.Hikaru Kawai. He alway discussed with me, and gave me various insights about physics at the Planck scale. I also thank Koji Tsumura for teaching me various phenomenological aspects of physics beyond the SM. I am also grateful to my collaborators Yuta Hamada and Katsuta Sakai for giving me various ideas of physics.

This work is supported by the Grant-in-Aid for Japan Society for the Promotion of Science (JSPS) Fellows No.27·1771.

A Renormalization Group equations

Here, we summarize the RGEs of the scalar extensions of the SM. Calculate are based on the general formula in Refs. [129].

- SM with a quadruplet scalar field

$$
\begin{aligned}
\frac{d\lambda}{dt} &= \frac{1}{16\pi^2}\Big(+ 24\lambda^2 - 6y_t^4 + \frac{3}{8}g_Y^4 + \frac{9}{8}g_2^4 + \frac{3}{4}g_Y^2 g_2^2 + 12\lambda y_t^2 - 3\lambda g_Y^2 - 9\lambda g_2^2 + 4\kappa^2 + \frac{5}{4}\kappa'^2 \\
&\quad + \frac{40}{9}|\lambda_{\Phi^{\dagger 2}X^2}|^2 + 8|\lambda_{\Phi\Phi^{\dagger 2}X}|^2 + 24\lambda^2_{\Phi^{\dagger 3}X}\Big), \\
\frac{d\lambda_X}{dt} &= \frac{1}{16\pi^2}\Big(+ 32\lambda_X^2 + 30\lambda_X\lambda_X' + \frac{99}{2}\lambda_X'^2 + 6Y_X^4 g_Y^4 + \frac{297}{8}g_2^4 - 12Y_X^2\lambda_X g_Y^2 - 45\lambda_X g_2^2 \\
&\quad + 2\kappa^2 + 2|\lambda_{\Phi^{\dagger 2}X^2}|^2\Big), \\
\frac{d\lambda_X'}{dt} &= \frac{1}{16\pi^2}\Big(+ 24\lambda_X\lambda_X' + 42\lambda_X'^2 + 12Y_X^2 g_Y^2 g_2^2 - 12Y_X^2\lambda_X' g_Y^2 - 45\lambda_X' g_2^2 + \frac{1}{2}\kappa'^2 - \frac{8}{9}|\lambda_{\Phi^{\dagger 2}X^2}|^2\Big), \\
\frac{d\kappa}{dt} &= \frac{1}{16\pi^2}\Big(+ 3Y_X^2 g_Y^4 + \frac{45}{4}g_2^4 + 4\kappa^2 + \frac{15}{4}\kappa'^2 + 6y_t^2\kappa - 6Y_X^2\kappa g_Y^2 - \frac{3}{2}\kappa g_Y^2 - 27\kappa g_2^2 \\
&\quad + 12\kappa\lambda + 20\kappa\lambda_X + 15\kappa\lambda_X' + 18\lambda^2_{\Phi^{\dagger 3}X} + \frac{40}{3}|\lambda_{\Phi^{\dagger 2}X^2}|^2 + 6|\lambda_{\Phi\Phi^{\dagger 2}X}|^2\Big), \\
\frac{d\kappa'}{dt} &= \frac{1}{16\pi^2}\Big(+ 12Y_X g_Y^2 g_2^2 + 6y_t^2\kappa' - \frac{3}{2}\kappa' g_Y^2 - 6Y_X^2\kappa' g_Y^2 - 27\kappa' g_2^2 + 8\kappa\kappa' + 4\kappa'\lambda + 4\kappa'\lambda_X + 31\kappa'\lambda_X' \\
&\quad + 24\lambda^2_{\Phi^{\dagger 3}X} + \frac{64}{9}|\lambda_{\Phi^{\dagger 2}X^2}|^2 + \frac{8}{3}|\lambda_{\Phi\Phi^{\dagger 2}X}|^2\Big), \\
\frac{d\lambda_{\Phi^{\dagger 2}X^2}}{dt} &= \frac{1}{16\pi^2}\Big(- 4\lambda^2_{\Phi\Phi^{\dagger 2}X} + 6y_t^2\lambda_{\Phi^{\dagger 2}X^2} - \frac{3}{2}\lambda_{\Phi^{\dagger 2}X^2} g_Y^2 - 6Y_X^2\lambda_{\Phi^{\dagger 2}X^2} g_Y^2 - 27\lambda_{\Phi^{\dagger 2}X^2} g_2^2 \\
&\quad + 8\kappa\lambda_{\Phi^{\dagger 2}X^2} + 4\kappa'\lambda_{\Phi^{\dagger 2}X^2} + 4\lambda\lambda_{\Phi^{\dagger 2}X^2} + 4\lambda_X\lambda_{\Phi^{\dagger 2}X^2} - 11\lambda_X'\lambda_{\Phi^{\dagger 2}X^2}\Big), \\
\frac{d\lambda_{\Phi\Phi^{\dagger 2}X}}{dt} &= \frac{1}{16\pi^2}\Big(+ 12\lambda\lambda_{\Phi\Phi^{\dagger 2}X} + 9y_t^2\lambda_{\Phi\Phi^{\dagger 2}X} - \frac{9}{4}g_Y^2\lambda_{\Phi\Phi^{\dagger 2}X} - 3Y_X^2 g_Y^2\lambda_{\Phi\Phi^{\dagger 2}X} - 18g_2^2\lambda_{\Phi\Phi^{\dagger 2}X} \\
&\quad + 6\kappa\lambda_{\Phi\Phi^{\dagger 2}X} + \frac{5}{2}\kappa'\lambda_{\Phi\Phi^{\dagger 2}X} - \frac{40}{3}\lambda_{\Phi^{\dagger 2}X^2}\lambda^*_{\Phi\Phi^{\dagger 2}X}\Big), \\
\frac{d\lambda_{\Phi^{\dagger 3}X}}{dt} &= \frac{\lambda_{\Phi^{\dagger 3}X}}{16\pi^2}\Big(+ 12\lambda + 9y_t^2 - 18g_2^2 - \frac{9}{4}g_Y^2 - 3Y_X^2 g_Y^2 + 6\kappa + \frac{15}{2}\kappa'\Big).
\end{aligned}
\tag{217}
$$

- SM with a real quintet scalar field

$$\frac{d\lambda}{dt} = \frac{1}{16\pi^2}\Big(+ 24\lambda^2 - 6y_t^4 + \frac{3}{8}g_Y^4 + \frac{9}{8}g_2^4 + \frac{3}{4}g_Y^2 g_2^2 + \frac{5}{2}\kappa^2 + 12\lambda y_t^2 - 3\lambda g_Y^2 - 9\lambda g_2^2\Big),$$
$$\frac{d\lambda_X}{dt} = \frac{1}{16\pi^2}\Big(+ 26\lambda_X^2 + 108 g_2^4 - 72\lambda_X g_2^2 + 2\kappa^2\Big),$$
$$\frac{d\kappa}{dt} = \frac{1}{16\pi^2}\Big(+ 18 g_2^4 + 12\kappa\lambda + 14\kappa\lambda_X + 6y_t^2\kappa - \frac{3}{2}\kappa g_Y^2 - \frac{81}{2}\kappa g_2^2 + 4\kappa^2\Big). \tag{218}$$

- SM with a complex quintet scalar field

$$\frac{d\lambda}{dt} = \frac{1}{16\pi^2}\Big(+ 24\lambda^2 - 6y_t^4 + \frac{3}{8}g_Y^4 + \frac{9}{8}g_2^4 + \frac{3}{4}g_Y^2 g_2^2 + 12\lambda y_t^2 - 3\lambda g_Y^2 - 9\lambda g_2^2 + 5\kappa^2 + \frac{5}{2}\kappa'^2\Big),$$
$$\frac{d\lambda_X}{dt} = \frac{1}{16\pi^2}\big(+ 36\lambda_X^2 + 48\lambda_X\lambda_X' + 720\lambda_X\lambda_X'' + 1152\lambda_X'\lambda_X'' + 3168\lambda_X''^2$$
$$+ 6Y_X^4 g_Y^4 - 12Y_X^2\lambda_X g_Y^2 - 72\lambda_X g_2^2 + 2\kappa^2\big),$$
$$\frac{d\lambda_X'}{dt} = \frac{1}{16\pi^2}\Big(+ 24\lambda_X\lambda_X' + 84\lambda_X'^2 + 408\lambda_X'\lambda_X'' - 84\lambda_X''^2 + 3g_2^4 + 12Y_X^2 g_Y^2 g_2^2 - 12Y_X^2\lambda_X' g_Y^2$$
$$- 72\lambda_X' g_2^2 + \frac{1}{2}\kappa'^2\Big),$$
$$\frac{d\lambda_X''}{dt} = \frac{1}{16\pi^2}\big(+ 8\lambda_X'^2 + 24\lambda_X\lambda_X'' - 32\lambda_X'\lambda_X'' + 368\lambda_X''^2 + 6g_2^4 - 12Y_X^2\lambda_X'' g_Y^2 - 72\lambda_X'' g_2^2\big),$$
$$\frac{d\kappa}{dt} = \frac{1}{16\pi^2}\Big(+ 3Y_X^2 g_Y^4 + 18 g_2^4 + 12\kappa\lambda + 24\kappa\lambda_X + 24\kappa\lambda_X' + 360\kappa\lambda_X'' + 6y_t^2\kappa$$
$$- \frac{3}{2}\kappa g_Y^2 - 6Y_X^2\kappa g_Y^2 - \frac{81}{2}\kappa g_2^2 + 4\kappa^2 + 6\kappa'^2\Big),$$
$$\frac{d\kappa'}{dt} = \frac{1}{16\pi^2}\Big(+ 12Y_X g_Y^2 g_2^2 + 4\kappa'\lambda + 4\kappa'\lambda_X + 60\kappa'\lambda_X' + 60\kappa'\lambda_X'' + 6y_t^2\kappa'$$
$$- \frac{3}{2}\kappa' g_Y^2 - 6Y_X^2\kappa' g_Y^2 - \frac{81}{2}\kappa' g_2^2 + 8\kappa\kappa'\Big). \tag{219}$$

- SM with a sextet scalar field

$$
\begin{aligned}
\frac{d\lambda}{dt} &= \frac{1}{16\pi^2}\Big(+ 24\lambda^2 - 6y_t^4 + \frac{3}{8}g_Y^4 + \frac{9}{8}g_2^4 + 12\lambda y_t^2 - 3\lambda g_Y^2 - 9\lambda g_2^2 + \frac{3}{4}g_Y^2 g_2^2 + 6\kappa^2 + \frac{35}{8}\kappa'^2 \\
&\quad + \frac{28}{5}|\lambda_{\Phi^{\dagger 2}X^2}|^2\Big), \\
\frac{d\lambda_X}{dt} &= \frac{1}{16\pi^2}\Big(+ 40\lambda_X^2 + 70\lambda_X\lambda_X' + \frac{3535}{2}\lambda_X\lambda_X'' + \frac{8525}{4}\lambda_X'\lambda_X'' + \frac{271975}{16}\lambda_X''^2 + 6Y_X^4 g_Y^4 \\
&\quad - 12Y_X^2\lambda_X g_Y^2 - 105\lambda_X g_2^2 + 2\kappa^2 - \frac{11}{8}|\lambda_{\Phi^{\dagger 2}X^2}|^2\Big), \\
\frac{d\lambda_X'}{dt} &= \frac{1}{16\pi^2}\Big(+ 24\lambda_X\lambda_X' + 136\lambda_X'^2 + \frac{2115}{2}\lambda_X'\lambda_X'' - \frac{265}{2}\lambda_X''^2 + 3g_2^4 + 12Y_X^2 g_Y^2 g_2^2 - 12Y_X^2\lambda_X' g_Y^2 \\
&\quad - 105\lambda_X' g_2^2 + \frac{1}{2}\kappa'^2 - \frac{7}{25}|\lambda_{\Phi^{\dagger 2}X^2}|^2\Big), \\
\frac{d\lambda_X''}{dt} &= \frac{1}{16\pi^2}\Big(+ 8\lambda_X'^2 + 24\lambda_X\lambda_X'' + 2\lambda_X'\lambda_X'' + \frac{1715}{2}\lambda_X''^2 + 6g_2^4 - 105\lambda_X'' g_2^2 - 12Y_X^2\lambda_X'' g_Y^2 + \frac{2}{25}|\lambda_{\Phi^{\dagger 2}X^2}|^2\Big), \\
\frac{d\kappa}{dt} &= \frac{1}{16\pi^2}\Big(+ 3Y_X^2 g_Y^4 + \frac{105}{4}g_2^4 + 12\kappa\lambda + 28\kappa\lambda_X + 35\kappa\lambda_X' + \frac{3535}{4}\kappa\lambda_X'' \\
&\quad + 6y_t^2\kappa - 57\kappa g_2^2 - \frac{3}{2}\kappa g_Y^2 - 6Y_X^2\kappa g_Y^2 + 4\kappa^2 + \frac{35}{4}\kappa'^2 + \frac{56}{5}|\lambda_{\Phi^{\dagger 2}X^2}|^2\Big), \\
\frac{d\kappa'}{dt} &= \frac{1}{16\pi^2}\Big(+ 12Y_X g_Y^2 g_2^2 + 4\kappa'\lambda + 4\kappa'\lambda_X + 101\kappa'\lambda_X' + \frac{697}{4}\kappa'\lambda_X'' + 6y_t^2\kappa' \\
&\quad - \frac{3}{2}\kappa' g_Y^2 - 6Y_X^2\kappa' g_Y^2 - 57\kappa' g_2^2 + 8\kappa\kappa' + \frac{64}{25}|\lambda_{\Phi^{\dagger 2}X^2}|^2\Big), \\
\frac{d\lambda_{\Phi^{\dagger 2}X^2}}{dt} &= \frac{\lambda_{\Phi^{\dagger 2}X^2}}{16\pi^2}\Big(+ 4\lambda + 4\lambda_X - 31\lambda_X' + \frac{961}{4}\lambda_X'' + 6y_t^2 - \frac{3}{2}g_Y^2 - 6Y_X^2 g_Y^2 - 57g_2^2 + 4\kappa' + 8\kappa\Big).
\end{aligned}
\tag{220}
$$

- SM with a real septet scalar field

$$
\begin{aligned}
\frac{d\lambda}{dt} &= \frac{1}{16\pi^2}\Big(+ 24\lambda^2 - 6y_t^4 + \frac{9}{8}g_2^4 + \frac{3}{8}g_Y^4 + 12\lambda y_t^2 - 3\lambda g_Y^2 - 9\lambda g_2^2 + \frac{3}{4}g_Y^2 g_2^2 + \frac{7}{2}\kappa^2\Big), \\
\frac{d\lambda_X}{dt} &= \frac{1}{16\pi^2}\big(+ 30\lambda_X^2 + 2448\lambda_X\lambda_X'' + 51840\lambda_X''^2 - 144\lambda_X g_2^2 + 2\kappa^2\big), \\
\frac{d\lambda_X''}{dt} &= \frac{1}{16\pi^2}\big(+ 6g_2^4 + 1530\lambda_X''^2 + 24\lambda_X\lambda_X'' - 144\lambda_X'' g_2^2\big), \\
\frac{d\kappa}{dt} &= \frac{1}{16\pi^2}\Big(+ 36g_2^4 + 12\kappa\lambda + 18\kappa\lambda_X + 6y_t^2\kappa - \frac{3}{2}\kappa g_Y^2 - \frac{153}{2}\kappa g_2^2 + 4\kappa^2\Big).
\end{aligned}
\tag{221}
$$

- SM with a complex septet scalar field

$$
\begin{aligned}
\frac{d\lambda}{dt} &= \frac{1}{16\pi^2}\Big(+ 24\lambda^2 - 6y_t^4 + \frac{3}{8}g_Y^4 + \frac{9}{8}g_2^4 + 12y_t^2\lambda - 9\lambda g_2^2 - 3\lambda g_Y^2 + \frac{3}{4}g_2^2 g_Y^2 + 7\kappa^2 + 7\kappa'^2\Big),\\
\frac{d\lambda_X}{dt} &= \frac{1}{16\pi^2}\big(+ 44\lambda_X^2 + 96\lambda_X\lambda_X' + 3744\lambda_X\lambda_X'' + 77184\lambda_X''^2 + 9216\lambda_X\lambda_X''' + 31104\lambda_X'\lambda_X'''\\
&\quad + 90432\lambda_X''\lambda_X''' + 2859264\lambda_X'''^2 + 6Y_X^4 g_Y^4 - 12Y_X^2\lambda_X g_Y^2 - 144\lambda_X g_2^2 + 2\kappa^2\big),\\
\frac{d\lambda_X'}{dt} &= \frac{1}{16\pi^2}\Big(+ 24\lambda_X\lambda_X' + 204\lambda_X'^2 + 768\lambda_X'\lambda_X'' + 7008\lambda_X''^2 + 44616\lambda_X'\lambda_X''' - 73824\lambda_X''\lambda_X'''\\
&\quad + 2408676\lambda_X'''^2 + 3g_2^4 - 12Y_X^2\lambda_X' g_Y^2 - 144\lambda_X' g_2^2 + 12Y_X^2 g_2^2 g_Y^2 + \frac{1}{2}\kappa'^2\Big),\\
\frac{d\lambda_X''}{dt} &= \frac{1}{16\pi^2}\big(+ 8\lambda_X'^2 + 24\lambda_X\lambda_X'' + 96\lambda_X'\lambda_X'' + 1588\lambda_X''^2 + 912\lambda_X'\lambda_X''' + 5312\lambda_X''\lambda_X''' + 22696\lambda_X'''^2\\
&\quad + 6g_2^4 - 144\lambda_X'' g_2^2 - 12Y_X^2\lambda_X'' g_Y^2\big),\\
\frac{d\lambda_X'''}{dt} &= \frac{1}{16\pi^2}\big(+ 16\lambda_X'\lambda_X'' - 80\lambda_X''^2 + 24\lambda_X\lambda_X''' - 128\lambda_X'\lambda_X''' + 3056\lambda_X''\lambda_X''' - 12200\lambda_X'''^2\\
&\quad - 12Y_X^2\lambda_X''' g_Y^2 - 144\lambda_X''' g_2^2\big),\\
\frac{d\kappa}{dt} &= \frac{1}{16\pi^2}\Big(+ 3Y_X^2 g_Y^4 + 36g_2^4 + 12\kappa\lambda + 32\kappa\lambda_X + 48\kappa\lambda_X' + 1872\kappa\lambda_X'' + 4608\kappa\lambda_X''' + 6y_t^2\kappa\\
&\quad - \frac{3}{2}\kappa g_Y^2 - 6Y_X^2\kappa g_Y^2 - \frac{153}{2}\kappa g_2^2 + 4\kappa^2 + 12\kappa'^2\Big),\\
\frac{d\kappa'}{dt} &= \frac{1}{16\pi^2}\Big(+ 12Y_X g_2^2 g_Y^2 + 4\kappa'\lambda + 4\kappa'\lambda_X + 156\kappa'\lambda_X' + 384\kappa'\lambda_X'' + 13236\kappa'\lambda_X''' + 6y_t^2\kappa'\\
&\quad - \frac{3}{2}\kappa' g_Y^2 - 6Y_X^2\kappa' g_Y^2 - \frac{153}{2}\kappa' g_2^2 + 8\kappa\kappa'\Big).
\end{aligned}
\tag{222}
$$

B Sphaleron process and relation between number densities

In this appendix, we summarize the foundations of Sphaleron and thermal number density.

□**Sphaleron process**

In the SM, the baryon and lepton number are not conserved as a consequence of the anomaly. This is related to the topological charge of the SU(2) gauge field,

$$B(t_f) - B(t_i) = N_f\{N_{cs}(t_f) - N_{cs}(t_i)\}, \tag{223}$$

where

$$N_{cs}(t) = \frac{g^2}{32\pi^2}\int d^3x\epsilon^{ijk}\mathrm{Tr}[A_i\partial_j A_k + \frac{2}{3}igA_iA_jA_k] \tag{224}$$

is the Cern-Simon number, and N_f is the number of the generations. The transition rate at zero temperature is given by the instanton action,

$$\begin{aligned}\Gamma &\simeq e^{-S_{\rm Ins}} = e^{-\frac{4\pi}{g^2}} \\ &= \mathcal{O}(10^{-165}).\end{aligned} \tag{225}$$

Since this rate is very small, the violation of B (or L) does not occur at zero temperature. However, in a thermal bath, one can make transition between the gauge vacua, through thermal fluctuations. This transition rate is determined by the sphaleron configuration, a classical solution of the field theory [51]. The transition rate of this process is [48]

$$\Gamma_{sph} \simeq \alpha_W^4 \times T \times e^{-\frac{E_{sph}}{T}} \tag{226}$$

where $\alpha_W = g_2^2/4\pi$ and E_{sph} is the sphaleron energy. If the expansion rate of the universe $\frac{\dot{a}}{a} = H$ becomes lager than Γ_{sph}, the sphaleron process does not occur, and the total baryon number is fixed. The decoupling temperature is determined by equating H and Γ_{sph};

$$H \simeq \frac{T_{dec}^2}{M_{pl}} \simeq \alpha_W^4 \times T_{dec} \times e^{-\frac{E_{sph}}{T_{dec}}}. \tag{227}$$

Note that we have used $H \simeq \frac{T^2}{M_{pl}}$ because this process happens in the radiation dominated era. The important fact is that, if T_{dec} is comparable with the mass of the heavy particle, its abundance is suppressed by the factor $e^{-\frac{m}{T_{dec}}}$. For the actual determination of the decoupling temperature, see Appendix in [62] where the recent numerical study [130] is used.

□**Number density in thermal bath**

The number density of the particle species i which is thermalized is given by

$$\begin{aligned}n_i &= \frac{g_i}{(2\pi)^3}\int \frac{dp^3}{\exp\left(\frac{\sqrt{p^2+m_i^2}-\mu_i}{T}\right)\pm 1} \\ &= 4\pi g_i\left(\frac{T}{2\pi}\right)^3\int_0^\infty dx\frac{x^2}{\exp\left(\sqrt{x^2+(\frac{m_i}{T})^2}-\frac{\mu_i}{T}\right)\pm 1}\end{aligned} \tag{228}$$

where g_i represents the degree of freedom, and the sign $\pm$ is $-$ for bosons and $+$ for fermions. We can obtain the antiparticle density $\bar{n}_i$ by replacing μ_i with $-\mu_i$ in Eq.(228). Then, the difference

between the number density of particle and antiparticle is

$$
\begin{aligned}
n_i - \bar{n}_i &= 4\pi g_i \left(\frac{T}{2\pi}\right)^3 \int_0^\infty dx\, x^2 \times \left(\frac{1}{\exp\left(\sqrt{x^2 + (\frac{m_i}{T})^2} - \frac{\mu_i}{T}\right) \pm 1} - \frac{1}{\exp\left(\sqrt{x^2 + (\frac{m_i}{T})^2} + \frac{\mu_i}{T}\right) \pm 1} \right) \\
&\simeq 8\pi g_i \mu_i \frac{T^2}{(2\pi)^3} \int_0^\infty dx\, x^2 \times \frac{\exp\sqrt{x^2 + (m_i/T)^2}}{\left(\exp\sqrt{x^2 + (m_i/T)^2} \pm 1\right)^2} \\
&= 2\pi g_i \mu_i \frac{T^2}{(2\pi)^3} \int_0^\infty dx\, x^2 \begin{cases} \frac{1}{\cosh^2(\frac{\sqrt{x^2+(m_i/T)^2}}{2})} & \text{(for fermion)} \\ \\ \frac{1}{\sinh^2(\frac{\sqrt{x^2+(m_i/T)^2}}{2})} & \text{(for boson)} \end{cases} \\
&:= g_i \mu_i \frac{T^2}{6} \begin{cases} g_f(m_i) & \text{(for fermion)}, \\ \\ g_b(m_i) & \text{(for boson)}, \end{cases}
\end{aligned} \tag{229}
$$

where

$$
\begin{aligned}
g_f(m_i) &:= \frac{3}{2\pi^2} \int_0^\infty dx x^2 \frac{1}{\cosh^2(\frac{\sqrt{x^2+(m_i/T)^2}}{2})}, \\
g_b(m_i) &:= \frac{3}{2\pi^2} \int_0^\infty dx x^2 \frac{1}{\sinh^2(\frac{\sqrt{x^2+(m_i/T)^2}}{2})}.
\end{aligned} \tag{230}
$$

Here we can take $\frac{T^2}{6}$ as a unit:

$$
n_i - \bar{n}_i = g_i \mu_i \begin{cases} g_f(m_i) & \text{(for fermion)} \\ \\ g_b(m_i) & \text{(for boson)}. \end{cases} \tag{231}
$$

where $g_f(0) = 1, g_b(0) = 2$. From these results, one can see that the existence of asymmetry is equivalent to $\mu_i \neq 0$. In the following, we denote the chemical potentials for the conserved quantities as μ_a. Since the chemical potentials $\{\mu_i\}$ are conserved in thermal equilibrium, they can be written as linear combinations of the conserved quantum numbers;

$$
\mu_i = \sum_a q_{ia} \mu_a. \tag{232}
$$

In the broken phase, the conserved quantum numbers are $B - L$ and the electromagnetic charge Q, and we can write the chemical potential μ_i for each species as

$$
\mu_u = \frac{1}{3}\mu_{B-L} + \frac{2}{3}\mu_Q \tag{233}
$$

$$\mu_d = \frac{1}{3}\mu_{B-L} - \frac{1}{3}\mu_Q \tag{234}$$

$$\mu_e = -\mu_{B-L} - \mu_Q \tag{235}$$

$$\mu_{\nu_e} = -\mu_{B-L} \tag{236}$$

$$\mu_W = -\mu_Q. \tag{237}$$

We can eliminate μ_Q by using the fact that Q is zero:

$$\begin{aligned} Q =& \frac{2}{3}\sum_{i:\text{u sector}} g_i g_f(m_i)\left(\frac{1}{3}\mu_{B-L} + \frac{2}{3}\mu_Q\right) - \frac{1}{3}\sum_{i:\text{d sector}} g_i g_f(m_i)\left(\frac{1}{3}\mu_{B-L} - \frac{1}{3}\mu_Q\right) \\ &- \sum_{i:\text{e sector}} g_i g_f(m_i)(-\mu_{B-L} - \mu_Q) + 3g_b(m_W)\mu_Q = 0. \end{aligned} \tag{238}$$

This leads to

$$\mu_Q = -\mu_{B-L}\frac{4\sum_{i:\text{u}} g_f(m_i) - 2\sum_{i:\text{d}} g_f(m_i) + 6\sum_{i:\text{e}} g_f(m_i)}{8\sum_{i:\text{u}} g_f(m_i) + 2\sum_{i:\text{d}} g_f(m_i) + 6\sum_{i:\text{e}} g_f(m_i) + 9g_b(m_W)}. \tag{239}$$

As a result, the baryon and lepton number densities are given by

$$\begin{aligned} B :=& n_B - \bar{n}_B = 6\cdot\frac{1}{3}\left(\frac{1}{3}\mu_{B-L} + \frac{2}{3}\mu_Q\right)\cdot\sum_{i:\text{u sector}} g_f(m_i) + 6\cdot\frac{1}{3}\left(\frac{1}{3}\mu_{B-L} - \frac{1}{3}\mu_Q\right)\cdot\sum_{i:\text{d sector}} g_f(m_i) \\ =& \frac{2\mu_{B-L}}{3}\left[\frac{6\sum_{i:\text{d}} g_f(m_i) - 6\sum_{i:\text{e}} g_f(m_i) + 9g_b(m_W)}{8\sum_{i:\text{u}} g_f(m_i) + 2\sum_{i:\text{d}} g_f(m_i) + 6\sum_{i:\text{e}} g_f(m_i) + 9g_b(m_W)}\sum_{i:\text{u}} g_f(m_i)\right. \\ &\left. + \frac{12\sum_{i:\text{u}} g_f(m_i) + 12\sum_{i:\text{e}} g_f(m_i) + 9g_b(m_W)}{8\sum_{i:\text{u}} g_f(m_i) + 2\sum_{i:\text{d}} g_f(m_i) + 6\sum_{i:\text{e}} g_f(m_i) + 9g_b(m_W)}\sum_{i:\text{d}} g_f(m_i)\right] \end{aligned} \tag{240}$$

$$\begin{aligned} L :=& n_L - \bar{n}_L = 2\cdot(-\mu_{B-L} - \mu_Q)\sum_{i:e} g_f(m_i) - 3\mu_{B-L} \\ =& \mu_{B-L}\{-2\frac{4\{\sum_{i:\text{u}} g_f(m_i) + \sum_{i:\text{d}} g_f(m_i)\} + 9g_b(m_W)}{8\sum_{i:\text{u}} g_f(m_i) + 2\sum_{i:\text{d}} g_f(m_i) + 6\sum_{i:\text{e}} g_f(m_i) + 9g_b(m_W)}\sum_{i:\text{e}} g_f(m_i) - 3\} \end{aligned} \tag{241}$$

where we have assumed that neutrinos are massless. Once N_{B-L} is given, the baryon number is given by

$$N_B = \frac{B}{B-L}N_{B-L}. \tag{242}$$

Here, we do not write the explicit result because it is rather complicated. When all the particles massless, we obtain

$$N_B = \frac{8N_g + 4N_d}{22N_g + 13N_d}N_{B-L}, \tag{243}$$

where N_g is the generation number, N_d is the number of scalar doublet. In the SM, this leads to

$$N_B = \frac{28}{79}N_{B-L}. \tag{244}$$

C Multi-local theory from the matrix model

In this appendix, we discuss a concrete example of an appearance of the multi-local theory from the matrix model [79, 65]. In the original Coleman's argument, such a multi-locality was originated in wormholes. In the matrix model, however, the matrices itself become non-local objects. (See Fig.(25) for example.) In the following, we adopt the covariant derivative interpretation [80] of the matrix model because it has the manifest diffeomorphism invariance. Our aim is to show that the effective action in this interpretation is given by the multi-local action.

The action of the IIB matrix model is given by

$$S_{IIB} = \frac{1}{g^2}\mathrm{Tr}\left(\frac{1}{4}[X^a, X^b][X^c, X^d]\eta_{ac}\eta_{bd} + \frac{1}{2}\bar{\Psi}\Gamma^a[X^b, \Psi]\eta_{ab}\right), \tag{245}$$

where a, b, c, and d are the ten dimensional Lorentz indices, X^a and Ψ are a ten dimensional vector and a Majorana spinor respectively, and they are also $N \times N$ hermitian matrices. Eq.(245) has the manifest $SO(9,1)$ and $U(N)$ invariances. For now, it is sufficient to consider X^a only. In the covariant derivative interpretation, we interpret X^a as a linear operator acting on smooth functions on a given D (≤ 10) dimensional manifold $\mathcal{M}$:

$$X^a \in End(C^\infty(\mathcal{M})) = \{C^\infty(\mathcal{M}) \to C^\infty(\mathcal{M})\}\,., \tag{246}$$

and the operation of X^a can be explicitly written as

$$\begin{aligned}(X^a f)(x) &= \int d^D y\ X^a(x,y) f(y) \\ &= \left(S^a(x) + a^{a\mu}(x)\bigtriangledown_\mu + b^{a\mu\nu}(x)\bigtriangledown_\mu\bigtriangledown_\nu + \cdots\right) f(x) \\ &\qquad\qquad \text{for } {}^\forall f(x) \in C^\infty(\mathcal{M}),\end{aligned} \tag{247}$$

where we have expanded the kernel $X^a(x,y)$ by infinite local fields with integer spins and the covariant derivative $\bigtriangledown$ on $\mathcal{M}$. See Fig.25 for example. This represents a schematic explanation of Eq.(247), and one can see that matrices are non-local objects in this interpretation. As a result, they contain infinite local fields if we expand them around a point. Here, note that ten dimensional Lorentz index a has no relation to D dimensional index μ in general. The classical equation of motion of X^a's is given by

$$\eta_{ab}\left[X^a, \left[X^b, X^c\right]\right] = 0. \tag{248}$$

Among the various solutions, the following one

$$X_a = \begin{cases} i\bigtriangledown_a = e^\mu_a(x)\bigtriangledown_\mu & \text{for } a = 0, 1, \cdots, D-1, \\ 0 & \text{for } a = D, \cdots, 9 \end{cases} \tag{249}$$

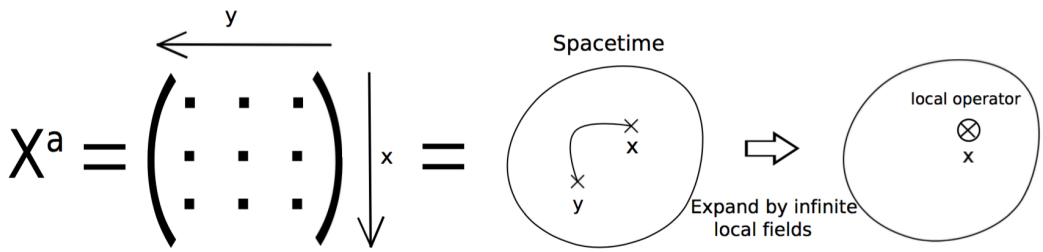

Figure 25: The covariant derivative interpretation of matrix model. i and j of a matrix $(X^a)_{ij}$ represent two points on a manifold $\mathcal{M}$ (left), and $(X^a)_{ij}$ operates on a function $f(x)$ as $\sum_{ij}(X^a)_{ij}f(x_i)$ (middle). However, by introducing infinite local fields, it can be also represented as a local operator (right).

is notable because Eq.(248) corresponds to the Einstein equation in this case:

$$\begin{aligned}[\nabla^a,[\nabla_a,\nabla_b]] &= \left[\nabla^a, R^{cd}_{ab}\times\hat{\mathcal{O}}_{cd}\right] \\ &= \left(\nabla^a R^{cd}_{ab}\right)\hat{\mathcal{O}}_{cd} - R^{cd}_{ab}\,\hat{\mathcal{O}}_{cd}\nabla^a = 0 \\ &\leftrightarrow \nabla^a\, R^{cd}_{ab} = 0,\ R_{ab} = 0 \end{aligned} \tag{250}$$

where $\hat{\mathcal{O}}_{cd}$ is the D dimensional Lorentz generator, and we have interpreted $e^\mu_a(x)$ as the vielbein field. This fact tells us that gravity can be actually contained in the degrees of freedom of matrices. Here, note that an existence of spacetime manifold is assumed from the beginning in the covariant interpretation of the matrix model.

Furthermore, we can find the diffeomorphism invariance within the original $U(N)$ symmetry:

$$\delta X^a = i\left[\Lambda, X^a\right],\ \Lambda\in N\times N \text{ Hermitian matrix.} \tag{251}$$

The explicit form of Λ in the large N limit is given by

$$\Lambda = \lambda(x) + \frac{i}{2}\left\{\lambda^\mu(x),\nabla_\mu\right\} + \frac{i^2}{2}\left\{\lambda^{\mu\nu}(x),\nabla_\mu\nabla_\nu\right\} + \cdots \tag{252}$$

as well as X^a. Here, we have introduced the anti-commutator $\{\ ,\ \}$ to make each terms hermitian. In fact, by taking the hermitian conjugate, we have

$$\Lambda^\dagger = \lambda(x) - \frac{i}{2}\left\{\nabla^\dagger_\mu,\lambda^\mu(x)\right\} + \frac{(-i)^2}{2}\left\{\nabla^\dagger_\mu\nabla^\dagger_\nu,\lambda^{\mu\nu}(x)\right\} + \cdots, \tag{253}$$

where $\nabla^\dagger_\mu$ is the derivative which acts on a function on the left (by definition). Thus, by neglecting the total derivative term, we obtain the same expression as Eq.(252). Note that we must take

the order of $\lambda^{\mu\nu\cdots}(x)$ and $\bigtriangledown_\mu$ into consideration to obtain the correct result. The second term in Eq.(252)

$$\Lambda = \frac{i}{2}\left\{\lambda^\mu(x), \bigtriangledown_\mu\right\} \tag{254}$$

represents the diffeomorphism of the fields appearing in Eq.(247). For example, the scalar $S^a(x)$ transforms as

$$\delta S^a(x) = i\left[\Lambda, S^a\right] = \lambda^\mu(x) \bigtriangledown_\mu S^a(x), \tag{255}$$

and this is actually the diffeomorphism transformation of scalar. Thus, one can see that all the information of a curved manifold $\mathcal{M}$ can be embedded in the matrices X^a's. However, the above argument is not mathematically rigorous because $X_a = e^\mu_a(x)\bigtriangledown_\mu$ is not in fact included in $End(C^\infty(\mathcal{M}))$. Naively, this is because $\bigtriangledown_i$ maps functions on $\mathcal{M}$ to vectors on it [25]. To overcome this situation, new covariant derivative interpretation was proposed in [80] where X^a's are interpreted as linear operators acting on smooth functions on the principal bundle E_{prin} whose base space is $\mathcal{M}$, and fibre is $Spin(D-1,1)$. The result of [80] is mathematically rigorous, so we can actually realize a curved spacetime by matrix. For our present purpose, however, we do not need such a rigorous result, and we proceed our discussion based on the above naive covariant derivative interpretation in the following [26].

To examine the effective action, we use the background field method:

$$X^a(x,y) = \tilde{X}^a(x,y) + \phi^a(x,y), \tag{258}$$

where $\tilde{X}^a(x,y)$ is the background field, and $\phi^a(x,y)$ represents the fluctuation which should be

[25] More concretely, $\bigtriangledown_\mu$ is explicitly written as $\bigtriangledown_\mu = \partial_\mu + \omega^{ab}_\mu(x)\hat{O}_{ab}$, where $\omega^{ab}_\mu(x)$ is a connection, and, as well as $\hat{\mathcal{O}}_{ab}$, its explicit form depends on the representation of a function it operates. For example, when they operate the Lorentz vector, we have $(\hat{O}_{ab})^\mu_\nu = \eta^{\mu a}\delta^b_\nu - \delta^a_\nu\eta^{\mu b}$, $2\omega^\nu_{\mu\lambda}(x) = \Gamma^\nu_{\mu\lambda}(x)$, where the raising or lowering of indices is done by flat metric. If we consider the product of $X_1 = i\bigtriangledown_1 := ie^\mu_1\bigtriangledown_\mu$ and $X_2 = i\bigtriangledown_2 = ie^\mu_2\bigtriangledown_\mu$, it is given by

$$X_1 \cdot X_2 = (i\bigtriangledown_1)(i\bigtriangledown_2) = -e^\mu_1\partial_\mu(e^\nu_2\bigtriangledown_\nu) - e^\mu_1\omega^{2c}_\mu\bigtriangledown_c = -e^\mu_1\partial_\mu(e^\nu_2\bigtriangledown_\nu) - e^\mu_1\omega^{2c}_\mu X_c, \tag{256}$$

from which we can see that the right hand side is not a product of X_1 and X_2, but contains other matrices. Therefore, in this naive covariant derivative interpretation, $\bigtriangledown_i$ is not included in $End(C^\infty(\mathcal{M}))$.

[26] There exist some subtle problems in the new interpretation. For example, because it also has degrees of freedom of fibre, more infinite number of fields appear if we expand the matrix:

$$X^a(x,g) = \sum_r R^r_{ij}(g)A_{ij}(x), \tag{257}$$

where r denotes the representation of $Spin(D-1,1)$. How these infinite fields are related to ordinary field theory is not yet understood.

integrated out. The bosonic part of the action Eq.(245) now becomes

$$S_{IIB}\Big|_{boson} = \frac{1}{4g^2}\mathrm{Tr}\Big([\tilde{X}^a,\tilde{X}^b][\tilde{X}_a,\tilde{X}_b] + 4[\tilde{X}^a,\tilde{X}^b][\tilde{X}_a,\phi_b] + 2[\tilde{X}^a,\phi^b][\tilde{X}_a,\phi_b] + 2[\tilde{X}^a,\tilde{X}^b][\phi_a,\phi_b] + 2[\tilde{X}^a,\phi^b][\phi_a,\tilde{X}_b] + 4[\phi^a,\tilde{X}^b][\phi_a,\phi_b] + [\phi^a,\phi^b][\phi_a,\phi_b]\Big), \tag{259}$$

where the second term can be always eliminated by the field redefinition of ϕ^a. Although there are three quadratic terms in Eq.(259), it is sufficient to consider the third term in Eq.(259) for our qualitative understanding:

$$S_{\phi^2} = \frac{1}{2}\mathrm{Tr}\left([\tilde{X}^a,\phi][\tilde{X}^a,\phi]\right), \tag{260}$$

where we have put $g = 1$, and picked up one component of ϕ^a's for simplicity. The effective theory on the flat spacetime can be obtained by expanding the background field around the flat derivative:

$$\tilde{X}^a(x,y) = \delta^{(D)}(x-y) \times \begin{cases} i\partial^a + A^a(x,\partial_x) & \text{for } a = 0,1,\cdots,D-1 \\ A^a(x,\partial_x) & \text{for } a = D,\cdots,9 \end{cases}, \tag{261}$$

where $A^a(x,\partial_x)$ is a function of x and its derivative, and contains infinite local fields like Eq.(247) and Eq.(252). In this case, Eq.(260) becomes

$$S_{\phi^2} = \frac{1}{2}\int d^Dx \int d^Dy \left[\left(\frac{\partial}{\partial x^\mu} + \frac{\partial}{\partial y^\mu} - i\mathcal{A}_\mu(x,\partial_x;y,\partial_y)\right)\phi(x,y)\right]^2 + \frac{1}{2}\int d^Dx \int d^Dy \left[\mathcal{A}_a(x,\partial_x;y,\partial_y)\phi(x,y)\right]^2, \tag{262}$$

where

$$\mathcal{A}_a(x,\partial_x;y,\partial_y) = A_a(x,\partial_x) - A_a(y,\partial_y). \tag{263}$$

From Eq.(262), we can read the propagator of $\phi(x,y)$ as

$$D(x_1,y_1;x_2,y_2) = G((x_1+y_1)-(x_2+y_2)) \times \delta^{(D)}((x_1-y_1)-(x_2-y_2)), \tag{264}$$

where $G(x)$ is the propagator of free massless scalar. We represent this propagator and the three (four) point vertex between ϕ and the background $A_a(x,\partial_x)$ or $A_a(y,\partial_y)$ by the double lines and the circled cross mark respectively. See Fig.26 for example. Note that only one external wavy line sticks to the vertex because $\phi(x,y)$ interacts $A_a(x,\partial_x)$ or $A_a(y,\partial_y)$.

We can now calculate the effective action

$$\exp\left(iS_{\mathrm{eff}}[\mathcal{A}]\right) = \int \mathcal{D}\phi \ \exp\left(iS_{\phi^2}\right) \tag{265}$$

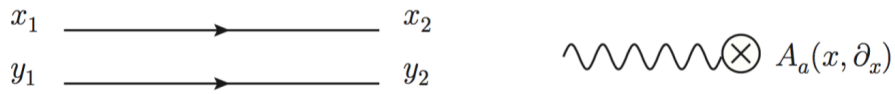

Figure 26: Left: The propagator of the fluctuation $\phi(x, y)$. Right: The background field $A_a(x, \partial_x)$ or $A_a(y, \partial_y)$.

based on the loop expansion. This is absolutely the same calculation as the effective potential in QFT [27]. For example, at two-loop level[28], we must calculate the one-loop closed diagram of $\phi(x, y)$ with arbitrary n insertions of A_a:

$$\int d^D x \int d^D y \prod_{i=1}^{n} \Bigg[\int d^D x_i \int d^D y_i D(x_{i+1}, y_{i+1}; x_i, y_i) \times \begin{cases} \partial^\mu A_\mu(x_i, \partial_{x_i}),\ \partial^\mu A_\mu(y_i, \partial_{y_i}) \\ \qquad \text{or} \\ A_a(x_i, \partial_{x_i})^2,\ A_a(y_i, \partial_{y_i})^2,\ 2A^a(x_i, \partial_{x_i}) A_a(y_i, \partial_{y_i}) \end{cases} \Bigg] \times D(x_1, y_1; x, y) \tag{267}$$

where $x_{n+1} = x$, $y_{n+1} = y$. See the left figure in Fig.27 for example. For our present purpose, it is sufficient to consider the cubic interaction $\phi\phi\partial^\mu A_\mu$ because our conclusion does not change even if we consider the quartic interaction $\phi\phi A_a^2$. In order to obtain the effective action written by local

[27]For example, if we neglect the quartic interaction $\phi\phi\mathcal{A}_a^2$ in Eq.(262), $S_{\text{eff}}[\mathcal{A}]$ can be understood as the generating functional of n point correlation function of ϕ. Thus, it can be expanded as

$$S_{\text{eff}}[\mathcal{A}] = \sum_{n=0}^{\infty} \int d^D x_1 \int d^D y_1 \cdots \int d^D x_n \int d^D y_n G^{(n)}(x_1, y_1; x_2, y_2; \cdots; x_n, y_n) \partial^\mu \mathcal{A}_\mu(x_1, \partial_{x_1}; y_1, \partial_{y_1}) \times \cdots \times \partial^\mu \mathcal{A}_\mu(x_n, \partial_{x_n}; y_n, \partial_{y_n}), \tag{266}$$

where $G^{(n)}$ is the n point correlation function. The one-loop effective action corresponds to considering the one-loop diagram of $G^{(n)}$.

[28]Here, we use the term "n-loop" as the number of the spacetime integrals. Thus, one-loop of ϕ corresponds to two-loop in our case.

fields, let us expand each $A_a(x_i, \partial_{x_i})$'s like Eq.(252):

$$\begin{aligned}
A^a(x_i, \partial_{x_i}) &= \hat{A}^a(x_i) + \frac{i}{2}\left\{\hat{A}^{a\mu}(x_i), \partial^{(i)}_\mu\right\} + \frac{i^2}{2}\left\{\hat{A}^{a\mu\nu}(x_i), \partial^{(i)}_\mu \partial^{(i)}_\nu\right\} + \cdots \\
&= \sum_{k=0}^{\infty} \frac{i^n}{k!}\{\hat{A}^{a\mu_1\cdots\mu_k}(x_i), \partial^{(i)}_{\mu_1}\cdots\partial^{(i)}_{\mu_k}\} \\
&= \sum_{k=0}^{\infty} \frac{i^n}{k!} \sum_{m=0}^{\infty} \frac{1}{m!} \hat{A}^{a\mu_1\cdots\mu_k}_{\nu_1\cdots\nu_m}(x)\{\tilde{x}_i^{\nu_1}\cdots\tilde{x}_i^{\nu_m}, \tilde{\partial}^{(i)}_{\mu_1}\cdots\tilde{\partial}^{(i)}_{\mu_k}\} \\
&:= \sum_{k=0}^{\infty} \frac{i^n}{k!} \sum_{m=0}^{\infty} \frac{1}{m!} \hat{A}^{a\{\mu\}}_{\{\nu\}}(x)\hat{\mathcal{P}}^{(i)\{\nu\}}_{\{\mu\}}(\tilde{x}_i, \tilde{\partial}^{(i)}).
\end{aligned} \tag{268}$$

where $\tilde{x}_i = x_i - x$, $\tilde{\partial}^{(i)}_\mu$ is the derivative with respect to $\tilde{x}_i^\mu$, and we have expanded $\hat{A}^{a\mu_1\cdots\mu_k}(x_i)$ around x from the second line to the third line. Note that we have also used

$$\frac{\partial}{\partial x_i^\mu} = \frac{\partial}{\partial \tilde{x}_i^\mu}. \tag{269}$$

By substituting Eq.(268) into Eq.(267), we generally obtain

$$\begin{aligned}
&\int d^D x \left(\hat{A}^{\alpha_1\{\mu_1\}}_{\{\nu_1\}}(x)\cdot\cdots\cdot\hat{A}^{\alpha_l\{\mu_l\}}_{\{\nu_l\}}(x)\right)\int d^D y\left(\hat{A}^{\beta_1\{\mu_1\}}_{\{\nu_1\}}(y)\cdot\cdots\cdot\hat{A}^{\beta_f\{\mu_f\}}_{\{\nu_f\}}(y)\right)\times\left(\prod_{j=1}^{n}\int d^D\tilde{x}_j\int d^D\tilde{y}_j\right) \\
&\times D(x,y;\tilde{x}_n,\tilde{y}_n)\times\begin{cases}\tilde{\partial}^{(n)}_\alpha\hat{\mathcal{P}}^{(n)\{\nu\}}_{\{\mu\}}(\tilde{x}_n,\tilde{\partial}^{(n)}) \\ \quad\text{or} \\ \tilde{\partial}^{(n)}_\beta\hat{\mathcal{P}}^{(n)\{\nu\}}_{\{\mu\}}(\tilde{y}_n,\tilde{\partial}^{(n)})\end{cases}\times D(\tilde{x}_n,\tilde{y}_n;\tilde{x}_{n-1},\tilde{y}_{n-1})\times\cdots\times\begin{cases}\tilde{\partial}^{(1)}_\alpha\hat{\mathcal{P}}^{(1)\{\nu\}}_{\{\mu\}}(\tilde{x}_1,\tilde{\partial}^{(1)}) \\ \quad\text{or} \\ \tilde{\partial}^{(1)}_\beta\hat{\mathcal{P}}^{(1)\{\nu\}}_{\{\mu\}}(\tilde{y}_1,\tilde{\partial}^{(1)})\end{cases} \\
&\times D(\tilde{x}_1,\tilde{y}_1;x,y),
\end{aligned} \tag{270}$$

where the numbers l and f depend on the choice of vertexes, and we have changed the variable of each of the integrations from x_i (y_i) to $\tilde{x}_i$ ($\tilde{y}_i$). Note that we have not explicitly written the lower index of α (β) in $\tilde{\partial}^{(i)}_\alpha$ ($\tilde{\partial}^{(i)}_\beta$) because there are many possible ways of their contractions. Furthermore, from Eq.(264), we can see that $D(\tilde{x}_1,\tilde{y}_1;x,y)$ and $D(x,y;\tilde{x}_n,\tilde{y}_n)$ do not depend on x and y; In fact, we have

$$\begin{aligned}
D(\tilde{x}_1,\tilde{y}_1;x,y) &= G(\tilde{x}_1+\tilde{y}_1+x+y-(x+y))\times\delta^{(D)}\left((\tilde{x}_1-\tilde{y}_1+x-y)-(x-y)\right) \\
&= G(\tilde{x}_1+\tilde{y}_1)\times\delta^{(D)}\left(\tilde{x}_1-\tilde{y}_1\right).
\end{aligned} \tag{271}$$

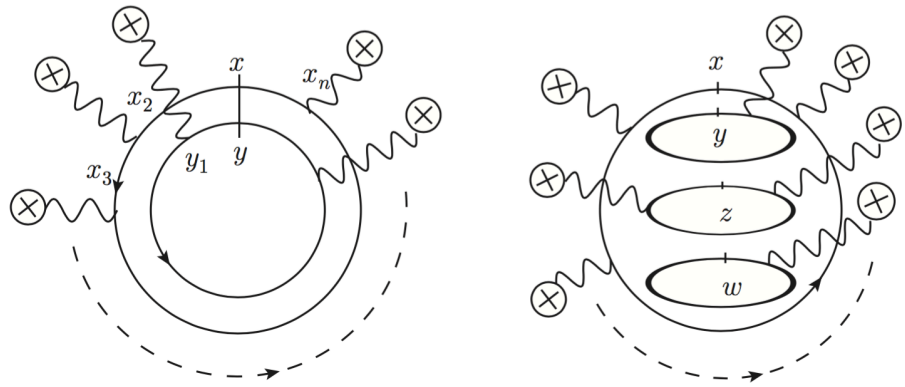

Figure 27: Typical two-loop (left) and four-loop (right) diagrams in the covariant derivative interpretation of the matrix model. The number of loops corresponds to the number of the products of the effective actions.

As a result, the underlined part in Eq.(270) is just a coefficient, and we finally obtain the factorized bi-local action:

$$c^{\{\nu_1\}\cdots\{\nu_l\},\{\nu_1\}\cdots\{\nu_f\}}_{\alpha_1\cdots\alpha_l\beta_1\cdots\beta_f\{\mu_1\}\cdots\{\mu_l\},\{\mu_1\}\cdots\{\mu_f\}} \int d^Dx \left(\hat{A}^{\alpha_1\{\mu_1\}}_{\{\nu_1\}}(x)\cdot\cdots\cdot\hat{A}^{\alpha_l\{\mu_l\}}_{\{\nu_l\}}(x)\right)\int d^Dy\left(\hat{A}^{\beta_1\{\mu_1\}}_{\{\nu_1\}}(y)\cdot\cdots\cdot\hat{A}^{\beta_f\{\mu_f\}}_{\{\nu_f\}}(y)\right). \tag{272}$$

The reason of the "bi-local" comes from the number of loops in a diagram: Because one-loop of ϕ corresponds to two-loop of the spacetime integrals, the corresponding effective action becomes bi-local. This feature descends to higher loop diagrams. When we consider m-loop diagram with arbitrary number of insertion of A_a's, we generally obtain

$$\sum_{i_1,\cdots,i_m} c_{i_1\cdots i_m}\int d^Dx_1\mathcal{O}_{i_1}(x_1)\times\int d^Dx_2\mathcal{O}_{i_2}(x_2)\times\cdots\times\int d^Dx_m\mathcal{O}_{i_m}(x_m), \tag{273}$$

where i_k's represent the various indexes. See the right figure of Fig.27 for example. Here we show a four-loop closed diagram where the self interaction of ϕ comes from the last term in Eq.(262). Thus, the effective action $S_{\text{eff}}[\mathcal{A}]$ in the covariant derivative interpretation of the matrix model generally contains many multi-local actions, and the effective couplings become dynamical by making the Fourier transform.

D Effect of the expansion of the universe

If we take the expansion of the universe into consideration, we can write the partition function of a system as

$$\begin{aligned} Z &= \int_{t=0}^{t=\infty} \mathcal{D}\phi \exp\left(iS_M\right) \psi_f^* \psi_i \\ &= \int d\overrightarrow{\lambda} f(\overrightarrow{\lambda}) \int_{t=0}^{t=\infty} \mathcal{D}\phi \exp\left(i \sum_i \lambda_i S_i\right) \psi_f^* \psi_i \\ &= \int d\overrightarrow{\lambda} f(\overrightarrow{\lambda}) \langle f | T \exp\left(-i \int_0^{+\infty} dt \hat{H}(\overrightarrow{\lambda}; a_{cl}(t))\right) | i \rangle, \end{aligned} \tag{274}$$

where $a_{cl}(t)$ is the radius of the universe determined by the Friedman equation, ψ_i and ψ_f represent initial and final states which are independent of $\overrightarrow{\lambda}$, and we have assumed that the universe eternally expands like our universe. At a first glance, it seems difficult to evaluate Z because it involves the total history of the universe. However, in almost all the time, the universe is sufficiently expanded, and its energy density is very close to that of the vacuum. More concretely, we have

$$T \exp\left(-i \int_0^{+\infty} dt \hat{H}(\overrightarrow{\lambda}; a_{cl}(t))\right) |i\rangle \sim \exp\left(-i\varepsilon(\overrightarrow{\lambda}) \int_{t^*}^{+\infty} dt V_3(a_{cl}(t))\right) |\psi(t^*; \overrightarrow{\lambda})\rangle, \tag{275}$$

where

$$|\psi(t; \overrightarrow{\lambda})\rangle = T \exp\left(-i \int_0^t dt' \hat{H}(\overrightarrow{\lambda}; a_{cl}(t'))\right) |i\rangle, \tag{276}$$

$V_3(a_{cl}(t))$ is the space volume, $\varepsilon(\overrightarrow{\lambda})$ is the vacuum energy density, and t^* is a time such that the energy density of the state $|\psi(t; \overrightarrow{\lambda})\rangle$ is sufficiently closed to $\varepsilon(\overrightarrow{\lambda})$. By substituting Eq.(275) to Eq.(274), we obtain

$$Z \sim \int d\overrightarrow{\lambda} f(\overrightarrow{\lambda}) \exp\left(-i\varepsilon(\overrightarrow{\lambda}) \int_{t^*}^{+\infty} dt V_3(a_{cl}(t))\right) \langle f | \psi(t^*; \overrightarrow{\lambda})\rangle. \tag{277}$$

Thus, as long as we concentrate on the expansion universe, the vacuum energy is inevitably going to dominate the energy density, and the partition function is also strongly dominated by it. In this sense, the effect of the expansion corresponds to the $i\epsilon$ in ordinary time independent QFT.

E Wheeler-Dewitt generalization

In this Appendix, we consider the generalization of Eq.(130) to the Wheeler-Dewitt wave function. As we mentioned in Section 4, considering the negative cosmological constant $\Lambda < 0$ is difficult

because we do not know the final state of the universe. On the other hand, in the positive region $\Lambda > 0$, we can consider the Wheeler-Dewitt wave function for the entire region of the radius of the universe, and examine which value of $\overrightarrow{\lambda}$ dominates. Therefore, we take only the region $\Lambda > 0$ into account in the path integral.

Then the generalization of Eq.(130) to the Wheeler-Dewitt wave function is given by

$$Z_{WD} = \int d\Lambda_B \int d\overrightarrow{\lambda} f(\Lambda_B, \overrightarrow{\lambda})\theta(\Lambda) \int_0^\infty dT \, \langle f_a| \otimes \langle f_{MR}| e^{-i\left(\hat{H}_G(\Lambda_B)+\hat{H}_{MR}(\overrightarrow{\lambda};\hat{a})\right)T} |\epsilon\rangle \otimes |i_{MR}\rangle, \quad (278)$$

where $\hat{H}_G(\Lambda_B) := -\hat{p}_a^2/\left(2\hat{a}M_{pl}^2\right) + \Lambda_B$ is the Hamiltonian for the radius of the universe a with a bare CC Λ_B [62], $\hat{H}_{MR}(\overrightarrow{\lambda};\hat{a})$ represents the other degrees of freedom, and $|\epsilon\rangle \otimes |i_{MR}\rangle$ ($|f_a\rangle \otimes |f_{MR}\rangle$) is an initial (a final) state of the universe. Here, we have assumed that the universe started with a tiny radius $a = \epsilon$. Note that the integration over T comes from the path integral for the lapse function $N(t)$ which is defined by

$$d^2s = -N(t)^2 d^2t + a(t)^2 d^2\mathbf{x}. \quad (279)$$

As for the final state, we take $|f_a\rangle = |a_\infty\rangle$ where a_∞ represents the large radius of the universe because it exponentially expands finally. In this generalization, the fine-tunings of other couplings than the CC can take place as follows: Eq.(278) differs from Eq.(130) in that it contains the integration over the time T. However, because our universe is well described by the classical Friedman universe, for a fixed value of a, the T integral is dominated by T_a at which the radius of the universe becomes a. See Fig.28 for example. More concretely, we have

$$\begin{aligned}\int_0^\infty dT \, \langle a| \otimes \langle f_{MR}| e^{-i\left(\hat{H}_G(\Lambda_B)+\hat{H}_{MR}(\overrightarrow{\lambda};\hat{a})\right)T} |\epsilon\rangle \otimes |i_{MR}\rangle &\sim \langle f_{MR}| T \exp\left(-i\int_0^{T_a} dt \hat{H}_{MR}(\overrightarrow{\lambda}; a_{cl}(t))\right) |i_{MR}\rangle \\ &:= \langle f_{MR}|\psi_{MR}(T_a)\rangle, \end{aligned} \quad (280)$$

where we have omitted the integrations over Λ_B and $\overrightarrow{\lambda}$ for simplicity. Here, $a_{cl}(t)$ satisfies the following Friedman equation and the boundary condition:

$$H^2 := \left(\frac{\dot{a_{cl}}}{a_{cl}}\right)^2 = \frac{1}{3M_{pl}^2}\left(\Lambda_B + \frac{\langle\psi_{MR}(t)|\hat{H}_{MR}(\overrightarrow{\lambda}; a_{cl}(t))|\psi_{MR}(t)\rangle}{V_3(a_{cl}(t))}\right) \ , \ a_{cl}(0) = \epsilon, \quad (281)$$

where $V_3(a_{cl}(t))$ is the volume of the space. We can understand Eq.(280) within the Born-Oppenheimer approximation [131] by assuming that the expansion rate H is very small compared with the energy scale of the other degrees of freedom.

Using Eq.(280), we can rederive the results of the previous Appendix. For a sufficiently large value of a, we can replace the Hamiltonian $\hat{H}_{MR}(\overrightarrow{\lambda}; a_{cl}(T_a))$ by the vacuum energy $E_0(\overrightarrow{\lambda}; a_{cl}(T_a)) =$

$$\int_0^\infty dt\, \langle a'|e^{-i\hat{H}t}|i\rangle\Big|_{\text{Born-Oppenheimer}} =$$

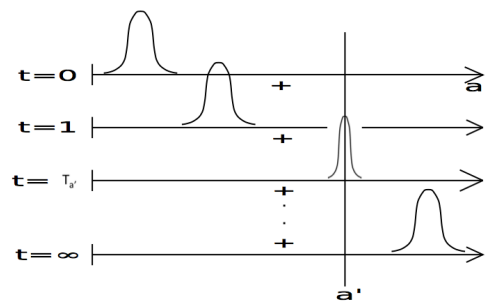

Figure 28: Image of the time integration of the wave function. Within the Born-Oppenheimer approximation, the center value of a evolves by the classical solution.

$\varepsilon(\overrightarrow{\lambda})V_3(a_{cl}(T_a))$ as in Eq.(277). Therefore, the right hand side of Eq.(280) becomes

$$\exp\left(-i\int_0^{T_a} dt\hat{H}_{MR}(\overrightarrow{\lambda}, a_{cl}(t))\right)|i_{MR}\rangle \sim \exp\left(-i\varepsilon(\overrightarrow{\lambda})\int_{t^*}^{T_a} dtV_3(a_{cl}(t))\right)|\psi_{MR}(t^*)\rangle, \tag{282}$$

where t^* is a time at which the energy density of the state $|\psi_{MR}(t^*)\rangle$ is sufficiently closed to that of the vacuum. Then, Eq.(278) can be written as

$$\int d\Lambda_B \int d\overrightarrow{\lambda} f(\Lambda_B, \overrightarrow{\lambda})\theta(\Lambda)\exp\left(-i\varepsilon(\overrightarrow{\lambda})\int_{t^*}^{T_a} dtV_3(a_{cl}(t))\right)\langle f_{MR}|\psi_{MR}(t^*)\rangle. \tag{283}$$

Thus, under the Born-Oppenheimer approximation, the partition function of matter sector is dominated by the vacuum energy. The is the same result of the previous Appendix.

F Principal value and Wheeler-Dewitt state

In this Appendix, we evaluate

$$PV\int_{-\infty}^{+\infty}\frac{dE}{E}\langle a|E;\Lambda\rangle\langle E;\Lambda|\epsilon\rangle \tag{284}$$

by using the WKB approximation. Because the universe is well described by the classical Friedman universe, we expect that $E=0$ dominates in it. The WKB solution of $\langle a|E;\Lambda\rangle$ is given by

$$\langle a|E;\Lambda\rangle = M_{pl}\sqrt{\frac{a}{p_{cl}}}\exp\left(i\int^a da' p_{cl}(a')\right), \tag{285}$$

where

$$p_{cl}(a) = M_{pl}a^2\sqrt{2\left(\frac{\rho(a)}{6}-\frac{E}{a^3}\right)} := M_{pl}a^2\sqrt{\frac{\tilde{\rho}(a)}{3}}. \tag{286}$$

Then, for a sufficiently large value of a, we have

$$\int_{a_M}^{a} da\, p_{cl}(a) = \frac{M_{pl}}{3^{\frac{3}{2}}}\left(a^3\sqrt{\tilde{\rho}(a)} - a_M^3\sqrt{\tilde{\rho}(a_M)} + \frac{M-E}{\sqrt{\Lambda}}\log\left[\frac{a^{\frac{3}{2}}(\Lambda+\sqrt{\Lambda\tilde{\rho}(a)})}{a_M^{\frac{3}{2}}(\Lambda+\sqrt{\Lambda\tilde{\rho}(a_M)})}\right]\right)$$
$$:= \frac{M_{pl}a^3}{3^{\frac{3}{2}}}g(\Lambda,E,a) \underset{a\gg a_M}{\simeq} \frac{M_{pl}a^3}{3^{\frac{3}{2}}}\sqrt{\tilde{\rho}(a)}, \tag{287}$$

By substituting Eq.(285) and Eq.(287) to Eq.(284), we obtain

$$PV\int_{-\infty}^{\infty}\frac{dE}{E}\, M_{pl}\sqrt{\frac{a}{p_{cl}}}\exp\left(i\frac{M_{pl}a^3}{3^{\frac{3}{2}}}\sqrt{\tilde{\rho}(a)}\right)\langle E;\Lambda|\epsilon\rangle \tag{288}$$

By expanding the exponent around $E=0$, we have

$$M_{pl}\sqrt{\frac{a}{p_{cl}}}\exp\left(i\frac{M_{pl}a^3}{3^{\frac{3}{2}}}\sqrt{\rho(a)} - i\frac{M_{pl}E}{3^{\frac{3}{2}}\sqrt{\rho(a)}} + \mathcal{O}(E^2)\right) = \langle a|0;\Lambda\rangle\exp\left(-i\frac{M_{pl}E}{3^{\frac{3}{2}}\sqrt{\rho(a)}} + \mathcal{O}(E^2)\right). \tag{289}$$

Therefore, only the region

$$|E| \lesssim \frac{\sqrt{\rho(a)}}{M_{pl}} \sim \frac{\sqrt{\Lambda}}{M_{pl}} \tag{290}$$

contributes to the integral [29]. Therefore, it is self-consistent to show $\Lambda = 0$ by using only the zero energy eigenstate $|0\rangle$.

References

[1] G. Aad *et al.* [ATLAS Collaboration], "Observation of a new particle in the search for the Standard Model Higgs boson with the ATLAS detector at the LHC," Phys. Lett. B **716**, 1 (2012) [arXiv:1207.7214 [hep-ex]].

[2] S. Chatrchyan *et al.* [CMS Collaboration], "Observation of a new boson at a mass of 125 GeV with the CMS experiment at the LHC," Phys. Lett. B **716**, 30 (2012) [arXiv:1207.7235 [hep-ex]].

[29] More concretely, by substituting Eq.(289) to Eq.(284), and neglecting the E dependence of $\langle E;\Lambda|\epsilon\rangle$, we obtain

$$\langle a|0;\Lambda\rangle PV\int_{-\infty}^{a^3\rho(a)}\frac{dE}{E}\exp\left(-i\frac{M_{pl}E}{3^{\frac{3}{2}}\sqrt{\rho(a)}}\right) = \langle a|0;\Lambda\rangle PV\int_{-\infty}^{k}\frac{dx}{x}e^{-ix} \underset{k\to+\infty}{\to} -i\pi\langle a|0;\Lambda\rangle,$$

where $k := M_{pl}a^3\sqrt{\rho(a)}/3^{\frac{3}{2}}$.

[3] D. Buttazzo, G. Degrassi, P. P. Giardino, G. F. Giudice, F. Sala, A. Salvio and A. Strumia, "Investigating the near-criticality of the Higgs boson," JHEP **1312**, 089 (2013) doi:10.1007/JHEP12(2013)089 [arXiv:1307.3536 [hep-ph]].

[4] F. Bezrukov, M. Y. Kalmykov, B. A. Kniehl and M. Shaposhnikov, *"Higgs boson mass and new physics,"* JHEP **1210** (2012) 140 [arXiv:1205.2893 [hep-ph]]; G. Degrassi, S. Di Vita, J. Elias-Miro, J. R. Espinosa, G. F. Giudice, G. Isidori and A. Strumia, JHEP **1208** (2012) 098 [arXiv:1205.6497 [hep-ph]];

[5] S. Alekhin, A. Djouadi and S. Moch, *"The top quark and Higgs boson masses and the stability of the electroweak vacuum,"* Phys. Lett. B **716** (2012) 214 [arXiv:1207.0980 [hep-ph]].

[6] Y. Hamada, H. Kawai and K. y. Oda, *"Bare Higgs mass at Planck scale,"* Phys. Rev. D **87** (2013) 5, 053009 [Phys. Rev. D **89** (2014) 5, 059901] [arXiv:1210.2538 [hep-ph]].

[7] F. Jegerlehner, *"The Standard model as a low-energy effective theory: what is triggering the Higgs mechanism?,"* Acta Phys. Polon. B **45** (2014) 6, 1167 [arXiv:1304.7813 [hep-ph]].

[8] F. Jegerlehner, *"The hierarchy problem of the electroweak Standard Model revisited,"* arXiv:1305.6652 [hep-ph].

[9] Y. Hamada, H. Kawai and K. y. Oda, *"Bare Higgs mass and potential at ultraviolet cutoff,"* arXiv:1305.7055 [hep-ph].

[10] P. A. R. Ade *et al.* [Planck Collaboration], "Planck 2015 results. XIII. Cosmological parameters," arXiv:1502.01589 [astro-ph.CO].:

[11] D. Clowe, M. Bradac, A. H. Gonzalez, M. Markevitch, S. W. Randall, C. Jones and D. Zaritsky, "A direct empirical proof of the existence of dark matter," Astrophys. J. **648**, L109 (2006) doi:10.1086/508162 [astro-ph/0608407].

[12] M. Tegmark *et al.* [SDSS Collaboration], "The 3-D power spectrum of galaxies from the SDSS," Astrophys. J. **606**, 702 (2004) doi:10.1086/382125 [astro-ph/0310725].

[13] G. R. Blumenthal, S. M. Faber, J. R. Primack and M. J. Rees, "Formation of Galaxies and Large Scale Structure with Cold Dark Matter," Nature **311**, 517 (1984). doi:10.1038/311517a0

[14] V. C. Rubin and W. K. Ford, Jr., "Rotation of the Andromeda Nebula from a Spectroscopic Survey of Emission Regions," Astrophys. J. **159**, 379 (1970). doi:10.1086/150317

[15] M. S. Roberts and R. N. Whitehurst. “The rotation curve and geometry of M31 at large galactocentric distances.” - 1975. Astrophys.J.,201,327

[16] M. Cirelli, N. Fornengo and A. Strumia, “Minimal dark matter,” Nucl. Phys. B **753**, 178 (2006) [hep-ph/0512090].

[17] J. Hisano, S. Matsumoto, M. Nagai, O. Saito and M. Senami, “Non-perturbative effect on thermal relic abundance of dark matter,” Phys. Lett. B **646**, 34 (2007) [hep-ph/0610249].

[18] M. Cirelli, A. Strumia and M. Tamburini, “Cosmology and Astrophysics of Minimal Dark Matter,” Nucl. Phys. B **787**, 152 (2007) [arXiv:0706.4071 [hep-ph]].

[19] M. Cirelli and A. Strumia, “Minimal Dark Matter: Model and results,” New J. Phys. **11**, 105005 (2009) [arXiv:0903.3381 [hep-ph]].

[20] Y. Hamada, H. Kawai and K. y. Oda, “Predictions on mass of Higgs portal scalar dark matter from Higgs inflation and flat potential,” JHEP **1407**, 026 (2014) doi:10.1007/JHEP07(2014)026 [arXiv:1404.6141 [hep-ph]].

[21] M. Hashimoto, S. Iso and Y. Orikasa, “Radiative symmetry breaking from flat potential in various U(1) models,” Phys. Rev. D **89**, no. 5, 056010 (2014) doi:10.1103/PhysRevD.89.056010 [arXiv:1401.5944 [hep-ph]].

[22] M. Hashimoto, S. Iso and Y. Orikasa, “Radiative symmetry breaking at the Fermi scale and flat potential at the Planck scale,” Phys. Rev. D **89**, no. 1, 016019 (2014) doi:10.1103/PhysRevD.89.016019 [arXiv:1310.4304 [hep-ph]].

[23] S. Iso and Y. Orikasa, “TeV Scale B-L model with a flat Higgs potential at the Planck scale - in view of the hierarchy problem -,” PTEP **2013**, 023B08 (2013) doi:10.1093/ptep/pts099 [arXiv:1210.2848 [hep-ph]].

[24] K. Kawana, “Multiple Point Principle of the Standard Model with Scalar Singlet Dark Matter and Right Handed Neutrinos,” PTEP **2015**, 023B04 (2015) doi:10.1093/ptep/ptv006 [arXiv:1411.2097 [hep-ph]].

[25] K. Kawana, “Criticality and inflation of the gauged B L model,” PTEP **2015**, 073B04 (2015) doi:10.1093/ptep/ptv093 [arXiv:1501.04482 [hep-ph]].

[26] Y. Hamada and K. Kawana, “Vanishing Higgs Potential in Minimal Dark Matter Models,” Phys. Lett. B **751**, 164 (2015) doi:10.1016/j.physletb.2015.10.006 [arXiv:1506.06553 [hep-ph]].

[27] N. Haba and Y. Yamaguchi, "Vacuum stability in the $U(1)_\chi$ extended model with vanishing scalar potential at the Planck scale," PTEP **2015**, no. 9, 093B05 (2015) doi:10.1093/ptep/ptv121 [arXiv:1504.05669 [hep-ph]].

[28] N. Haba, H. Ishida, R. Takahashi and Y. Yamaguchi, "Gauge coupling unification in a classically scale invariant model," JHEP **1602**, 058 (2016) doi:10.1007/JHEP02(2016)058 [arXiv:1511.02107 [hep-ph]].

[29] N. Haba, H. Ishida, N. Kitazawa and Y. Yamaguchi, "A new dynamics of electroweak symmetry breaking with classically scale invariance," Phys. Lett. B **755**, 439 (2016) doi:10.1016/j.physletb.2016.02.052 [arXiv:1512.05061 [hep-ph]].

[30] N. Haba, H. Ishida, N. Okada and Y. Yamaguchi, "Multiple-point principle with a scalar singlet extension of the Standard Model," arXiv:1608.00087 [hep-ph].

[31] K. Kawana, "Classical conformality in the Standard Model from Coleman's theory," Mod. Phys. Lett. A **31**, no. 31, 1650176 (2016) doi:10.1142/S0217732316501765 [arXiv:1605.00436 [hep-ph]].

[32] F. L. Bezrukov and M. Shaposhnikov, *"The Standard Model Higgs boson as the inflaton,"* Phys. Lett. B **659** (2008) 703 [arXiv:0710.3755 [hep-th]].

[33] A. Salvio, *"Higgs Inflation at NNLO after the Boson Discovery,"* Phys. Lett. B **727** (2013) 234 [arXiv:1308.2244 [hep-ph]].

[34] Y. Hamada, H. Kawai and K. y. Oda, *"Minimal Higgs inflation,"* PTEP **2014** (2014) 023B02 [arXiv:1308.6651 [hep-ph]].

[35] Y. Hamada, H. Kawai, K. y. Oda and S. C. Park, *"Higgs Inflation is Still Alive after the Results from BICEP2,"* Phys. Rev. Lett. **112** (2014) 24, 241301 [arXiv:1403.5043 [hep-ph]].

[36] F. Bezrukov and M. Shaposhnikov, *"Higgs inflation at the critical point,"* Phys. Lett. B **734** (2014) 249 [arXiv:1403.6078 [hep-ph]].

[37] Y. Hamada, H. Kawai, K. y. Oda and S. C. Park, *"Higgs inflation from Standard Model criticality,"* Phys. Rev. D **91** (2015) 5, 053008 [arXiv:1408.4864 [hep-ph]].

[38] Y. Hamada, K. y. Oda and F. Takahashi, *"Topological Higgs inflation: Origin of Standard Model criticality,"* Phys. Rev. D **90** (2014) 9, 097301 [arXiv:1408.5556 [hep-ph]].

[39] F. Bezrukov, J. Rubio and M. Shaposhnikov, *"Living beyond the edge: Higgs inflation and vacuum metastability,"* arXiv:1412.3811 [hep-ph].

[40] Y. Hamada, H. Kawai and K. y. Oda, "Eternal Higgs inflation and the cosmological constant problem," Phys. Rev. D **92** (2015) 045009 [arXiv:1501.04455 [hep-ph]].

[41] M. Yoshimura, "Unified Gauge Theories and the Baryon Number of the Universe," Phys. Rev. Lett. **41** (1978) 281 [Phys. Rev. Lett. **42** (1979) 746].

[42] I. Affleck and M. Dine, "A New Mechanism for Baryogenesis," Nucl. Phys. B **249** (1985) 361.

[43] M. Fukugita and T. Yanagida, "Baryogenesis Without Grand Unification," Phys. Lett. B **174** (1986) 45.

[44] H. Aoki and H. Kawai, "String scale baryogenesis," Prog. Theor. Phys. **98** (1997) 449 [hep-ph/9703421].

[45] S. Davidson, E. Nardi and Y. Nir, "Leptogenesis," Phys. Rept. **466**, 105 (2008) doi:10.1016/j.physrep.2008.06.002 [arXiv:0802.2962 [hep-ph]].

[46] Y. Hamada and R. Kitano, "Primordial Lepton Oscillations and Baryogenesis," JHEP **1611**, 010 (2016) doi:10.1007/JHEP11(2016)010 [arXiv:1609.05028 [hep-ph]].

[47] Y. Hamada and S. Iso, "Baryon asymmetry from primordial black holes," arXiv:1610.02586 [hep-ph].

[48] W. Buchmuller, R. D. Peccei and T. Yanagida, "Leptogenesis as the origin of matter," Ann. Rev. Nucl. Part. Sci. **55**, 311 (2005) doi:10.1146/annurev.nucl.55.090704.151558 [hep-ph/0502169].

[49] V. A. Kuzmin, V. A. Rubakov and M. E. Shaposhnikov, "On the Anomalous Electroweak Baryon Number Nonconservation in the Early Universe," Phys. Lett. **155B**, 36 (1985). doi:10.1016/0370-2693(85)91028-7

[50] G. 't Hooft, "Computation of the Quantum Effects Due to a Four-Dimensional Pseudoparticle," Phys. Rev. D **14** (1976) 3432 [Phys. Rev. D **18** (1978) 2199].

[51] F. R. Klinkhamer and N. S. Manton, "A Saddle Point Solution in the Weinberg-Salam Theory," Phys. Rev. D **30** (1984) 2212.

[52] Y. Hamada, K. Tsumura and D. Yasuhara, "The reheating era leptogenesis in models with seesaw mechanism," arXiv:1608.05256 [hep-ph].

[53] R. D. Peccei, "The Strong CP problem and axions," Lect. Notes Phys. **741**, 3 (2008) doi:$10.1007/978-3-540-73518-2_1$ [hep-ph/0607268].

[54] S. Weinberg, "The Cosmological Constant Problem," Rev. Mod. Phys. **61**, 1 (1989). doi:10.1103/RevModPhys.61.1

[55] J. Martin, "Everything You Always Wanted To Know About The Cosmological Constant Problem (But Were Afraid To Ask)," Comptes Rendus Physique **13**, 566 (2012) doi:10.1016/j.crhy.2012.04.008 [arXiv:1205.3365 [astro-ph.CO]].

[56] C. D. Froggatt and H. B. Nielsen, "Standard model criticality prediction: Top mass 173 +- 5-GeV and Higgs mass 135 +- 9-GeV," Phys. Lett. B **368**, 96 (1996) doi:10.1016/0370-2693(95)01480-2 [hep-ph/9511371].

[57] C. D. Froggatt, H. B. Nielsen and Y. Takanishi, "Standard model Higgs boson mass from borderline metastability of the vacuum," Phys. Rev. D **64**, 113014 (2001) doi:10.1103/PhysRevD.64.113014 [hep-ph/0104161].

[58] C. D. Froggatt, H. B. Nielsen and L. V. Laperashvili, "Hierarchy-problem and a bound state of 6 t and 6 anti-t," Int. J. Mod. Phys. A **20**, 1268 (2005) doi:10.1142/S0217751X0502416X [hep-ph/0406110].

[59] H. B. Nielsen, "PREdicted the Higgs Mass," Bled Workshops Phys. **13**, no. 2, 94 (2012) [arXiv:1212.5716 [hep-ph]].

[60] H. Kawai and T. Okada, "Solving the Naturalness Problem by Baby Universes in the Lorentzian Multiverse," Prog. Theor. Phys. **127**, 689 (2012) doi:10.1143/PTP.127.689 [arXiv:1110.2303 [hep-th]].

[61] H. Kawai, "Low energy effective action of quantum gravity and the naturalness problem," Int. J. Mod. Phys. A **28**, 1340001 (2013). doi:10.1142/S0217751X13400010

[62] Y. Hamada, H. Kawai and K. Kawana, "Evidence of the Big Fix," Int. J. Mod. Phys. A **29**, 1450099 (2014) doi:10.1142/S0217751X14500997 [arXiv:1405.1310 [hep-ph]].

[63] Y. Hamada, H. Kawai and K. Kawana, "Weak Scale From the Maximum Entropy Principle," PTEP **2015**, 033B06 (2015) doi:10.1093/ptep/ptv011 [arXiv:1409.6508 [hep-ph]].

[64] Y. Hamada, H. Kawai and K. Kawana, "Natural solution to the naturalness problem: The universe does fine-tuning," PTEP **2015**, no. 12, 123B03 (2015) doi:10.1093/ptep/ptv168 [arXiv:1509.05955 [hep-th]].

[65] K. Kawana, "Possible explanations for fine-tuning of the universe," arXiv:1609.00513 [hep-th].

[66] S. R. Coleman, "Why There Is Nothing Rather Than Something: A Theory of the Cosmological Constant," Nucl. Phys. B **310**, 643 (1988). doi:10.1016/0550-3213(88)90097-1.

[67] S. R. Coleman, "The Uses of Instantons," Subnucl. Ser. **15**, 805 (1979).

[68] S. R. Coleman, "Black Holes as Red Herrings: Topological Fluctuations and the Loss of Quantum Coherence," Nucl. Phys. B **307**, 867 (1988).

[69] N. Ishibashi, H. Kawai, Y. Kitazawa and A. Tsuchiya, "A Large N reduced model as superstring," Nucl. Phys. B **498**, 467 (1997) doi:10.1016/S0550-3213(97)00290-3 [hep-th/9612115].

[70] H. Aoki, S. Iso, H. Kawai, Y. Kitazawa, A. Tsuchiya and T. Tada, "IIB matrix model," Prog. Theor. Phys. Suppl. **134**, 47 (1999) doi:10.1143/PTPS.134.47 [hep-th/9908038].

[71] M. Fukuma, H. Kawai, Y. Kitazawa and A. Tsuchiya, "String field theory from IIB matrix model," Nucl. Phys. B **510**, 158 (1998) doi:10.1016/S0550-3213(98)81008-0, 10.1016/S0550-3213(97)00584-1 [hep-th/9705128].

[72] K. j. Hamada, "Supersymmetric Wilson loops in IIB matrix model," Phys. Rev. D **56**, R7503 (1997) doi:10.1103/PhysRevD.56.R7503 [hep-th/9706187].

[73] H. Aoki, S. Iso, H. Kawai, Y. Kitazawa and T. Tada, "Space-time structures from IIB matrix model," Prog. Theor. Phys. **99**, 713 (1998) doi:10.1143/PTP.99.713 [hep-th/9802085].

[74] S. Iso and H. Kawai, "Space-time and matter in IIB matrix model: Gauge symmetry and diffeomorphism," Int. J. Mod. Phys. A **15**, 651 (2000) doi:10.1142/S0217751X0000032X [hep-th/9903217].

[75] T. Imai, Y. Kitazawa, Y. Takayama and D. Tomino, "Quantum corrections on fuzzy sphere," Nucl. Phys. B **665**, 520 (2003) doi:10.1016/S0550-3213(03)00491-7 [hep-th/0303120].

[76] T. Imai, Y. Kitazawa, Y. Takayama and D. Tomino, "Effective actions of matrix models on homogeneous spaces," Nucl. Phys. B **679**, 143 (2004) doi:10.1016/j.nuclphysb.2003.11.038 [hep-th/0307007].

[77] H. Kaneko, Y. Kitazawa and D. Tomino, "Stability of fuzzy S**2 x S**2 x S**2 in IIB type matrix models," Nucl. Phys. B **725**, 93 (2005) doi:10.1016/j.nuclphysb.2005.07.009 [hep-th/0506033].

[78] S. W. Kim, J. Nishimura and A. Tsuchiya, "Expanding (3+1)-dimensional universe from a Lorentzian matrix model for superstring theory in (9+1)-dimensions," Phys. Rev. Lett. **108**, 011601 (2012) doi:10.1103/PhysRevLett.108.011601 [arXiv:1108.1540 [hep-th]].

[79] Y. Asano, H. Kawai and A. Tsuchiya, "Factorization of the Effective Action in the IIB Matrix Model," Int. J. Mod. Phys. A **27**, 1250089 (2012) doi:10.1142/S0217751X12500893 [arXiv:1205.1468 [hep-th]].

[80] M. Hanada, H. Kawai and Y. Kimura, "Describing curved spaces by matrices," Prog. Theor. Phys. **114**, 1295 (2006) doi:10.1143/PTP.114.1295 [hep-th/0508211].

[81] H. Kawai, "Curved space-times in matrix models," Prog. Theor. Phys. Suppl. **171**, 99 (2007). doi:10.1143/PTPS.171.99

[82] T. Eguchi and H. Kawai, "Reduction of Dynamical Degrees of Freedom in the Large N Gauge Theory," Phys. Rev. Lett. **48**, 1063 (1982). doi:10.1103/PhysRevLett.48.1063

[83] G. Bhanot, U. M. Heller and H. Neuberger, "The Quenched Eguchi-Kawai Model," Phys. Lett. **113B**, 47 (1982). doi:10.1016/0370-2693(82)90106-X

[84] G. Parisi, "A Simple Expression for Planar Field Theories," Phys. Lett. **112B**, 463 (1982). doi:10.1016/0370-2693(82)90849-8

[85] H. Aoki, N. Ishibashi, S. Iso, H. Kawai, Y. Kitazawa and T. Tada, "Noncommutative Yang-Mills in IIB matrix model," Nucl. Phys. B **565**, 176 (2000) doi:10.1016/S0550-3213(99)00633-1 [hep-th/9908141].

[86] N. Ishibashi, S. Iso, H. Kawai and Y. Kitazawa, "Wilson loops in noncommutative Yang-Mills," Nucl. Phys. B **573**, 573 (2000) doi:10.1016/S0550-3213(99)00708-7 [hep-th/9910004].

[87] S. Iso, H. Kawai and Y. Kitazawa, "Bilocal fields in noncommutative field theory," Nucl. Phys. B **576**, 375 (2000) doi:10.1016/S0550-3213(00)00092-4 [hep-th/0001027].

[88] V. O. Rivelles, "Noncommutative field theories and gravity," Phys. Lett. B **558**, 191 (2003) doi:10.1016/S0370-2693(03)00271-5 [hep-th/0212262].

[89] H. S. Yang, "Exact Seiberg-Witten map and induced gravity from noncommutativity," Mod. Phys. Lett. A **21**, 2637 (2006) doi:10.1142/S0217732306021682 [hep-th/0402002].

[90] H. S. Yang, "On The Correspondence Between Noncommuative Field Theory And Gravity," Mod. Phys. Lett. A **22**, 1119 (2007) doi:10.1142/S0217732307023675 [hep-th/0612231].

[91] H. Steinacker, "Emergent Gravity from Noncommutative Gauge Theory," JHEP **0712**, 049 (2007) doi:10.1088/1126-6708/2007/12/049 [arXiv:0708.2426 [hep-th]].

[92] H. Steinacker, "Emergent Gravity and Noncommutative Branes from Yang-Mills Matrix Models," Nucl. Phys. B **810**, 1 (2009) doi:10.1016/j.nuclphysb.2008.10.014 [arXiv:0806.2032 [hep-th]].

[93] H. Grosse, H. Steinacker and M. Wohlgenannt, "Emergent Gravity, Matrix Models and UV/IR Mixing," JHEP **0804**, 023 (2008) doi:10.1088/1126-6708/2008/04/023 [arXiv:0802.0973 [hep-th]].

[94] N. Kuntner and H. Steinacker, "On Poisson geometries related to noncommutative emergent gravity," J. Geom. Phys. **62**, 1760 (2012) doi:10.1016/j.geomphys.2012.04.002 [arXiv:1111.2732 [math-ph]].

[95] H. Steinacker, "The curvature of branes, currents and gravity in matrix models," JHEP **1301**, 112 (2013) doi:10.1007/JHEP01(2013)112 [arXiv:1210.8364 [hep-th]].

[96] H. C. Steinacker, "Emergent 4D gravity on covariant quantum spaces in the IKKT model," arXiv:1606.00769 [hep-th].

[97] H. Steinacker, "Emergent Geometry and Gravity from Matrix Models: an Introduction," Class. Quant. Grav. **27**, 133001 (2010) doi:10.1088/0264-9381/27/13/133001 [arXiv:1003.4134 [hep-th]].

[98] H. Steinacker, "Non-commutative geometry and matrix models," PoS QGQGS **2011**, 004 (2011) [arXiv:1109.5521 [hep-th]].

[99] H. S. Yang, "Quantization of Emergent Gravity," Int. J. Mod. Phys. A **30**, 1550016 (2015) doi:10.1142/S0217751X15500165 [arXiv:1312.0580 [hep-th]].

[100] H. Kawai, K. Kawana and K. Sakai, "A note on graviton exchange in emergent gravity scenario," arXiv:1610.09844 [hep-th].

[101] E. Aprile *et al.* [XENON100 Collaboration], "Dark Matter Results from 225 Live Days of XENON100 Data," Phys. Rev. Lett. **109**, 181301 (2012) doi:10.1103/PhysRevLett.109.181301 [arXiv:1207.5988 [astro-ph.CO]].

[102] D. S. Akerib *et al.* [LUX Collaboration], "First results from the LUX dark matter experiment at the Sanford Underground Research Facility," Phys. Rev. Lett. **112**, 091303 (2014) doi:10.1103/PhysRevLett.112.091303 [arXiv:1310.8214 [astro-ph.CO]].

[103] M. W. Goodman and E. Witten, "Detectability of Certain Dark Matter Candidates," Phys. Rev. D **31**, 3059 (1985). doi:10.1103/PhysRevD.31.3059

[104] L. Di Luzio, R. Grber, J. F. Kamenik and M. Nardecchia, "Accidental matter at the LHC," JHEP **1507**, 074 (2015) doi:10.1007/JHEP07(2015)074 [arXiv:1504.00359 [hep-ph]].

[105] Y. Hamada, K. Kawana and K. Tsumura, "Landau pole in the Standard Model with weakly interacting scalar fields," Phys. Lett. B **747**, 238 (2015) doi:10.1016/j.physletb.2015.05.072 [arXiv:1505.01721 [hep-ph]].

[106] K. Hally, H. E. Logan and T. Pilkington, "Constraints on large scalar multiplets from perturbative unitarity," Phys. Rev. D **85** (2012) 095017.

[107] K. Earl, K. Hartling, H. E. Logan and T. Pilkington, "Constraining models with a large scalar multiplet," Phys. Rev. D **88** (2013) 015002.

[108] S. Moch, S. Weinzierl, S. Alekhin, J. Blumlein, L. de la Cruz, S. Dittmaier, M. Dowling and J. Erler *et al.*, "High precision fundamental constants at the TeV scale," arXiv:1405.4781 [hep-ph].

[109] [ATLAS and CDF and CMS and D0 Collaborations], "First combination of Tevatron and LHC measurements of the top-quark mass," arXiv:1403.4427 [hep-ex].

[110] CMS Collaboration [CMS Collaboration], "Combination of the CMS top-quark mass measurements from Run 1 of the LHC," CMS-PAS-TOP-14-015.

[111] G. Aad *et al.* [ATLAS and CMS Collaborations], "Combined Measurement of the Higgs Boson Mass in pp Collisions at $\sqrt{s} = 7$ and 8 TeV with the ATLAS and CMS Experiments," Phys. Rev. Lett. **114**, 191803 (2015) [arXiv:1503.07589 [hep-ex]].

[112] M. J. G. Veltman, "The Infrared - Ultraviolet Connection," Acta Phys. Polon. B **12** (1981) 437.

[113] W. Buchmuller, P. Di Bari and M. Plumacher, "Leptogenesis for pedestrians," Annals Phys. **315**, 305 (2005) doi:10.1016/j.aop.2004.02.003 [hep-ph/0401240].

[114] G. Lazarides and Q. Shafi, "Origin of matter in the inflationary cosmology," Phys. Lett. B **258** (1991) 305.

[115] T. Asaka, K. Hamaguchi, M. Kawasaki and T. Yanagida, "Leptogenesis in inflaton decay," Phys. Lett. B **464**, 12 (1999) doi:10.1016/S0370-2693(99)01020-5 [hep-ph/9906366].

[116] T. Asaka, K. Hamaguchi, M. Kawasaki and T. Yanagida, "Leptogenesis in inflationary universe," Phys. Rev. D **61**, 083512 (2000) doi:10.1103/PhysRevD.61.083512 [hep-ph/9907559].

[117] B. Grzadkowski, M. Iskrzynski, M. Misiak and J. Rosiek, "Dimension-Six Terms in the Standard Model Lagrangian," JHEP **1010** (2010) 085 [arXiv:1008.4884 [hep-ph]].

[118] L. D. Landau and I. Pomeranchuk, "Limits of applicability of the theory of bremsstrahlung electrons and pair production at high-energies," Dokl. Akad. Nauk Ser. Fiz. **92**, 535 (1953).

[119] A. B. Migdal, "Bremsstrahlung and pair production in condensed media at high-energies," Phys. Rev. **103**, 1811 (1956). doi:10.1103/PhysRev.103.1811

[120] K. Harigaya and K. Mukaida, "Thermalization after/during Reheating," JHEP **1405**, 006 (2014) doi:10.1007/JHEP05(2014)006 [arXiv:1312.3097 [hep-ph]].

[121] K. Harigaya, M. Kawasaki, K. Mukaida and M. Yamada, "Dark Matter Production in Late Time Reheating," Phys. Rev. D **89**, no. 8, 083532 (2014) doi:10.1103/PhysRevD.89.083532 [arXiv:1402.2846 [hep-ph]].

[122] S. Weinberg, *Cosmology*, first edition, Oxford 2008.

[123] R. Kallosh, A. Linde and D. Roest, "Universal Attractor for Inflation at Strong Coupling," Phys. Rev. Lett. **112** (2014) no.1, 011303 [arXiv:1310.3950 [hep-th]].

[124] A. D. Linde, "Chaotic Inflation," Phys. Lett. B **129** (1983) 177.

[125] M. Aaboud *et al.* [ATLAS Collaboration], "Measurement of the top quark mass in the $t\bar{t} \to$ dilepton channel from $\sqrt{s} = 8$ TeV ATLAS data," arXiv:1606.02179 [hep-ex].

[126] V. Khachatryan *et al.* [CMS Collaboration], "Measurement of the top quark mass using proton-proton data at $\sqrt{(s)} = 7$ and 8 TeV," Phys. Rev. D **93**, no. 7, 072004 (2016) doi:10.1103/PhysRevD.93.072004 [arXiv:1509.04044 [hep-ex]].

[127] C. A. Baker, D. D. Doyle, P. Geltenbort, K. Green, M. G. D. van der Grinten, P. G. Harris, P. Iaydjiev and S. N. Ivanov *et al.*, "An Improved experimental limit on the electric dipole moment of the neutron," Phys. Rev. Lett. **97**, 131801 (2006) [hep-ex/0602020].

[128] S. Afach *et al.*, "A Revised Experimental Upper Limit on the Electric Dipole Moment of the Neutron," arXiv:1509.04411 [hep-ex].

[129] T. P. Cheng, E. Eichten and L. F. Li, "Higgs Phenomena in Asymptotically Free Gauge Theories," Phys. Rev. D **9** (1974) 2259.

[130] M. D'Onofrio, K. Rummukainen and A. Tranberg, "The sphaleron rate at the electroweak crossover with 125 GeV Higgs mass," PoS LATTICE **2012**, 055 (2012) [arXiv:1212.3206].

[131] M. Born and J. R. Oppenheimer, Ann. Phys. 84, (1927) 457.